**Heated Crevice - Design, Experimental Methods, and Data Interpretation**

**Jesse Lumsden**
**Rockwell Science Center**

**Keith Fruzzetti**
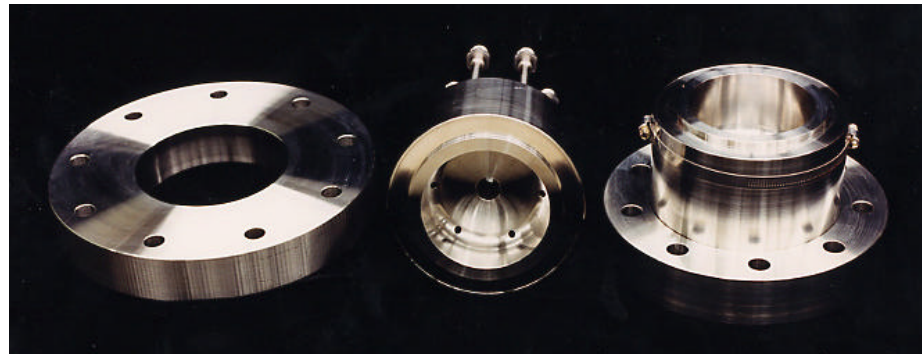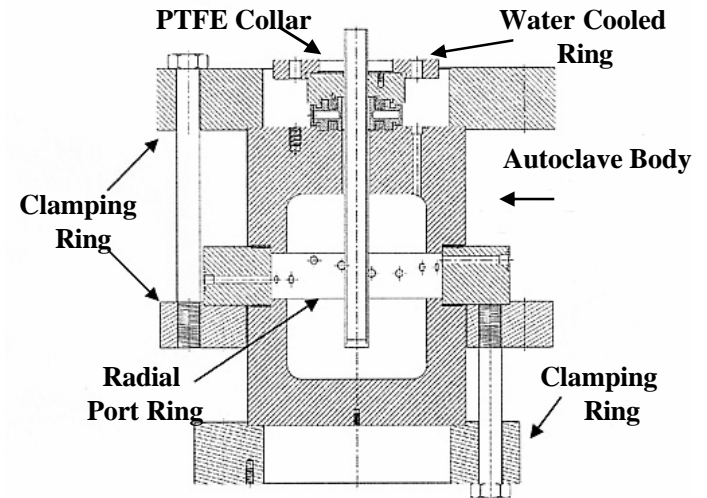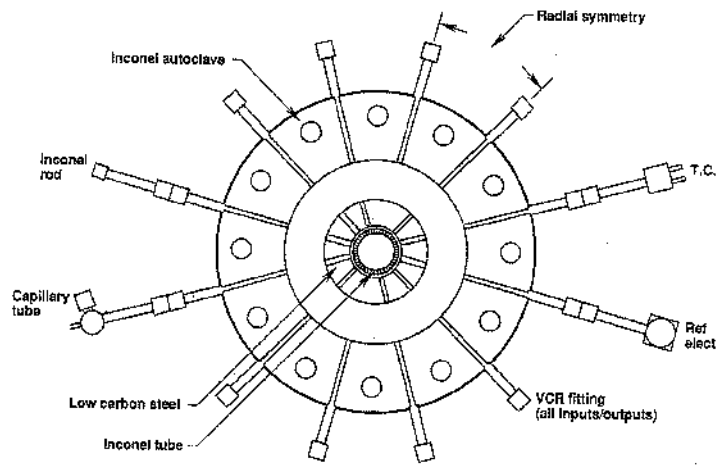**EPRI**

**Heated Crevice Seminar**
**Argonne National Laboratory**
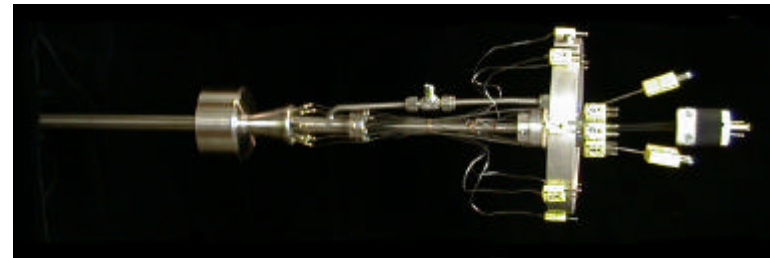
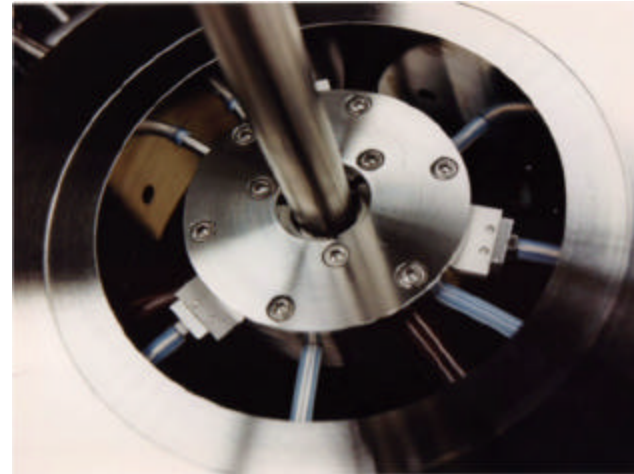# Heated Crevice - Design

- **Desired Flexibility**
  - **Easily Change Geometric Configuration/ Crevice Dimensions**
  - **Open Crevice, Packed Crevice, Closed Bottom Options**
  - **Disassemble & Tube Inspection Easy**
- **Clam Shell Design for Autoclave Body**
- **Tube Assembly Detachable from Autoclave**
- **Ring (Support Plate) Mounted Using Support Rods from the Side**

# Heated Crevice - Design

# Heated Crevice - Design



Alloy 600 tube wall

0.10"

0.010" — 0.010" Inconel 600 type k

400°C solder

ELOX holes from inside of tube

# Heated Crevice - Design



**Clamping Ring**

**Radial Port Ring**

**Clamping Ring**
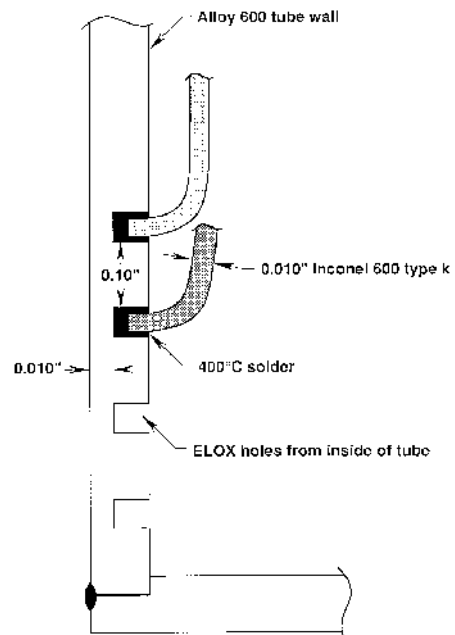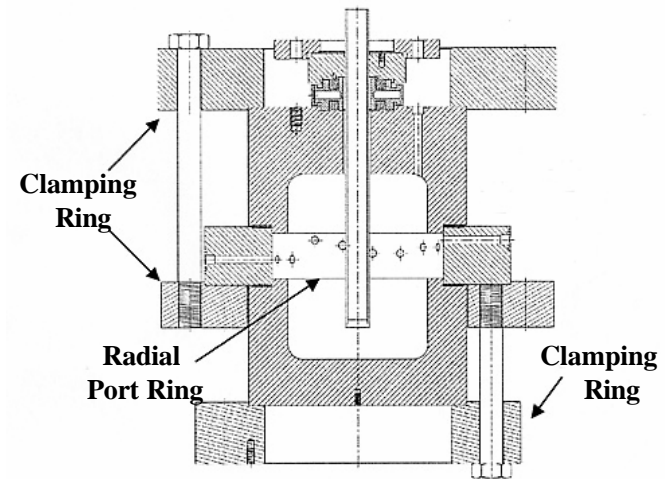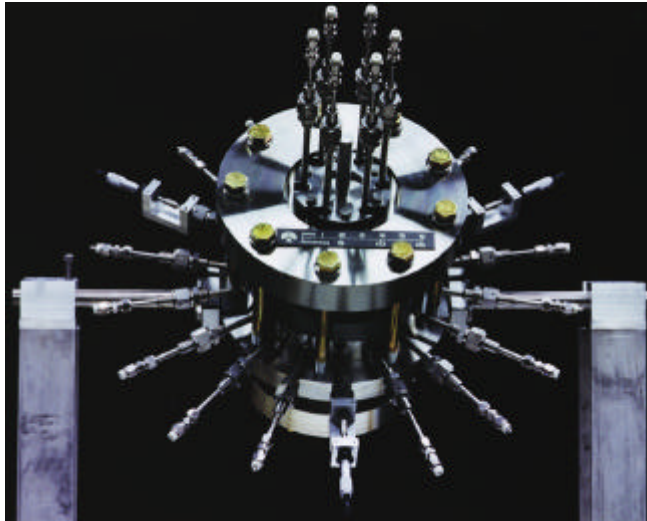
- Temperature of tube wall in crevice
- Bulk solution extraction for analysis
- Crevice solution extraction for analysis
- ECP of Freespan (NWT- Ag/AgCl)
- ECP of Alloy 600 Tube in crevice (NWT- Ag/AgCl)
- Temperature vs. elevation in crevice
- Electrochemical Noise
- AC Impedance
- pH Electrode
- Raman Spectroscopy

# Heated Crevice - Design
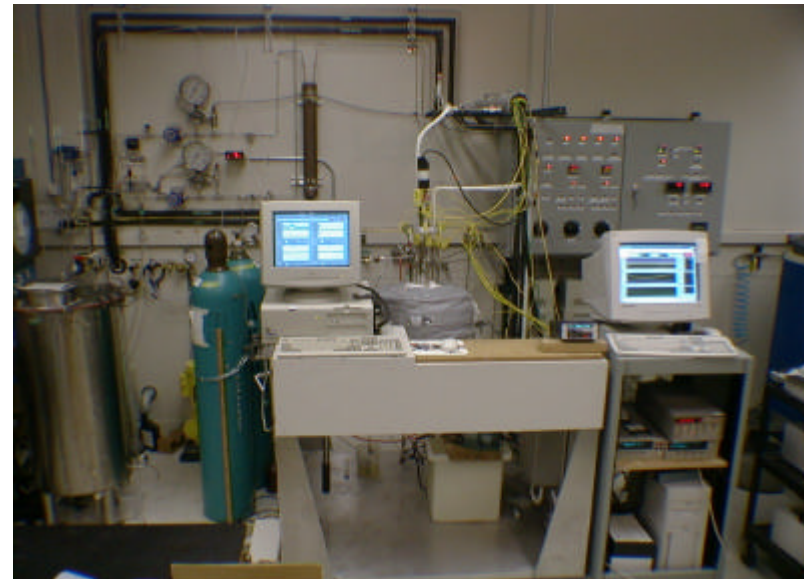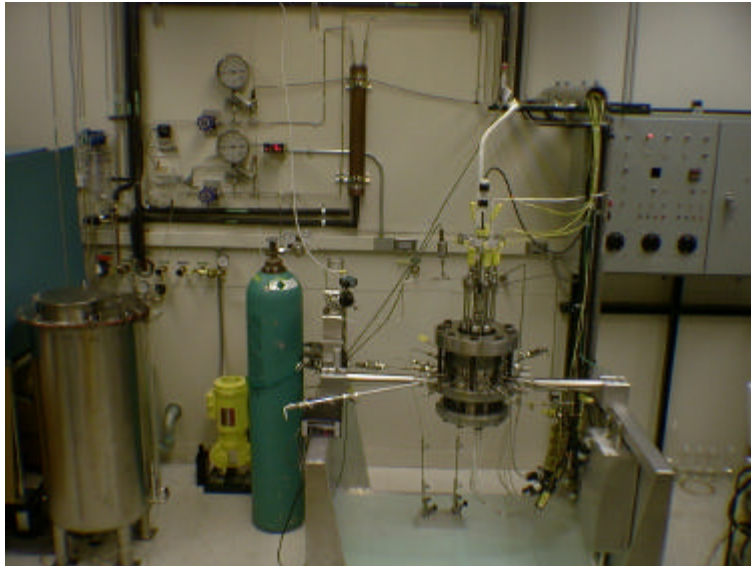


**Secondary Water System**
- **Once through or recirculating**
- **Deaerated**
- **Adjustable Saturation Temperature – 280 C Typical**

# Heated Crevice - Design



**Options for Heat Input to the Crevice**

- **Cartridge Heater**
  - Constant Heat Flux
  - Maximum rate of hideout accumulation
    $$dm/dt = QC/L \quad (100\% \text{ efficiency})$$
    $m$ = mass of salt
    $Q$ = Heat Flux,
    $C$ = Concentration of impurity in Bulk
    $L$ = Heat of Evaporation
    $$m = (QC/L)t$$
- **Primary Circulating Loop**
  - Constant Temperature
  - Maximum rate of hide accumulation
    $$dm/dt = QxC/SL \quad (100\% \text{ efficiency})$$
    $x$ = length of crevice not fully wetted
    $L$ = total length of crevice
    $$m = m_0[1 - \exp(-QCt/Lm_o)]$$
    m  = mass of hideout at equilibrium
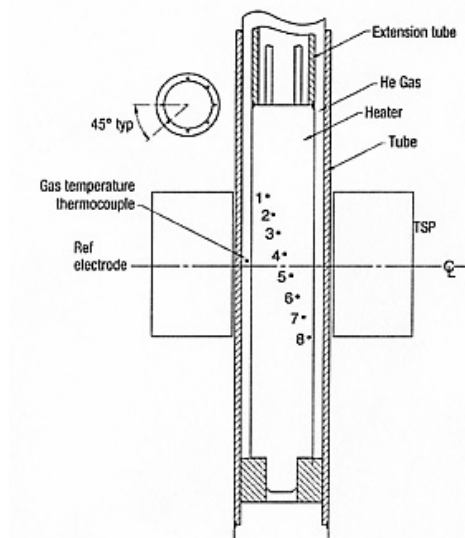
# Hideout Model For Loosely Packed Crevice
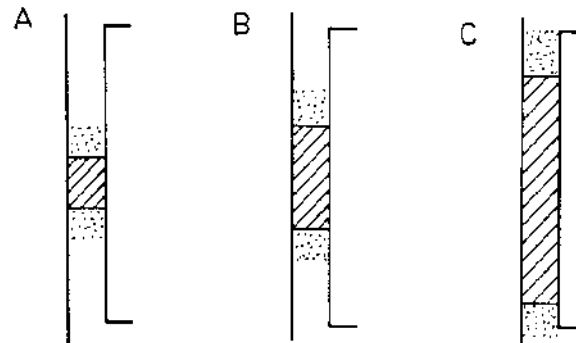


NON—BOILING SOLUTION; CONCENTRATION LIMITED BY $\Delta T$

After Mann

ZONE OF CONCENTRATION GRADIENT

- **Salt Initially Concentrates Deep in Crevice**
- **Boiling Point of Concentrated Solution Equals Superheat**
- **Boundary of Liquid Region Moves Toward Open End(s) of Crevice**
- **At Constant Heat Flux**
    - **Transition from Boiling to Fully Wetted Condition Marked by Increase in Temperate**
    - **Liquid has lower heat transfer coefficient**

# System Test
## Hypothesized Hideout Model For Tightly Packed Crevice
### Simple systems - NaOH, NaCl



STEAM

NON-BOILING SOLUTION; CONCENTRATION LIMITED BY $\Delta T$

ZONE OF CONCENTRATION GRADIENT
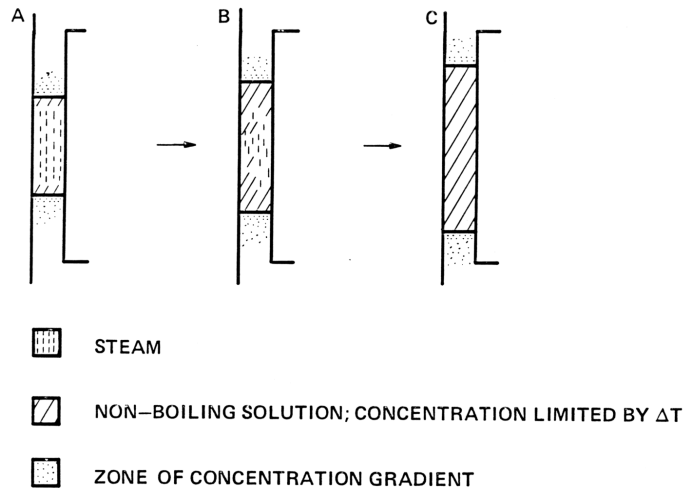
- **Most of Crevice Initially Steam Blanketed**
- **Hideout Begins at Top & Bottom Of Steam Blanket**
- **Concentrated Solution Penetrates into Steam Filled Region By Capillary Action**
- **Boiling Point of Concentrated Solution Equals Superheat**
- **At Constant Heat Flux**
    - **Transition from Steam Blanket to Boiling Marked by Temperature Decrease**
    - **Steam poorly conducting**
- **Successfully Quantitatively Modeled**
- **Multi-component Feedwater Chemistries & Precipitation not Yet Investigated**

# Heat Transfer Crevice/Thermo-Hydraulics

- **Open T/TSP Crevice**
- **Unrestricted flow**
- **Boiling heat transfer in crevice**
- **No hideout - no temperature gradient**



**40 ppm NaOH Feedwater**
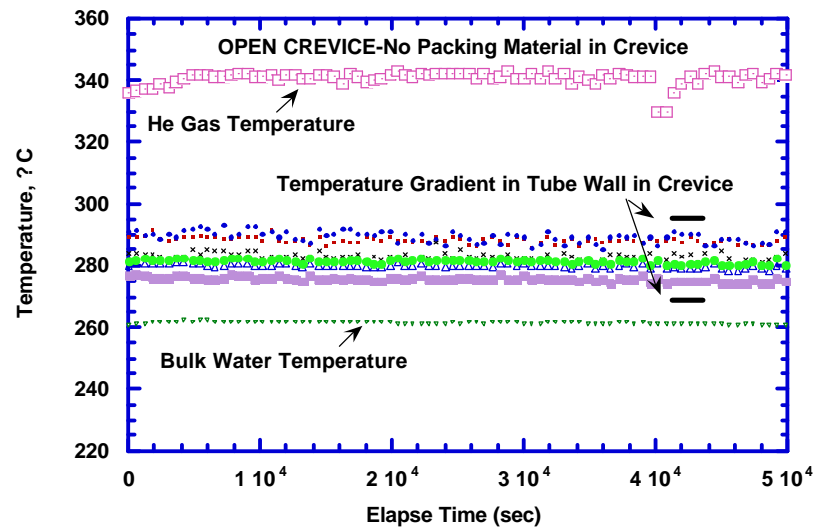
# Effects of Hideout on Crevice Wall Temperature

- **Crevice packed with diamond dust**
  - **52% porosity**
- **Feedwater at 2l/hr**
- **Constant heat flux**
- **$T_{SAT} = 280°C$**

**Temperature at Tube Surface DI Water**

Thermo1
Thermo2
Thermo3
Thermo4
Thermo5
Thermo6
Thermo7
Thermo8

**No Hideout**
**No Change in T**

**Temperature at Tube Surface 40 ppm NaOH**

Thermo1
Thermo2
Thermo3
Thermo4
Thermo5
Thermo6
Thermo7
Thermo8
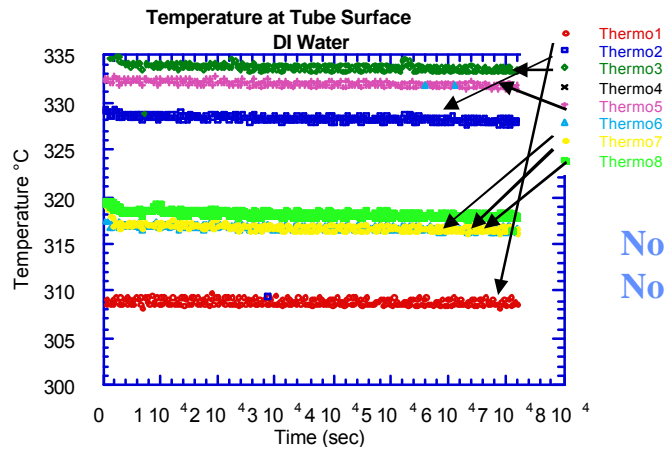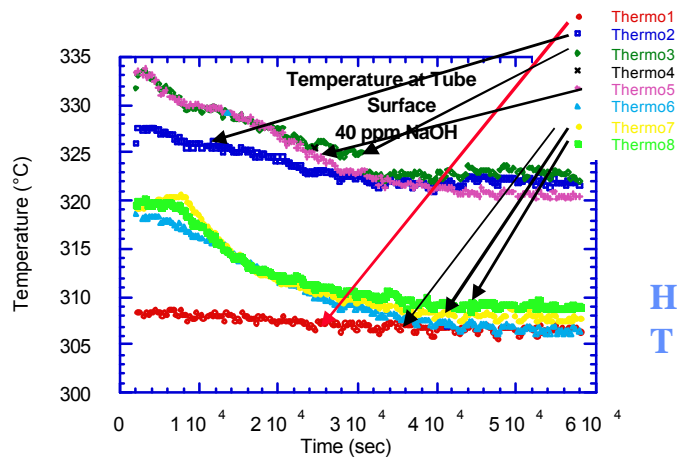
**Hideout**
**T Changes with time**

Extension tube
He Gas
Heater
Tube
45° typ
Gas temperature thermocouple
Ref electrode
TSP
CL
RSC0769.071701

# Extraction Results TSP- Type Crevice : Na Concentration

| Time of Superheat Crevice(Open) | Feedwater | Bulk | Crevice |
|---|---|---|---|
| **Open Crevice--No Significant Hideout** | | | |
| 2   hours | 19.2 ppm | 22.5 ppm | 860  ppm |
| | | | |
| **Packed Crevice (25% Porosity)** | | | |
| 2  hours | 19.5 ppm | 19.5 ppm | $8.23 \times 10^4$ ppm |
| 6 | 19.4 | 19.6 | $1.15 \times 10^5$ |
| 14 | 19.6 | 23.0 | $3.31 \times 10^5$ |
| 25 | 18.2 | 21.7 | $3.60 \times 10^5$ |

# Effect of Packing Density on Hideout

## Extraction Results - 52% Porosity Crevice - Constant Heat Flux

**20 ppm Na $^+$ Feedwater** (top graph, mg of Na Ions vs time (hrs))

**2 ppm Na $^+$ Feedwater** (bottom graph, mg of Na Ions vs time (hrs))
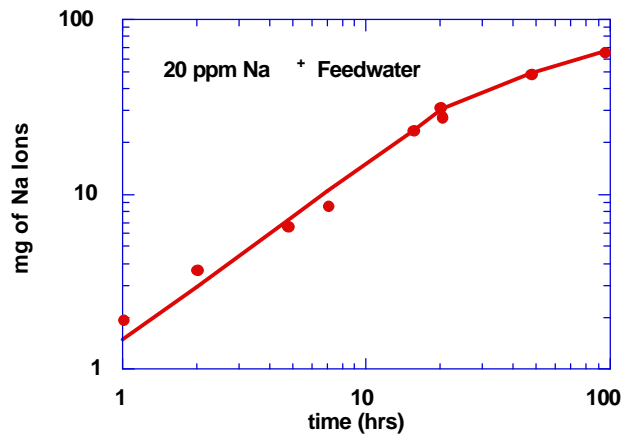
- **Initial Slope Equals One Implies Linear Hideout Rate**
- **Maximum possible Hideout Rate**
  $$dm/dt = QC/L$$
  **Q = Heat Flux From Section of Heater in Crevice**
  **C = Bulk Concentration of Sodium Ions**
  **L= Heat of Vaporization**

**Efficiency of Hideout Approx. 67% in Linear Region**
- **Higher Na+ than for 36% porosity**
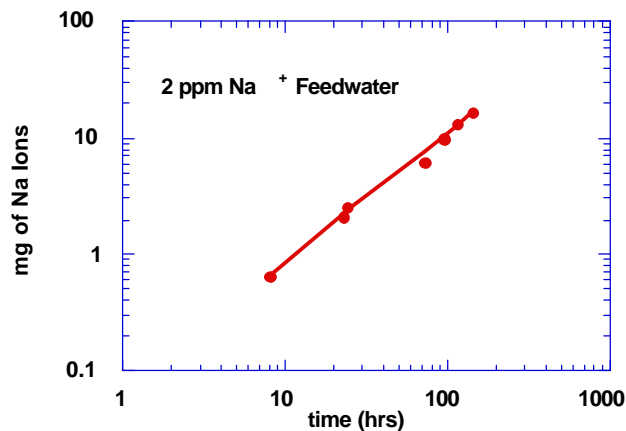
Max hideout rate = 2.17 mg/hr @ 20 ppm
Hideout rate, 20 ppm = 1.46 mg/hr
Hideout rate, 2 ppm = 0.126 mg/hr

110

# Tightly Packed Crevice - Model Calculations
## Computer Code Results

**23 ppm Na⁺ in Feedwater**

- **Hideout in good agreement with Millett model for a single concentrating specie in a packed crevice**
    - **Water drawn into crevice by capillary action**
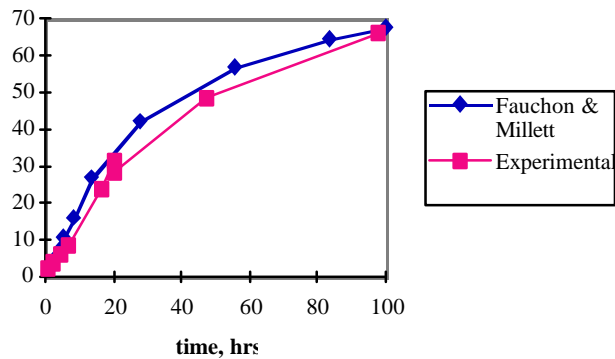    - **When water boils all salt drawn into crevice remains**
    - **Saturation concentration occurs when boiling point reaches available superheat**
    - **Applies conservation of energy, mass & momentum to transport within pores**
    - **Code solves set of differential equations**



- **Experimental Results in Excellent Agreement with Model Predictions**
    - **Model Predicts 14% of Crevice Initially Wetted**
    - **Predicts Initial Linear Rate of Accumulation**
    - **Predicts Steam Blanket Gradually Replaced with Concentrated Solution**

# Hideout and Hideout Return Kinetics

**Hideout**
**20 ppm Na in Feedwater**

*(Left chart: mg of sodium vs TIME (hrs), 0–50)*

**Hideout Return -Concentrated 16 hrs**
**Composite of 3 Runs**
**Tube Heater off at t=0**

**Best Fit Curve**

$y = A(1 - e^{-at})$

*(Right chart: HIDEOUT RETURN Na (mg) vs TIME (min), 0–70)*
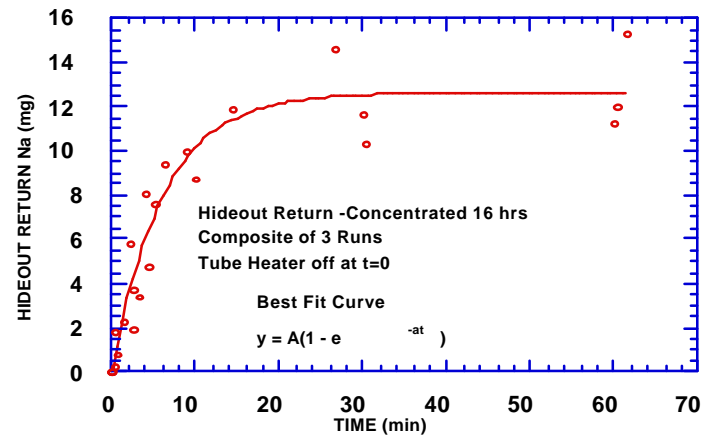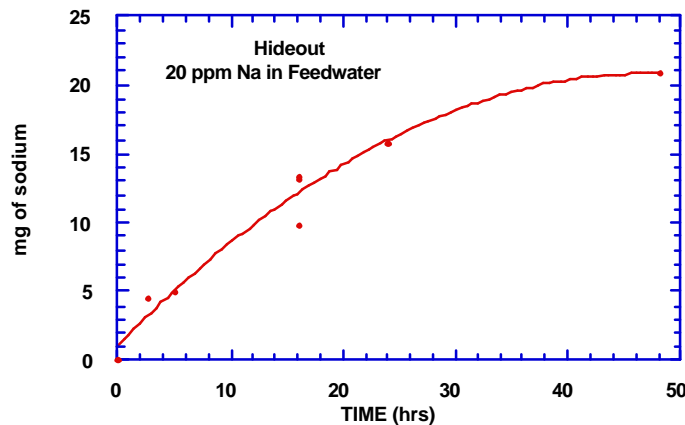
- Hideout in good agreement with Millett model for a single concentrating specie in a packed crevice
  - Water drawn into crevice by capillary action
  - When water boils all salt drawn into crevice remain
  - Saturation concentration occurs when boiling point reaches available superheat

- Cumulative hideout return of Na from a single crevice follows exponential model
- Mass balance for hideout and hideout return in good agreement

$$D = aS^2/p^2 \longrightarrow 1.47 \times 10^{-7} \text{ m}^2/\text{sec}$$

# Electrochemical Potential Measurement

- **ECP not measurable during heat flux**
  - **Steam in Crevice if packed with diamond powder**
- **ECP measurable after tube heater turned off**
  - **Fully liquid path 1- 2 min after tube off**
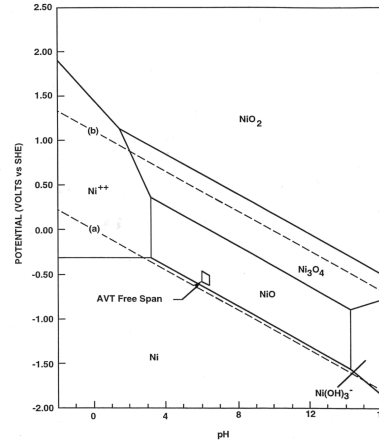- **Crevice less than free span ECP with NaOH**
  - **Indicates caustic crevice**
  - **Approx. 110mV per pH unit**
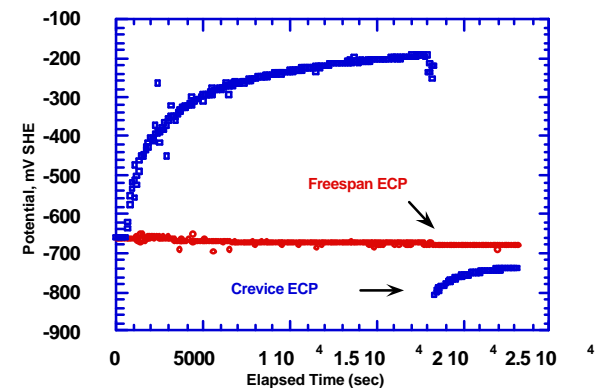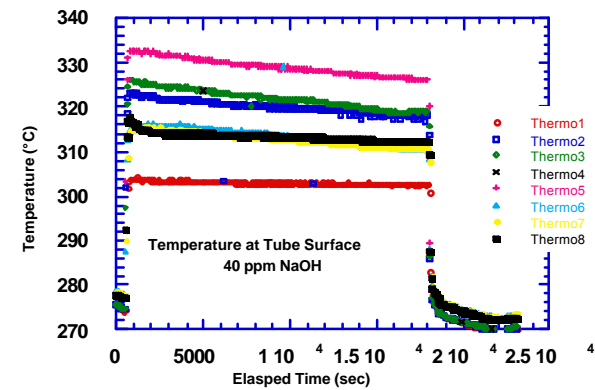
# Electrochemical Potential Measurement



- Assuming Corrosion Kinetics of alloy 600 Under Cathodic Control ECP is the reversible hydrogen electrode

$$E_{H2/H+} = 2.303\ RT/F\ (\log a_{H+}) - 2.303\ RT/2F\ (\log p_{H2})$$
Or
$$E_{H2/H+} = -0.110\ pH - 0.056\ \log p_{H2}$$

$p_{H2} = 0.0025$ atm, calculated from the bulk ECP

- **Crevice ECP < Bulk ECP if the crevice is caustic**
- **Crevice ECP > Bulk ECP if the crevice is acidic**

# BENCHMARKING ECP MEASUREMENT METHODOLOGY

- **Crevice pH calculated from potential measurement and by MULTEQ using results from extraction as input**
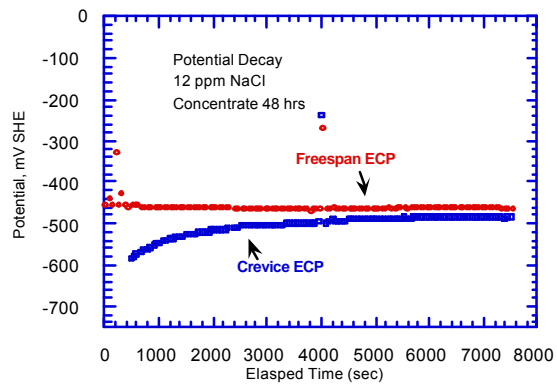
**Feedwater with 40 ppm NaOH**

| Time | $E_{crv}$ (SHE) | $E_{bulk}$ (SHE) | $\Delta E$ | pH (MULTEQ) | pH (ECP) |
|------|-----------------|------------------|------------|-------------|----------|
| 2.5 hrs | -780 mV | - 690 mV | 90 mV | 10.1 | 9.1 |
| 5 | - 820 | - 680 | 140 | 10.15 | 9.6 |
| 16 | - 830 | - 640 | 190 | 10.4 | 10.0 |

**Results**

**1. Crevice ECP Decreases with Concentrating Time**
- **Suggests Increase in pH**

**2. Difference between pH values calculated by MULTEQ (extraction results) & from ECP decrease as concentration time increases**
- **Volume occupied by steam decreases as hideout increases**
- **Volume of bulk liquid drawn into crevice after heat flux removed is greater**

# BENCHMARKING ECP MEASUREMENT METHODOLOGY
## Molar Ratio

Potential Decay
12 ppm NaCl
Concentrate 48 hrs

Freespan ECP

Crevice ECP

Potential, mV SHE

Elasped Time (sec)

Potential Decay
12 ppm NaCl + 11 ppm NH$_4$Cl
Concentrate 48 hrs

Crevice ECP

Freespan ECP

Potential, mV SHE

Elasped Time (sec)

- **Na/Cl Molar Ratio = 1**
  - **Crevice ECP > Bulk ECP**
  - **Implies Crevice pH > Bulk pH**
  - **Implies Hideout Efficiency Cl$^-$ < Na$^+$**
  - **Na = 0.34  Cl = 0.36**
    **Na/Cl Molar Ratio = approx 1**
  - **Implies Hideout efficiency Cl$^-$ & Na$^+$ same**

**Reference electrode in the center of the crevice.**
**Is there a Na/Cl concentration gradient in the crevice?**
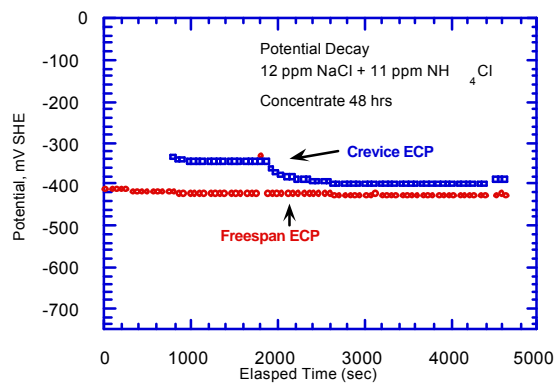
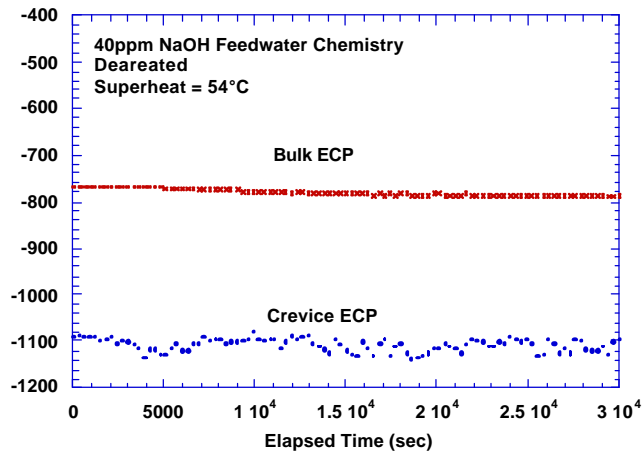- **Na/Cl Molar Ratio = 0.2**
  - **Crevice ECP< Bulk ECP**
  - **Implies Crevice pH< Bulk pH**
  - **HOR Results not yet available**

116

# BENCHMARKING ECP MEASUREMENT METHODOLOGY
## Magnetite Packed Crevice

---

– **Feedwater: Deaerated with 40 ppm NaOH**
– **Thermal Conditions: 340°C tube/280°C bulk**
– **Crevice packed with magnetite: 78% density**
  * **Apparently becomes "mud"**
– **Once through flow, 2l/min**



- **Bulk pH = 8.2 EPRI for 40 ppm NaOH**
  - **From EPRI Computer code, MULTEQ**
- **Crevice ECP is 320 mV less than bulk ECP**
  - **Implies crevice pH = 10.9 since 118mV/pH unit**
- **Places tube section in crevice in caustic cracking zone**

117
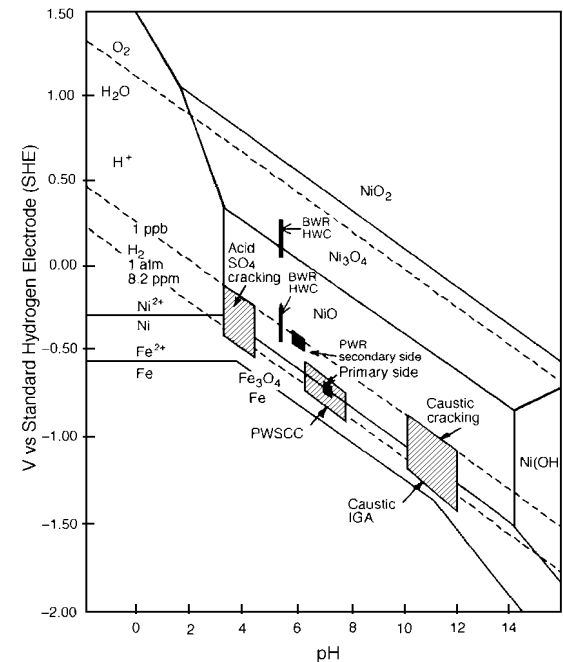
# Heat Transfer Crevice Program/Electrochemical Noise

- **Current fluctuations measured**
  - **Between Alloy 600 tube and Alloy 600 TSP**
  - **Use zero resistance ammeter**
- **Measure potential fluctuations**
  - **Between Alloy 600 tube and Ag/AgCl reference electrode Or Ni wire reference electrode**



- **Feedwater: Deaerated with 40 ppm NaOH**
- **Thermal Conditions: 340°C tube/280°C bulk**
- **Crevice packed with magnetite: 78% density**
  - **\* Apparently becomes "mud"**
- **Once through flow, 2l/min**
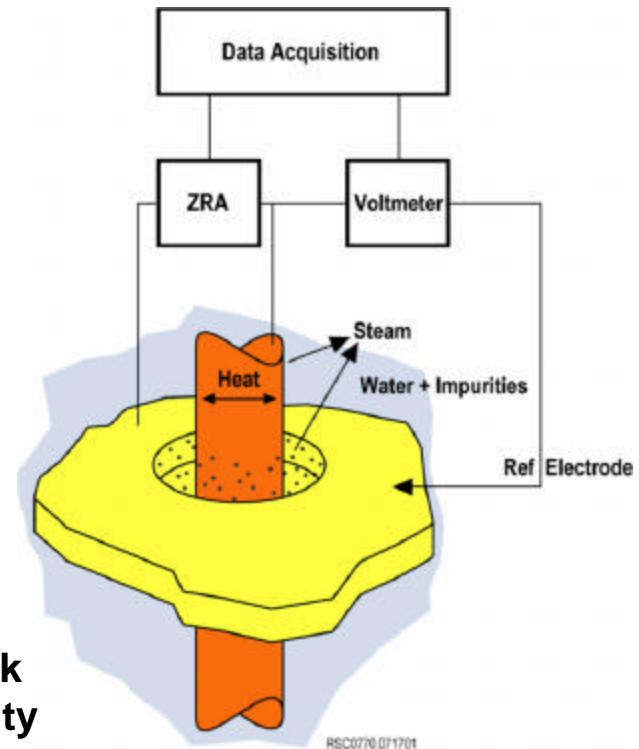
# Heat Transfer Crevice Program/**Electrochemical Noise**
### Noise intensity related to pressure (SCC?)

## Tube Pressurized @ 3000 psia
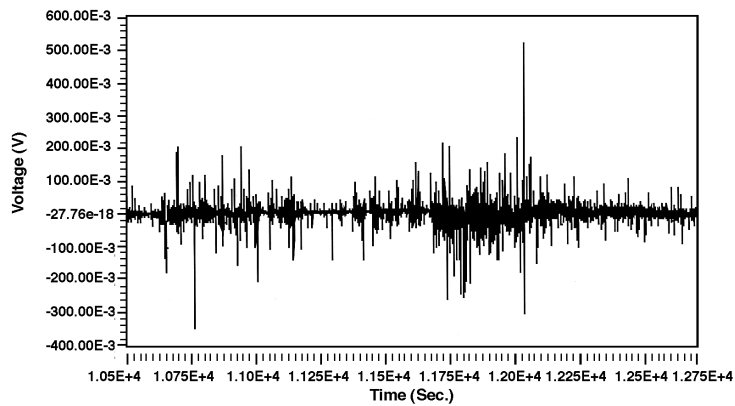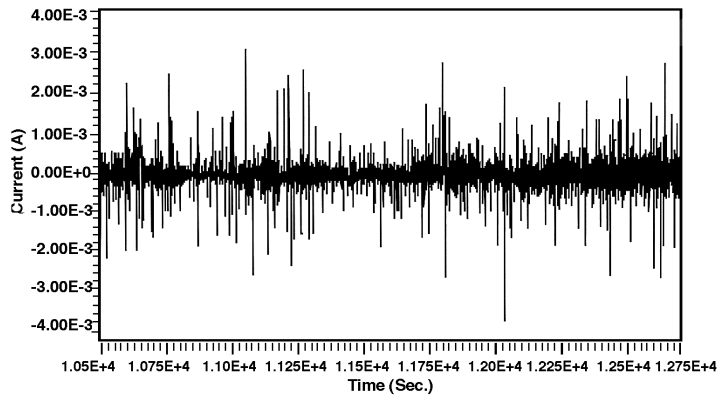


## Tube Depressurized



Current Noise
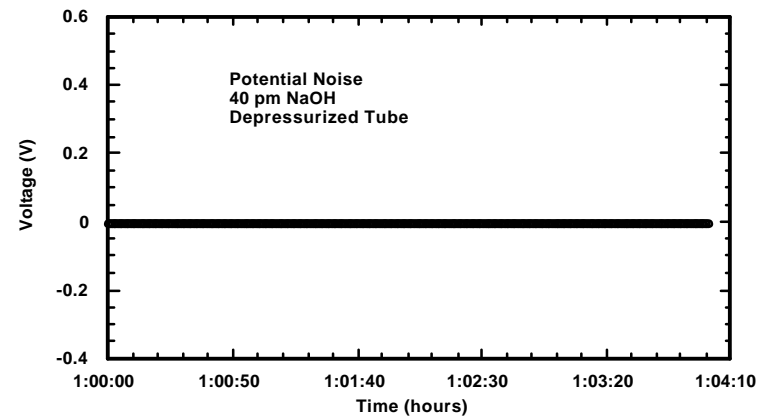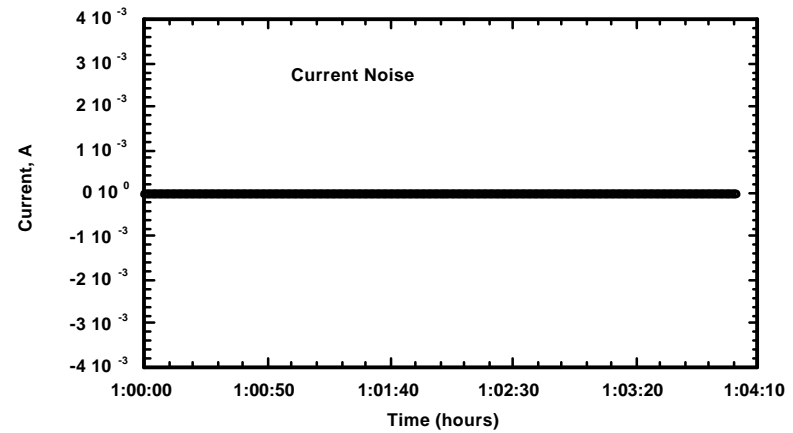
Potential Noise
40 pm NaOH
Depressurized Tube

## Effect of Chemistry on Crack Initiation
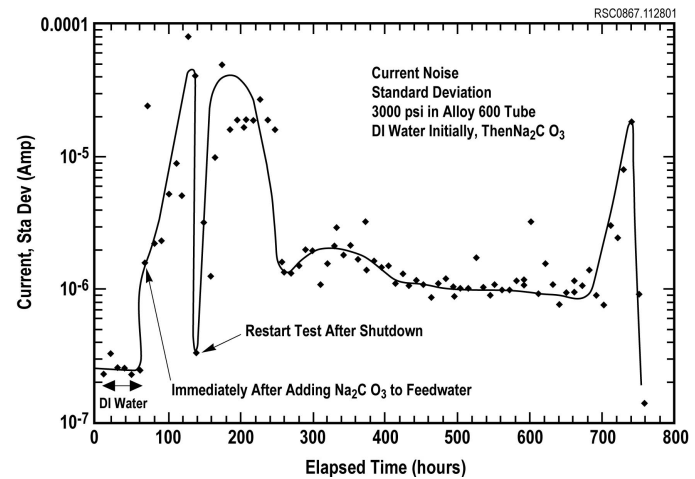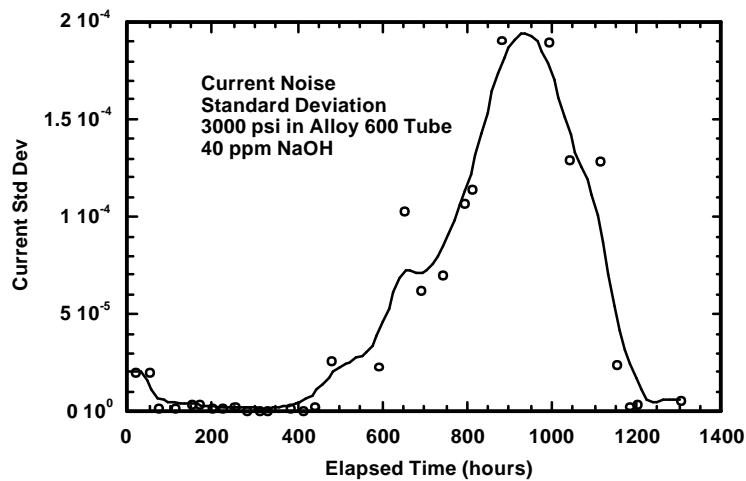
# Heat Transfer Crevice Program/baseline



Crack

Crack cut from tube

Rotated 180°
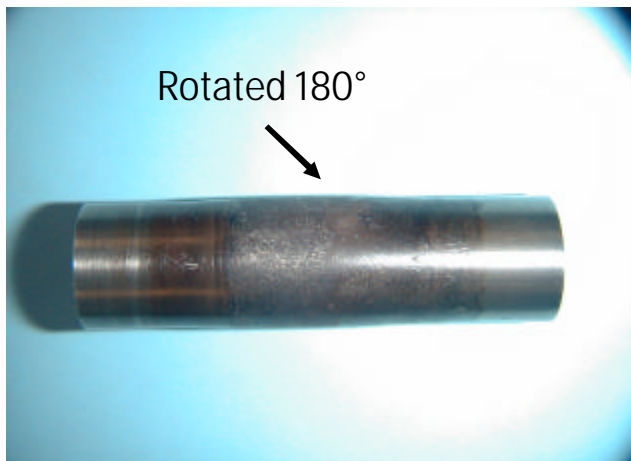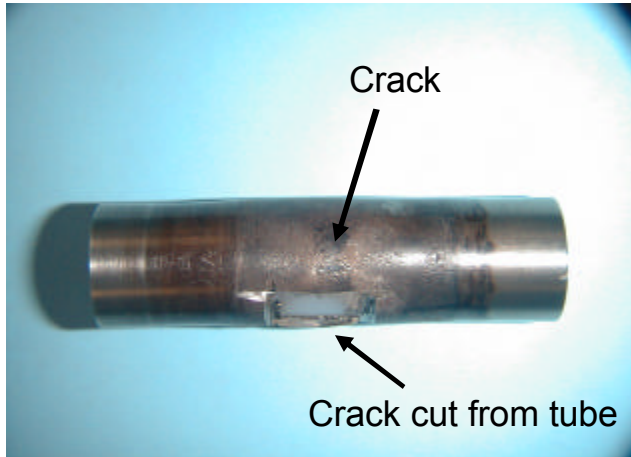
- **Crevice Section Expanded**
- **Compressed polymer Plug**
- **Opened cracks for observation**

# Heat Transfer Crevice Program

- **Regions of IGA**
  - **Uniform**
  - **Shallow**
- **Localized SCC**
  - **Deep penetrations**
  - **Intergranular**



122
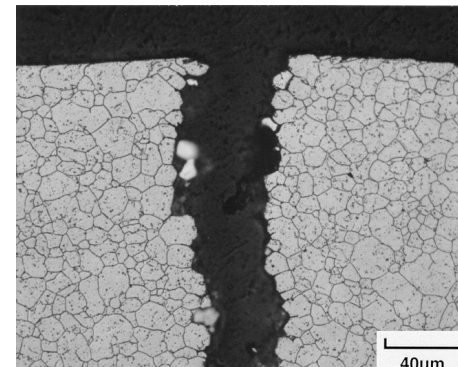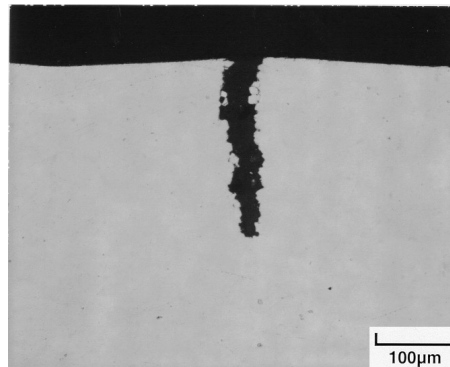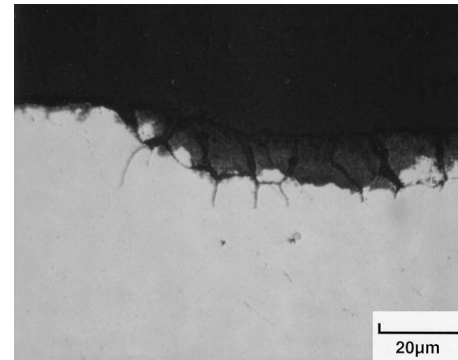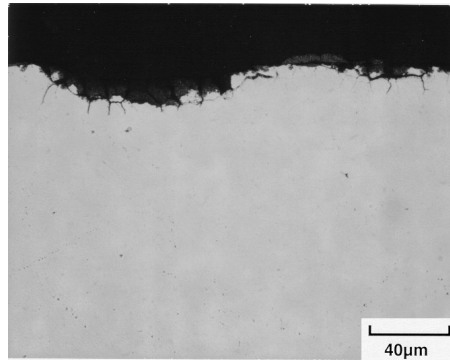
# Heat Transfer Crevice Program

- **Scanning electron microscopy view of fracture face**
  - **Intergranular with secondary cracks**
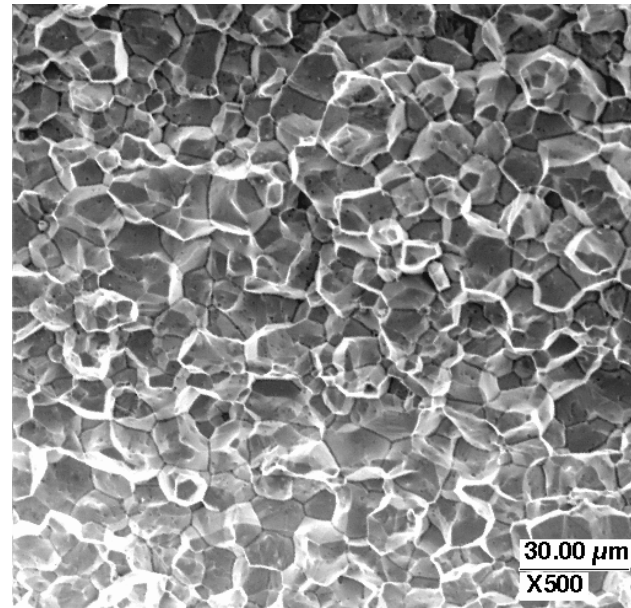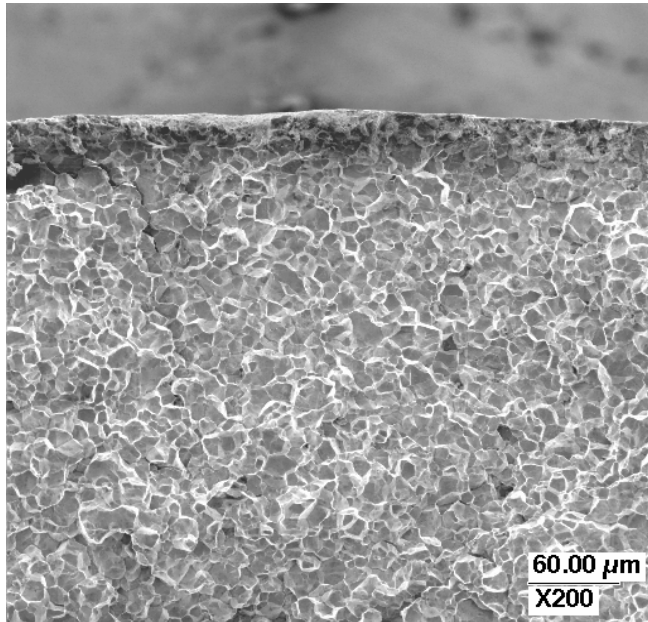
# Heat Transfer Crevice Program

- **Oxide film decreases in thickness as crack tip approached**
- **Ni enriched on surface, Negligible Na on fracture face**

# Raman Spectroscopy



**Laser** Incident Light · Scattered Light · Sample

**Liquid or solid**
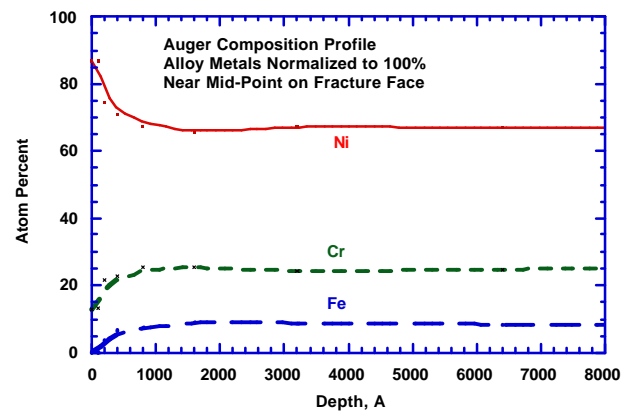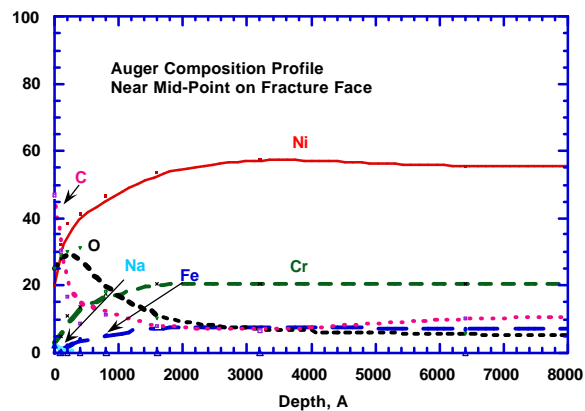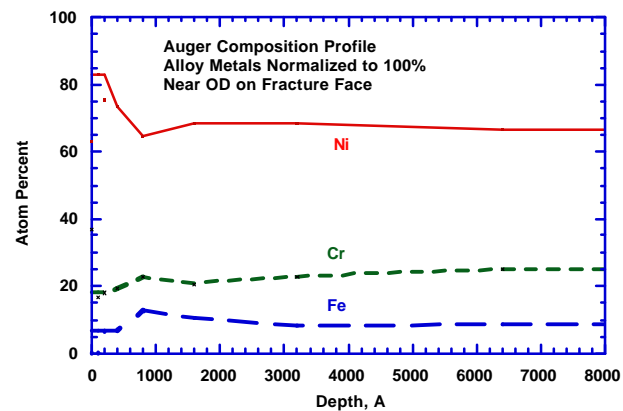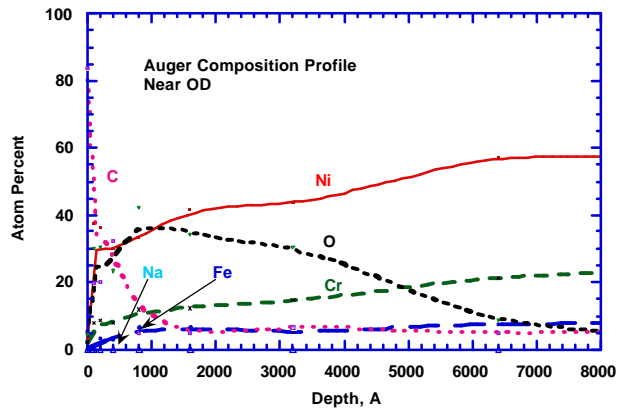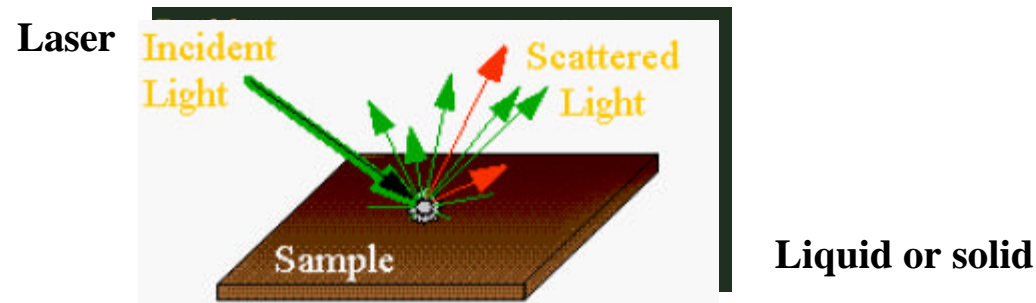
**Two Types of Scattered Light**

**Same wavelength as incident light**
**Different wavelength as incident light (Raman Scatter)**

$E_i$ energy of incident light
$E_s$ energy of Raman scattered light
$E_v$ energy of molecular vibration state
$E_s = E_i - E_v$ (visible range)

# Raman Spectroscopy
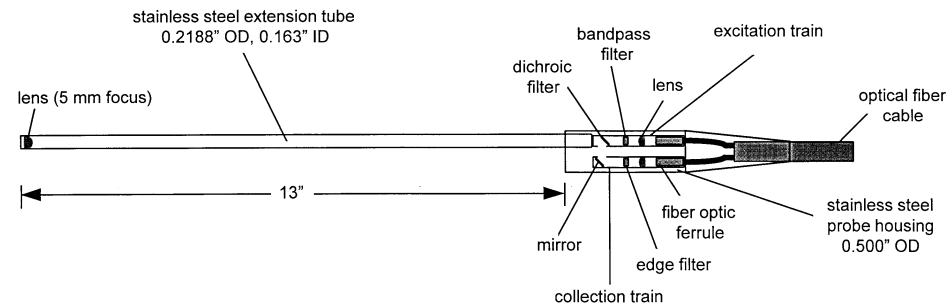


- **Designed uniquely for the heated crevice**
- **Stainless steel tube for light path**
- **Variable focal point for the laser exciting light and coincident collection point for the signal**
- **Filters at end of probe to remove "stray" light scattered from the incident laser beam**
- **Fiber optics from probe to spectrometer**

# Raman Spectroscopy



**Diamond Window**



Optics
Chamber

Autoclave Fitting
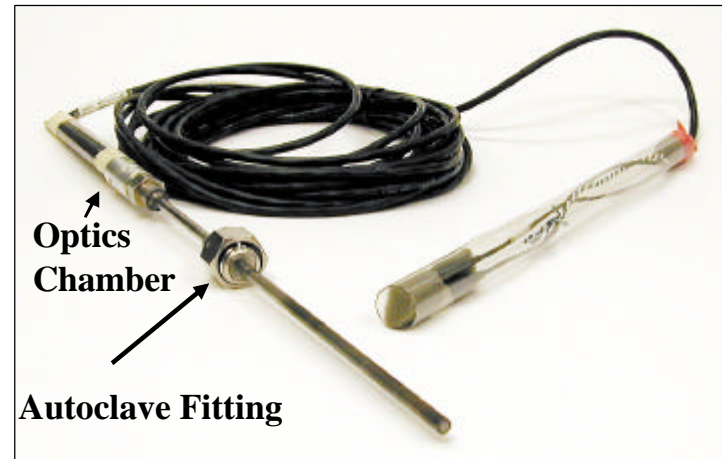
**Probe/Fiber Optic Cable**

# Raman Spectroscopy

## Effects of Temperature on the Water Line
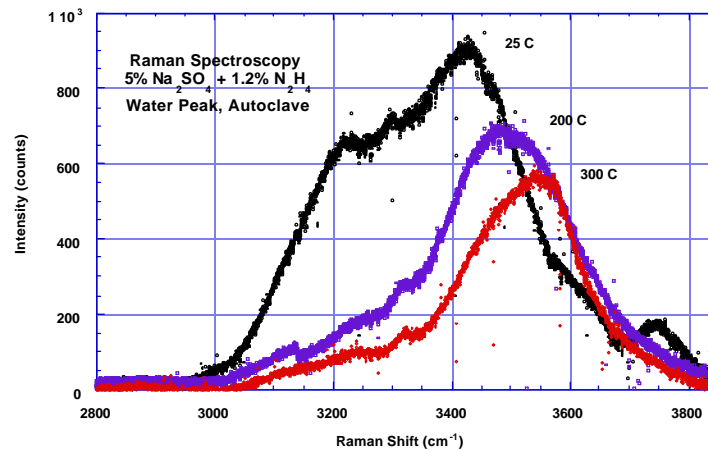


- **H-bonding causes a distribution of O-H bond strengths and vibration freq.**
  - **Causes broadening at room temperature**
- **Increase in temperature decreases H-bonding**
  - **Causes line to narrow**
  - **Increases O-H bond strength leading to shift to higher frequencies**
- **Decrease in density of water at high temperatures leads to intensity decrease**

# Raman Spectroscopy

- **Development work uses closed bottom crevice**
    - **No deposits needed for hideout**
    - **Hideout is the same, kinetics are different**
- **Next step will use packed Tube/TSP-type crevice**
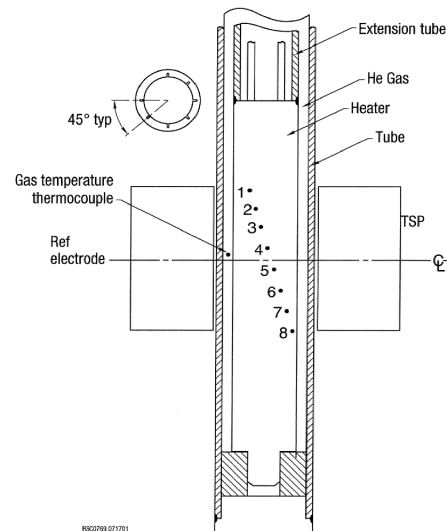
# Closed Bottom Heated Crevice/Thermal- Hydraulics

**Temperature of Tube Wall at Various Elevations in the Crevice During Hideout**
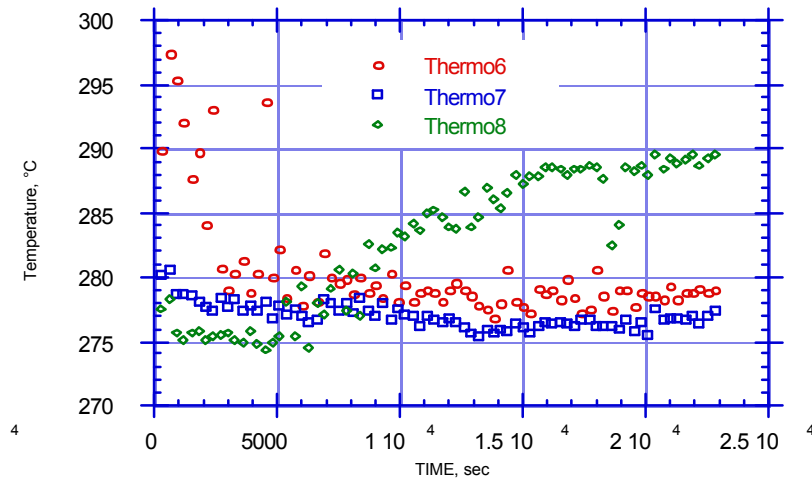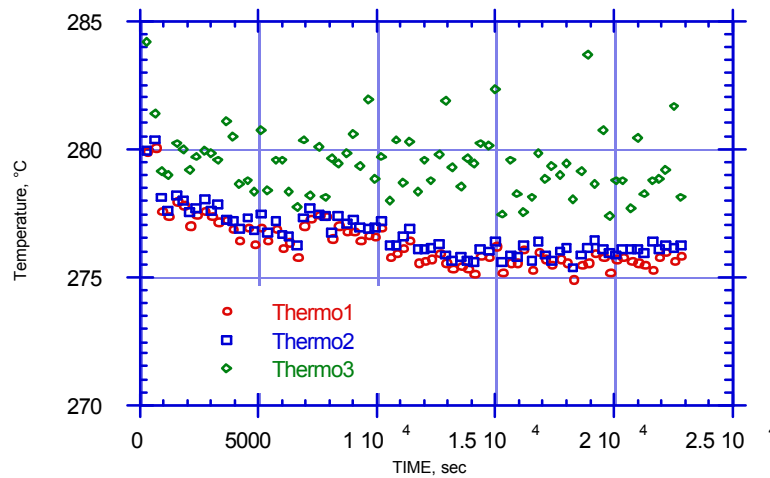


- **Boiling at locations 1, 2, & 3**

- **Steam blanketed to boiling at 6**
  - **Boiling to fully wetted at location 8**
    - **Indicated by increase in temp**

**Extraction Results--25.2 w/o**
**MULTEQ gives 27°C BPE**
**Measured BPE - 22°C  $T_{SAT} = 270°C$**

# Raman Results-Caustic

## First Raman Results from the  Heated Crevice (closed bottom)
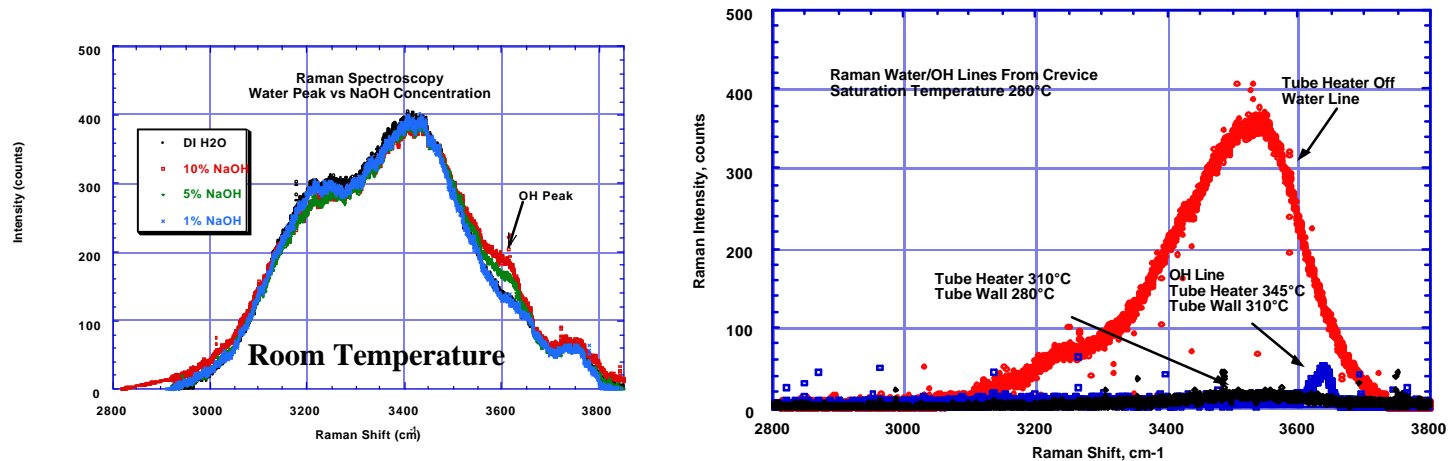


- **At a saturation temperature of 280°C with tube heater off**
  - **Water line same as static autoclave results**
- **At low super heats, no Raman lines from the crevice**
  - **Steam blanketed**
- **He heat transfer gas at 345°C, average wall temperature at 310°C**
  - **Hydroxide line, no water line**
  - **MULTEQ gives 25w/o NaOH for a boiling pt. Elevation of 30°C**
- **Every water bound to NaOH**

# Raman Spectroscopy

## Is NaOH Molten?
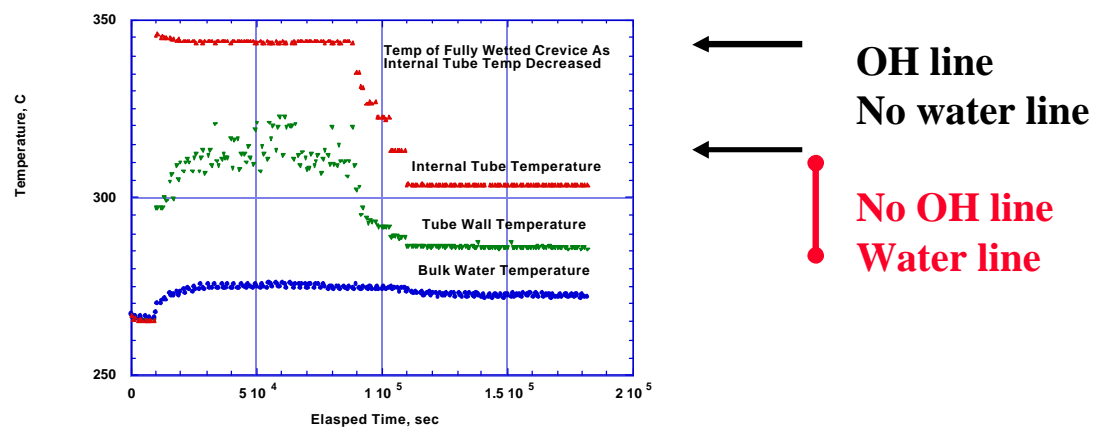


- **Temperature of He decreased in steps, 335°C, 330°C, 325°C, 320°C, 315°C, 305°C**
    - **Raman spectrum OH line until 305°C**
- **Wall temperature did not change until interior temperature was 305°C**
- **Water line appeared at 305°C**
- **Suggests region of Raman probe fully wetted**

# Raman Spectroscopy

**Is NaOH Molten, melting point is 318°C?**
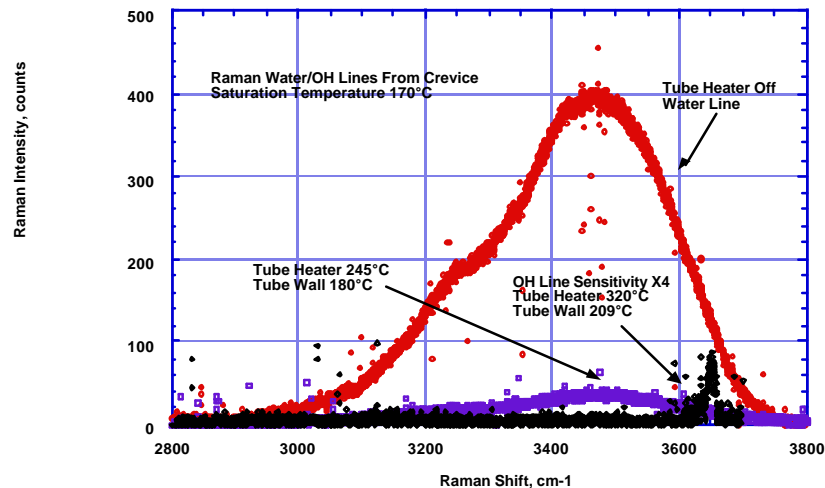


- **Pressure lowered to give a saturation temperature of 170°C**
- **At 170°C with tube heater off, water line**
- **When He temp below 209°C, no Raman signal from the crevice**
- **At a He temp. of 209°C, hydroxide line appeared, same as 280°C $T_{sat}$**
- **Suggests OH line from concentrated NaOH solution, not molten**

Room Temperature Measurements

solid NaOH

solid KOH

Arbitrary Y / Raman Shift (cm-1)

File # 1 : 21102B_SOLID NAOH_532NM_100S

532.201, 100000, solid NaOH 532nm 100 sec w/o Bkg Sub

Overlay Z-Zoom CUR

Res=0.4 cm

134
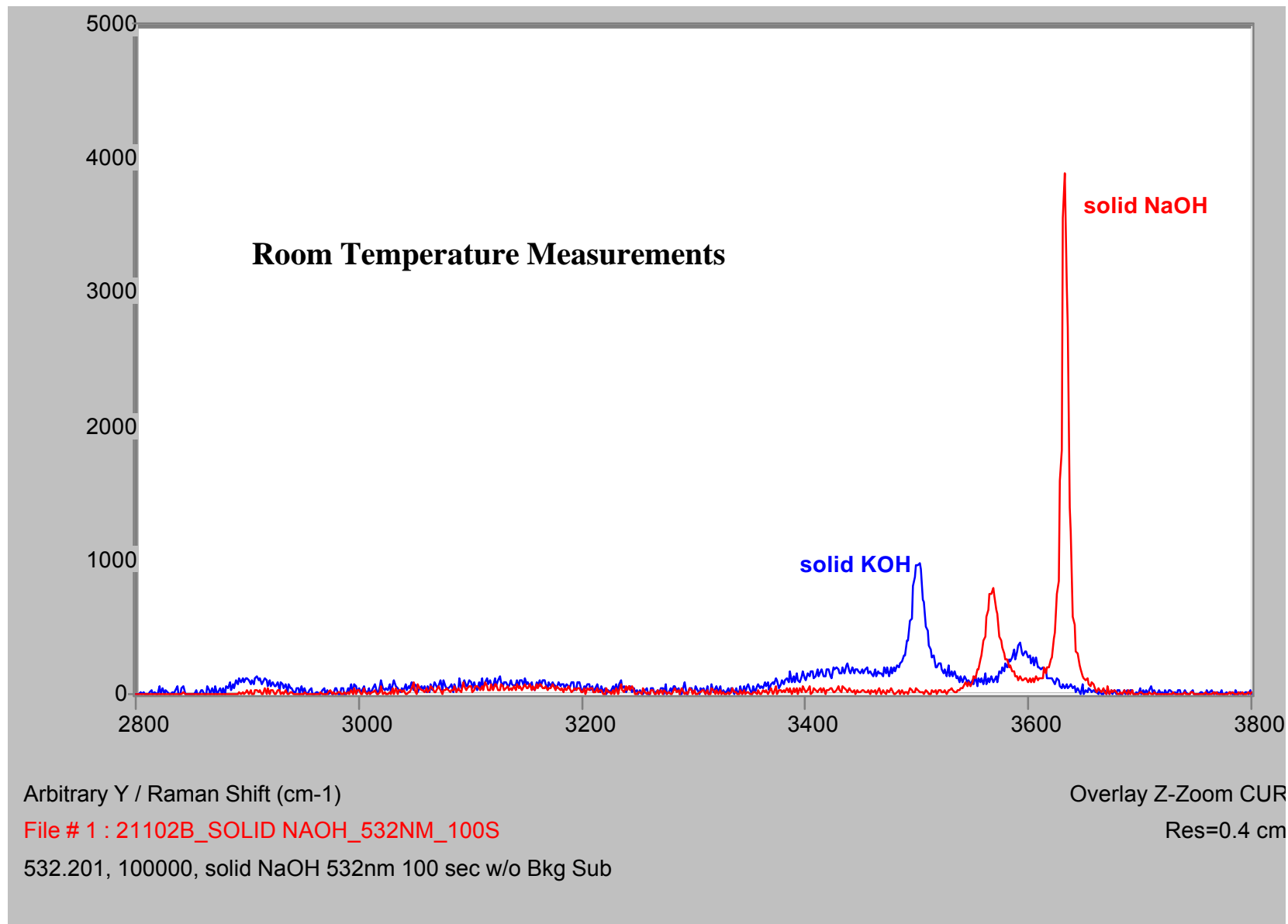
# Raman Spectroscopy

Raman spectroscopy ideally suited to investigating build up of deposits and precipitates in crevices

**Do the high impurity concentrations in the feedwater of a heated crevice correctly accelerate processes occurring in plants?**

- **Sodium hideout results in lab experiments linearly extrapolate to results from identical system installed in Ohi Nuclear Power Station**
- **IGA/SCC pattern, chemistry of OD film and fracture face are similar to observations from examinations in pulled tubes**
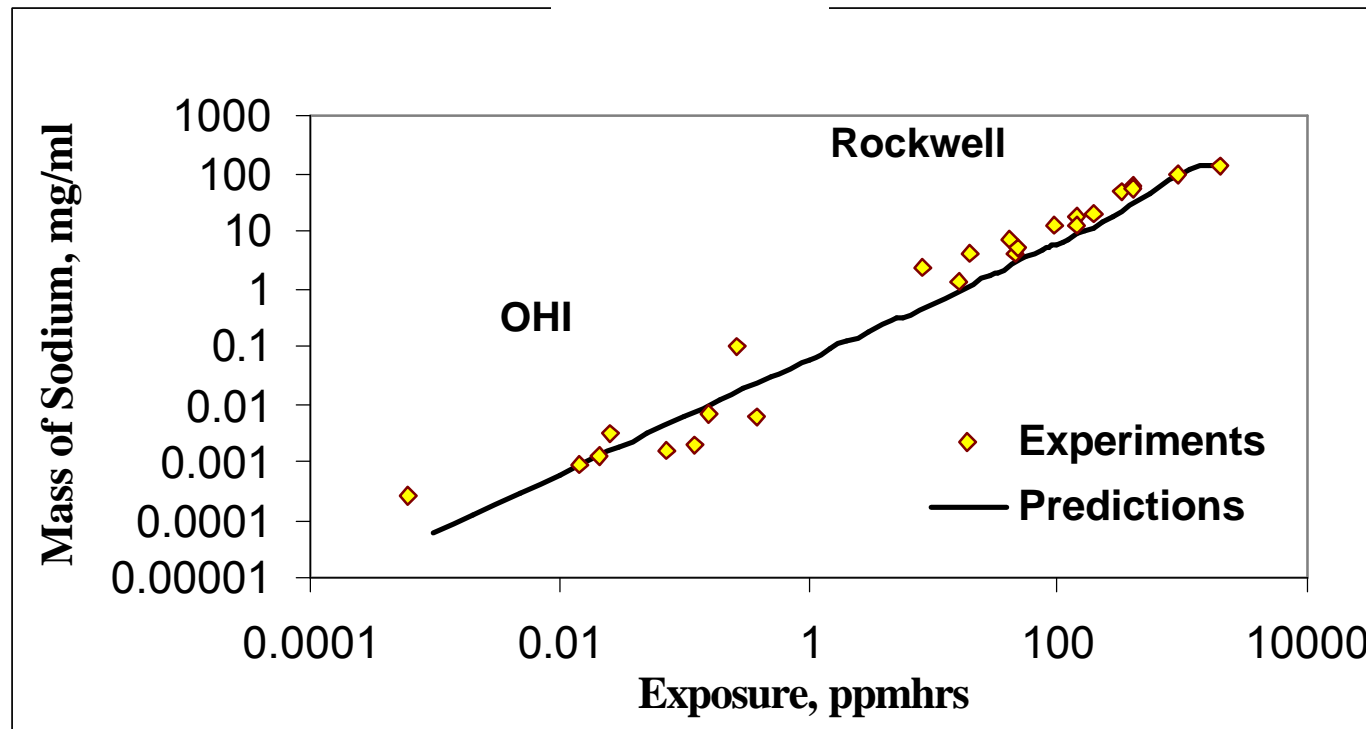
# Experimental Simulation of Crevice Chemistry Evolution

Chi Bum Bahn, Si Hyoung Oh, and Il Soon Hwang
Seoul National University

October 7-11, 2002
Argonne Guest House, ANL

# Outline

- Introduction
- Literature Review
- Goals & Approach
- Experimental System
- Results & Discussion
  - Open Crevice Test
  - Packed Crevice Test
- Summary & Conclusions

# Introduction

- In a locally restricted SG geometry, such as tube/TSP crevice, tubesheet crevice, or sludge pile, trace impurities in the bulk water can be concentrated by boiling processes to extreme pH.

- These concentrated solutions may then cause ODSCC/IGA, which is the one of the primary degradation mechanisms.

- In order to find the mitigation method for tube degradation in crevice, the understanding of boiling crevice phenomena must be advanced.
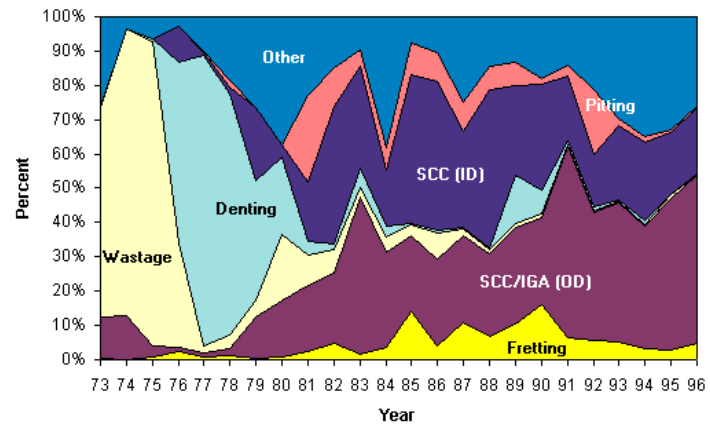
**Worldwide Causes of Tube Plugging**
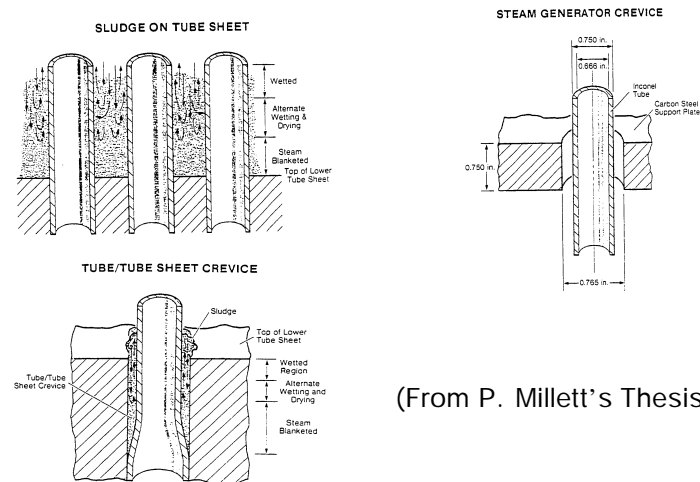
(From P. Millett's Thesis)

139

# Literature Review
## Thermal-hydraulic Aspects

| Author | Year | Experiment | Pressure Condition | Crevice Geometry | Packing | Heating Method | Control Method |
|---|---|---|---|---|---|---|---|
| M. K. Jensen | 1977 | Boiling heat transfer and CHF in annular geometries | Atmospheric | Horizontal TSP | Open | Electrically heated tube | q" |
| A. Baum | 1980 | Dryout and chemical concentration in confined geometries | High (5.5 MPa) | TSP | Open | Electric heater | q" |
| A. Baum | 1981 | Boiling heat transfer in porous bodies | High (5.5-7.6 MPa) | Tubesheet | Sludge Packed | Flowing water | ΔT |
| Y. Kozawa | 1982 | Alternate drying and rewetting of heat transfer surface | Atmospheric | Planar Tubesheet | Open | Flowing water | ΔT |
| S. Aoki | 1982 | Boiling phenomena within a narrow gap | Atmospheric | TSP & Tubesheet | Open | Electric heater | q" |
| S.-C. Yao | 1983 | Boiling heat transfer Boiling regimes thru visual observation | Atmospheric | Tubesheet | Open | Electrically heated tube | q" |
| Y. Chang | 1983 | CHF of narrow vertical annuli | Atmospheric | Tubesheet | Open | Electrically heated tube | q" |
| S. Tieszen | 1986 | Boiling regimes thru visual observation | Atmospheric High(1.5 MPa) | TSP | Open | Flowing water | ΔT |
| G. M. W. Mann | 1987 | NaCl hideout and return in heated crevices | High(6.4 MPa) | TSP | Carbon fiber packed | Electric Heater | q" & ΔT |
| J.-L. Campan | 1988 | Na hideout studies as a function of various parameters | High (~5.5 MPa) | TSP & Tubesheet | Magnetite packed | Flowing water | ΔT |

140

# Literature Review
## Electrochemical Aspects

| Author | Year | Experiment | Pressure Condition | Crevice Geometry | Packing | Heating Method | Control Method |
|--------|------|-----------|--------------------|------------------|---------|----------------|----------------|
| R. E. Hermer | 1988 | A600 ECP measurement by using 0.01 M KCl Ag/AgCl | High (5.5 MPa) | TSP | Sludge packed | Flowing water | $\Delta T$ |
| F. Damien | 1991 | Sodium & boric acid hideout with electrochemical impedance spectroscopy | High (6.4 MPa) | TSP | Open | Flowing water | $\Delta T$ |
| A. M. Brennenstuhl | 1997 | Electrochemical noise measurement to monitor the effects of chemical excursions on the corrosion response of A 800 | High (5.5 MPa) | Tubesheet | Magnetite packed | Electric heater | $\Delta T$ |
| J. Lumsden | 1997 1999 | NaCl hideout studies with ECP & temperature measurement | High (5.5 MPa) | TSP | Diamond Packed | Electric heater | $\Delta T$ & q" |
| H. Kawamura | 1999 | Na concentration factor measurement with high temperature conductivity cell | High (5.5-6.4 MPa) | TSP | Open | Flowing water | $\Delta T$ |
| A. Baum | 2001 | Crevice chemistry evaluation by measuring temperature, impedance, and pH difference | High (3.3 MPa) | TSP | Magnetite packed | Flowing water | $\Delta T$ |
| On-Site Model Boiler Test | | | | | | | |
| H. Takamatsu | 1991 | Direct solution sampling from crevice by using on-site model boiler | High (5.5 MPa) | Tubesheet | Open | Electric Heater | q" |

# Problem Statements

- Experimental Technique
  - Constant heat flux experiment may cause a overheated dryout area in crevice, which cannot be occurred in a real SG condition.
  - Constant temperature experiments using stagnant molten salt with an electric heater have a concern about axial temperature uniformity inside primary tubing.

- Water Chemistry Management
  - On-line crevice monitor that simulates a realistic SG crevice thermal condition and equipped with various probes, needs to be developed.

# Goals & Approach
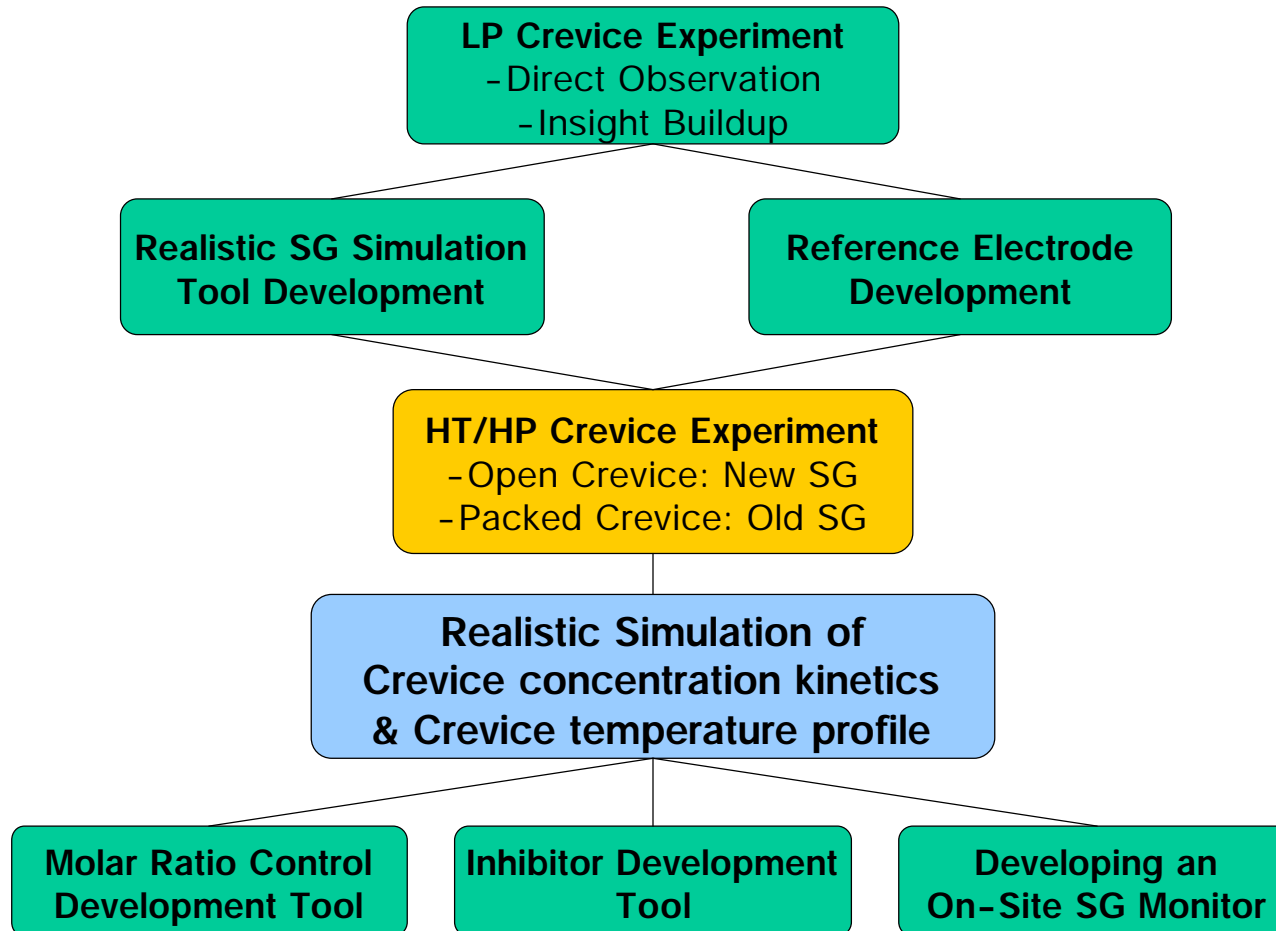
# High Temperature/High Pressure SG Crevice Simulation Experiment

- Experimental Systems
  - Two-Loop System Design for Constant $T_{primary}$ control
  - Electrode Development
- Results
  - Open Crevice Test
    - Temperature & Potential Data
    - Measured and Predicted Results
  - Packed Crevice Test
    - Temperature & Potential Data
    - Measured and Predicted Results

# Experimental
## Schematic View of Experimental System
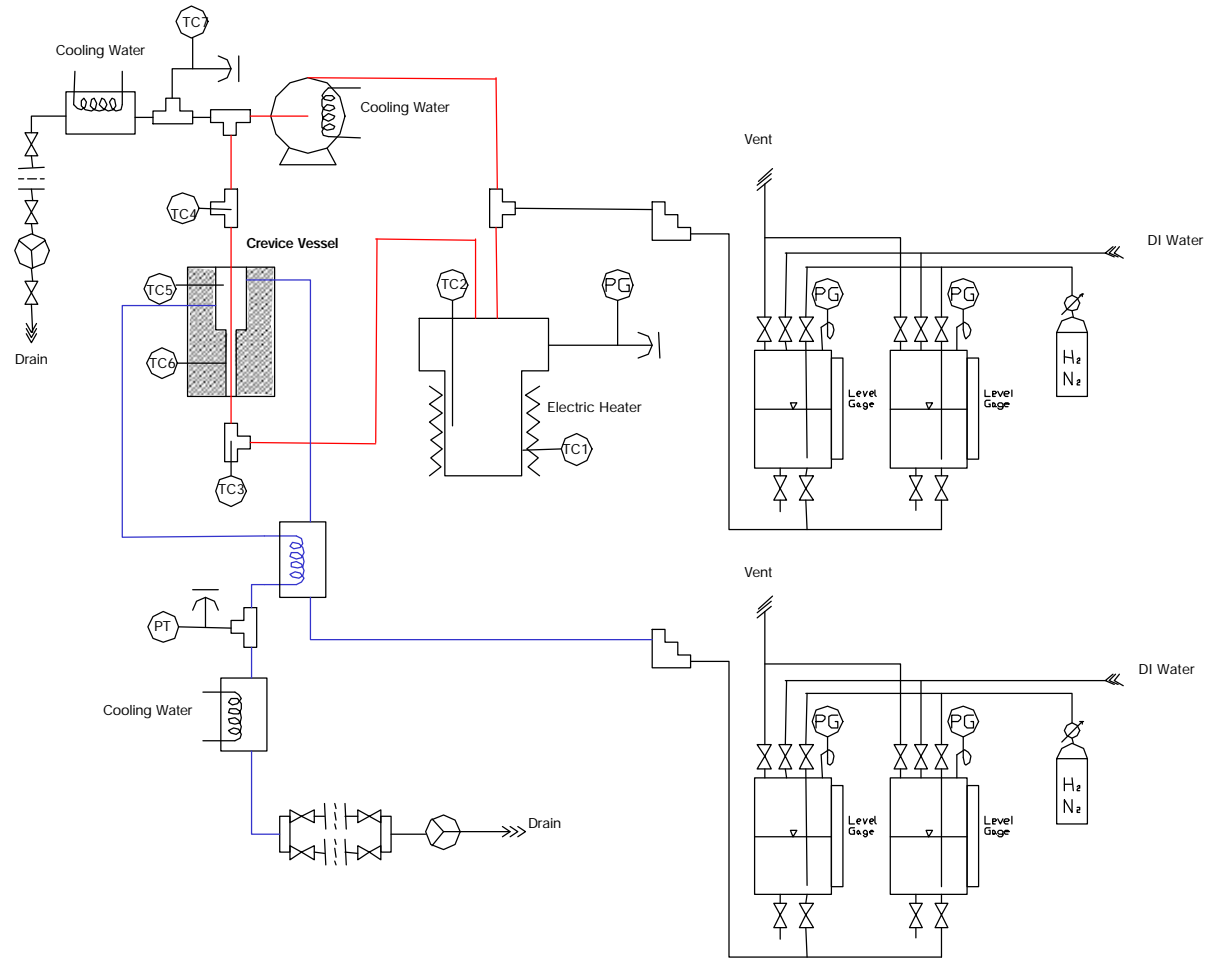
# Experimental
## Schematic View of Test Cell



Primary Outlet T/C

Compression Fitting

146mmφ

13 mm

62.5 mm

Bulk T/C #1
(70 mm from crevice mouth)

Bulk
(125 mm)

Bulk T/C #2
(30 mm from crevice mouth)

Ag/AgCl & Pt
Electrode

62.5 mm

240 mm

Crevice T/C

#1

#1: z/L=0.2
#2: z/L=0.4
#3: z/L=0.5
#4: z/L=0.6
#5: z/L=0.8

#2
#3
#4

#5

Crevice
(40 mm)

Ag/AgCl & Pt
Electrode

Ni-plated
316SS Vessel

Crevice depth: 40 mm
Crevice width: 0.15 mm

Electrolytic
Ni Plating

Conax® Fitting

3/4" OD Tubing

Primary Inlet T/C

# Experimental
## Monitoring Parameters

- Chemical & Electrochemical Parameters
  - pH monitoring
    - Pt electrode
    - Ni–plated Tubing & Autoclave
    - Reference electrode: Ext. Ag/AgCl (Pure Water) electrode
    - Measurement of Pt electrode and Ni potential vs. Reference electrode
  - Crevice solution monitoring
    - Conductivity measurement by AC impedance (failed)
    - *Crevice solution sampling: 1/16" OD Teflon tube (future work)*
- Thermal-hydraulic Parameters
  - temperature profile with crevice depth
  - local crevice temperature variation as a function of time

# Experimental
## Ag/AgCl (Water) Ref. Electrode Development
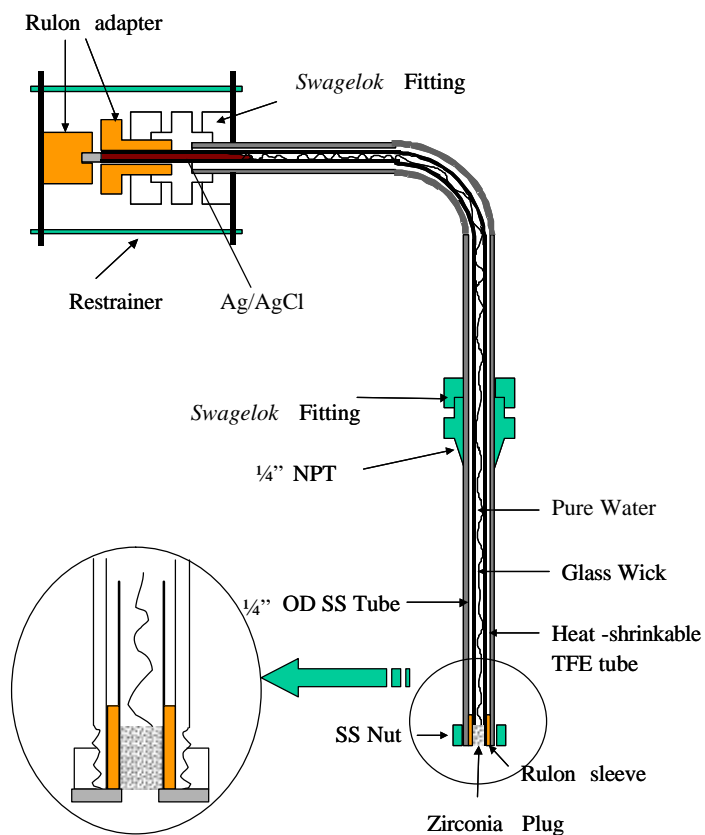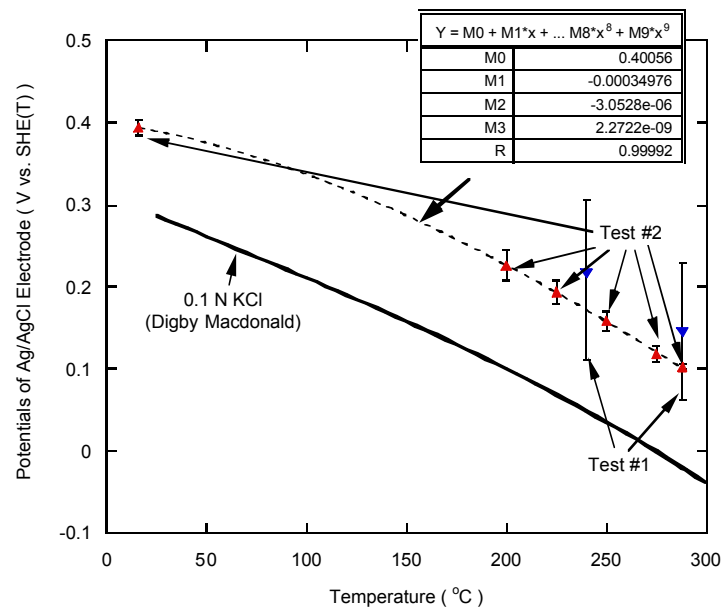
# Experimental
## Experimental Conditions

- Primary Side: Recirculating High Purity Water
- Secondary Side: Refreshed Water

|                        | Primary              | Secondary                |
|------------------------|----------------------|--------------------------|
| Temperature ($^o$C):   | max. 300             | 270                      |
| Pressure (MPa):        | 13-14                | 5.6                      |
| Flow Rate (L/hr):      | ~2000                | ~4                       |
| Water Chemistry:       | $H_2O$               | $H_2O$/NaOH              |
| ECP:                   | reducing($H_2$)      | reducing($H_2$)          |
| Crevice Materials:     | NA                   | open/packed(magnetite)   |

Experiment & Control:   Fully Computerized System

# Results
## Open Crevice Test

Axial Temperature Profile at a Steady States
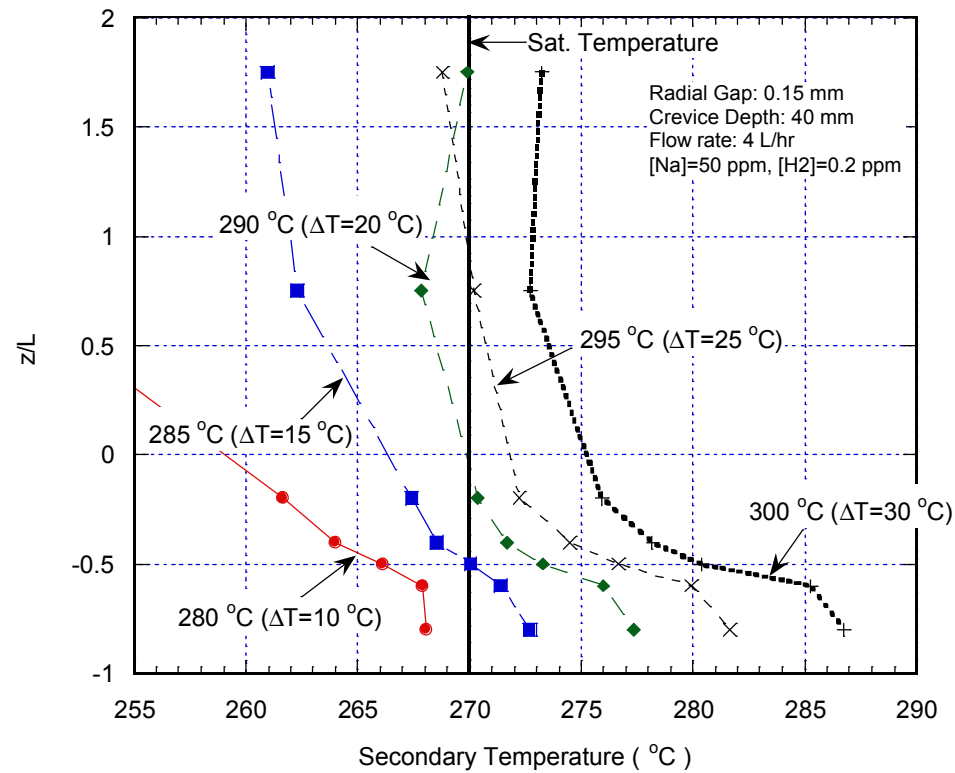
# Results
## Open Crevice Test

Local Temperature Variation with Time ($\Delta T=25$ °C)
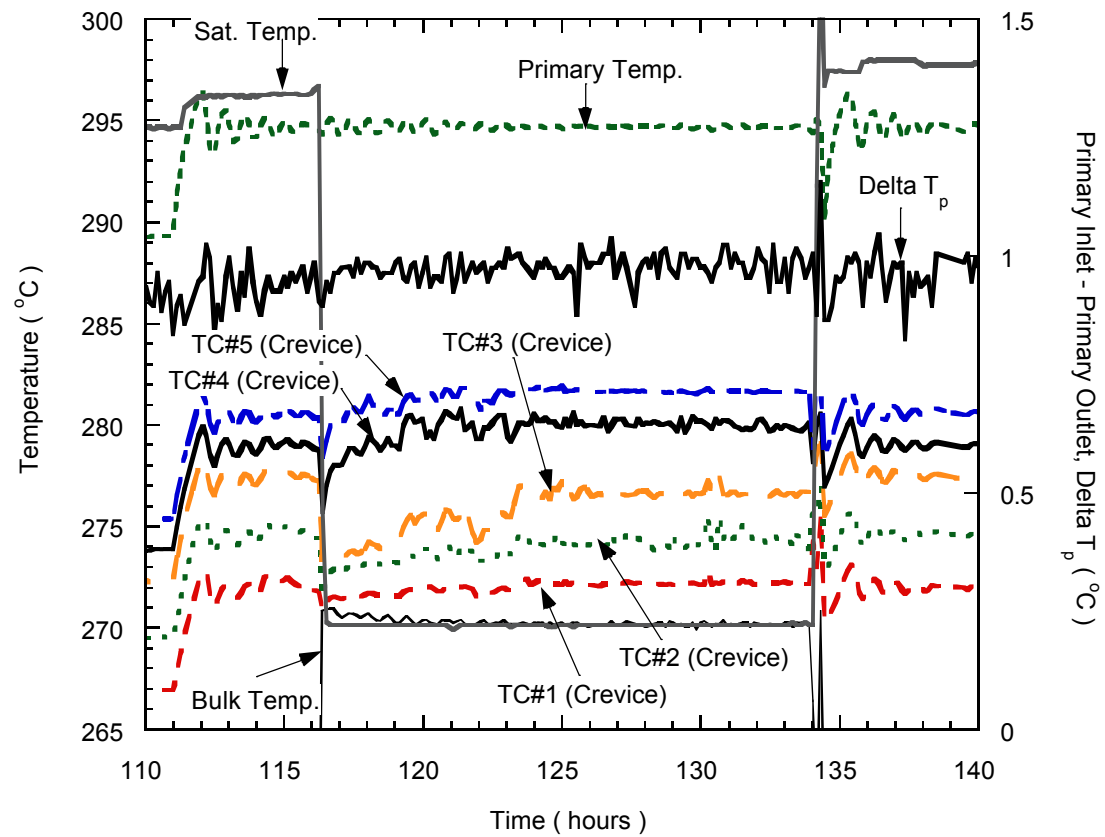
# Results
## Open Crevice Test

Bulk & Crevice Potential Variation with Time ($\Delta T = 25\ ^oC$)
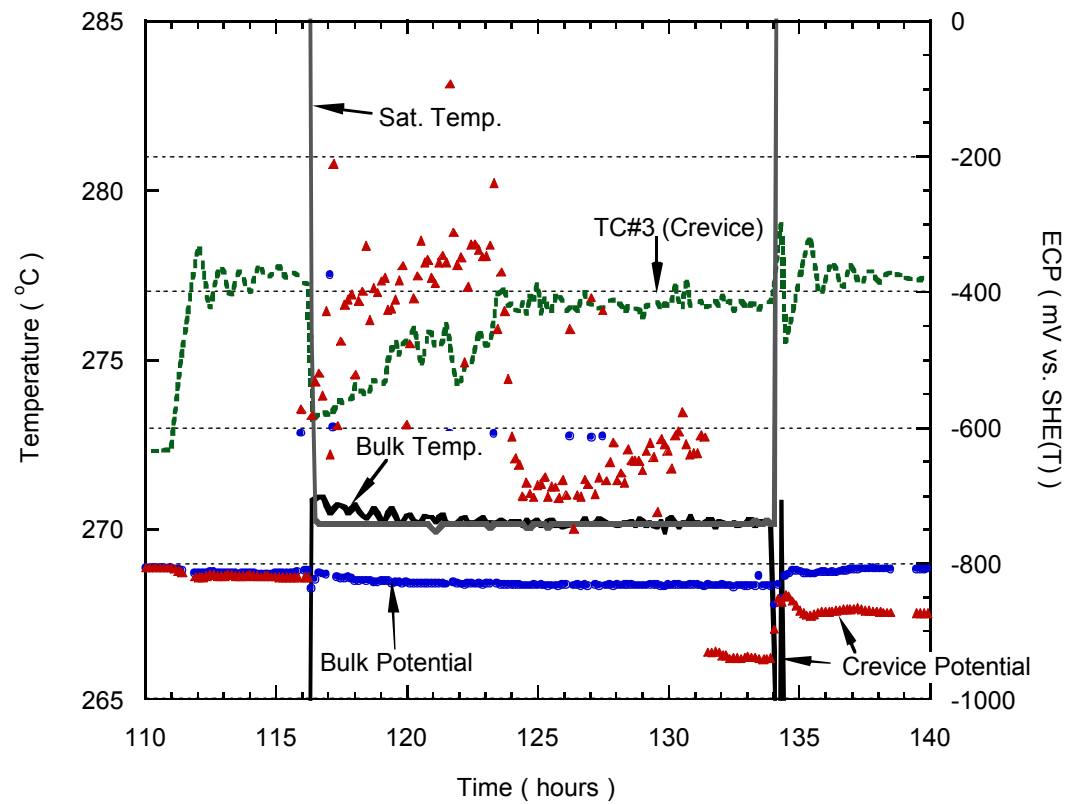
# Results & Discussion
## Open Crevice Test

**Boiling point elevation as a function of ΔT**
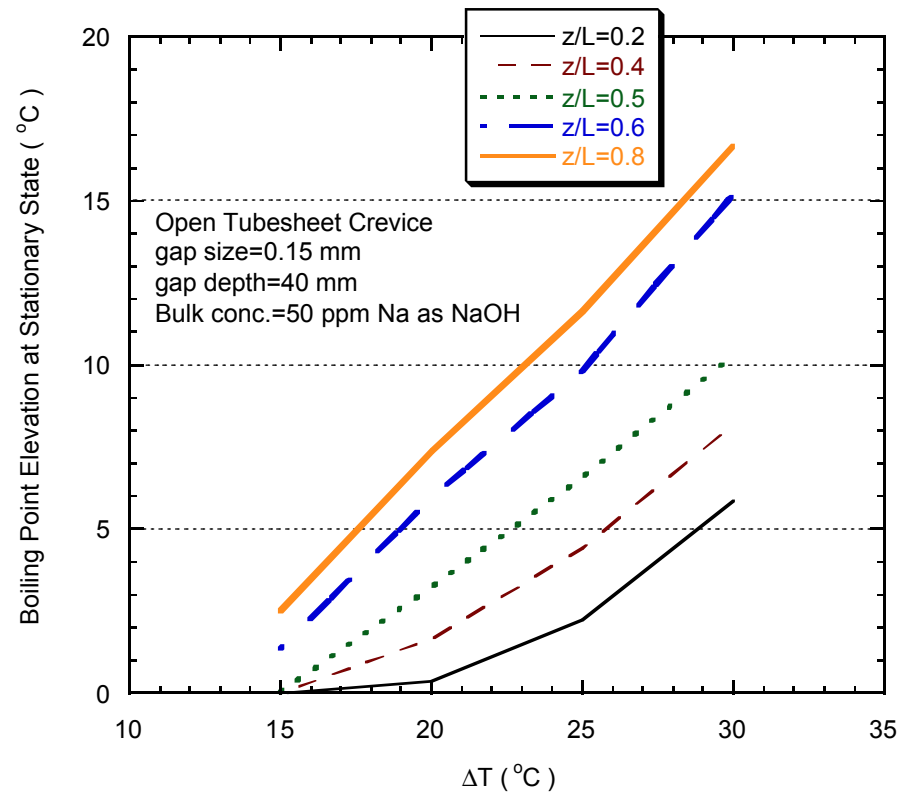
# Results & Discussion
## Open Crevice Test

Predicted solution pH and oxidation reduction potential as a function of boiling point elevation
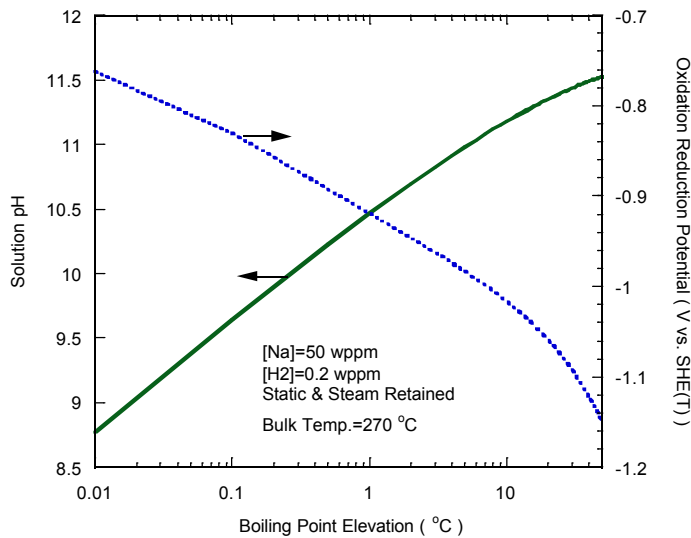
Comparison of Predicted Data with Measured Data
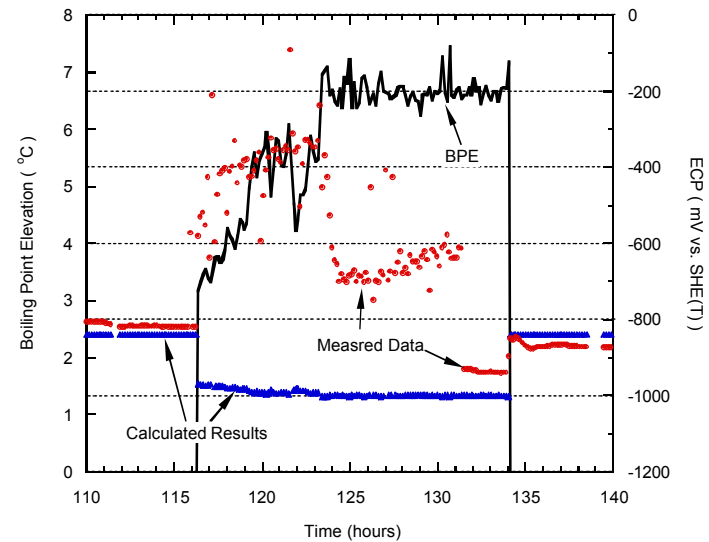
# Results
## Packed Crevice Test

Local Temperature Variation with Time ($\Delta T = 15\ ^oC$)
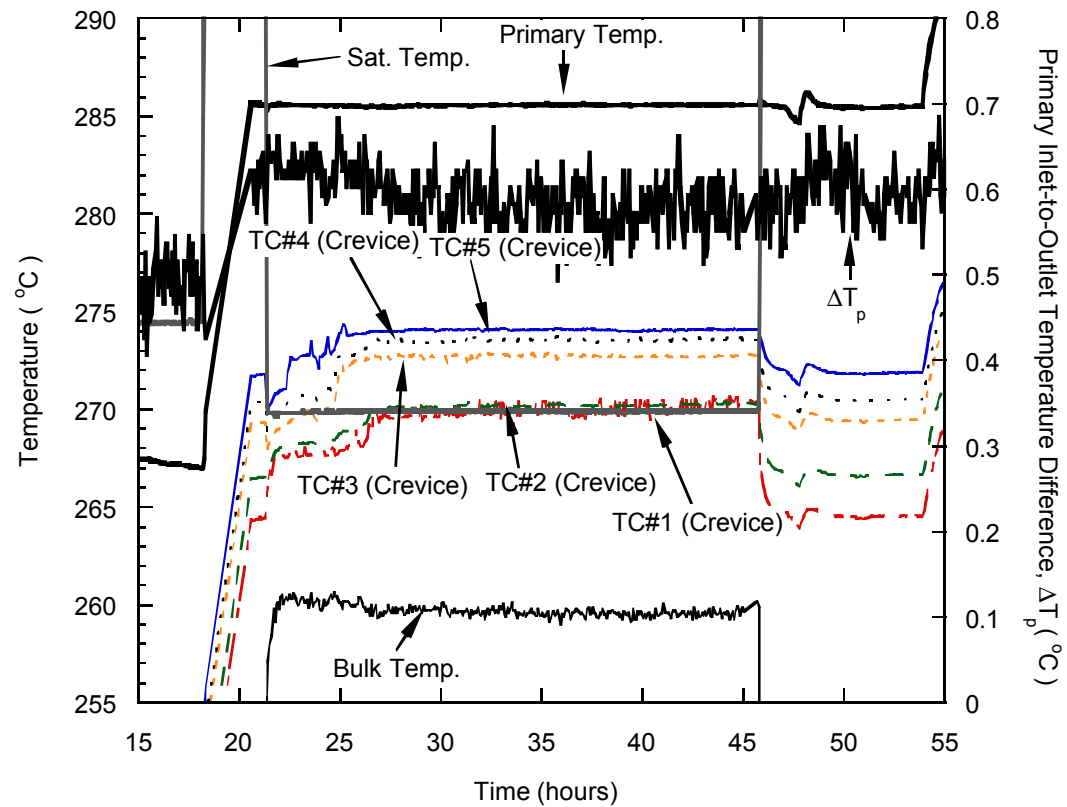
# Results
## Packed Crevice Test

Bulk & Crevice Potential Variation with Time ($\Delta T=15$ °C)
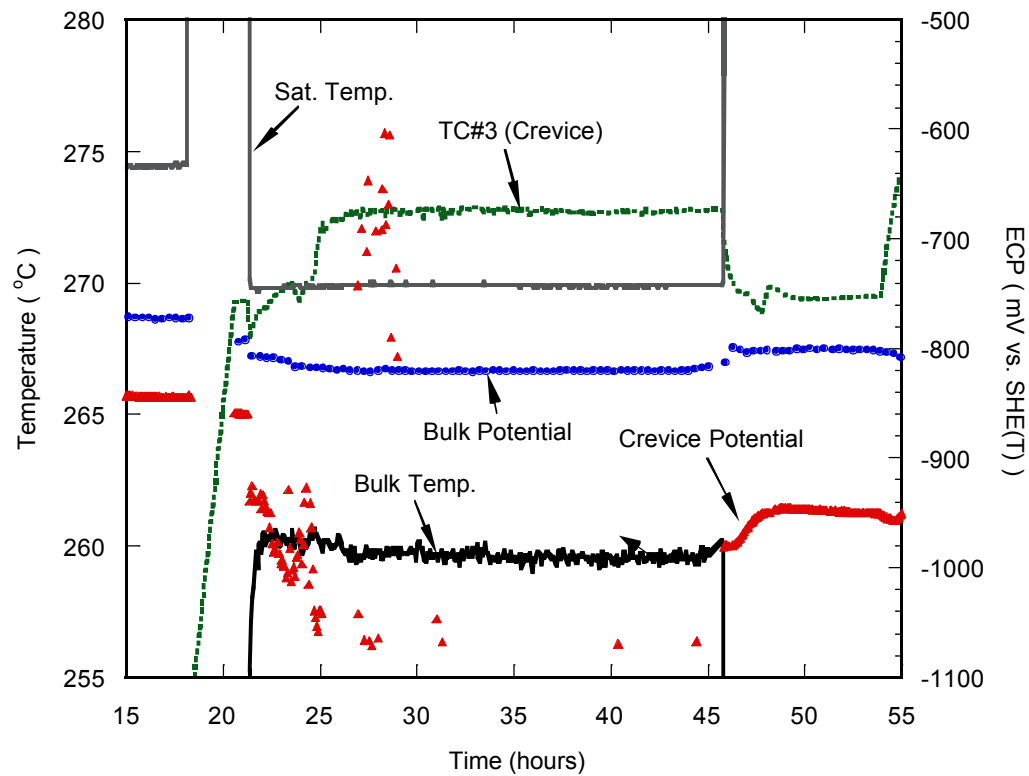
# Results & Discussion
## Comparison of Packed Crevice with Open Crevice



Axial Temperature Profiles
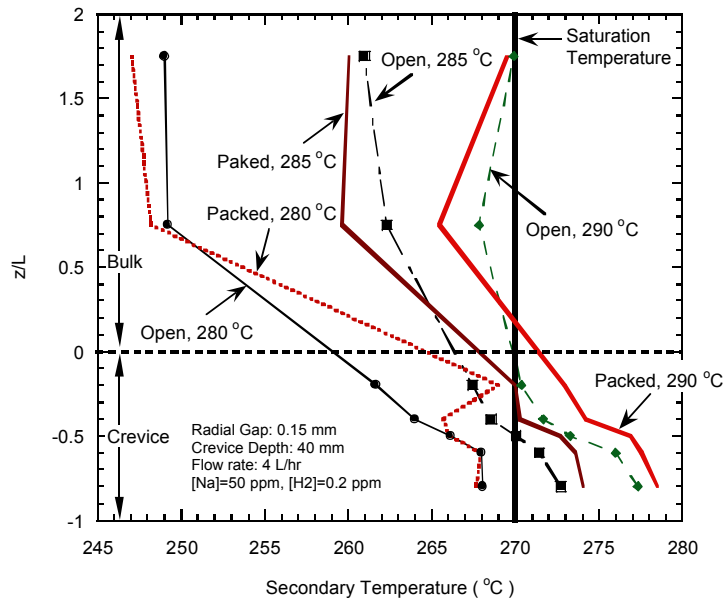
Concentration Behaviors
As a Function of Time
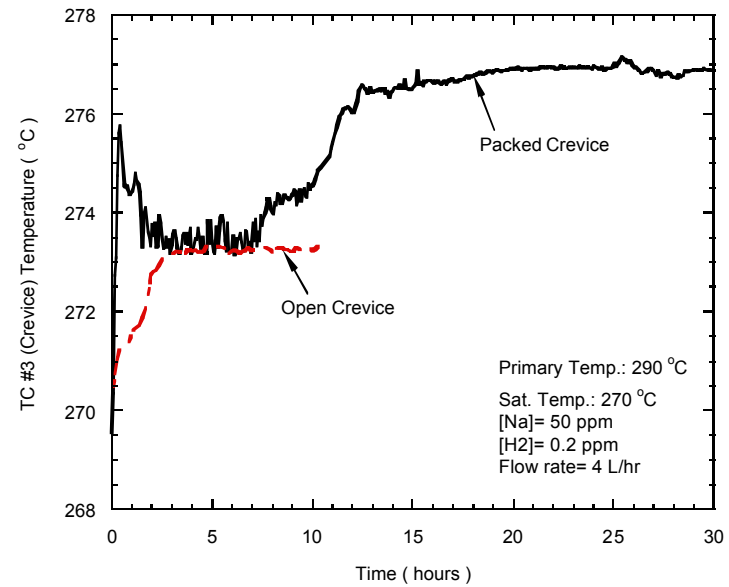
# Results & Discussion
## Measured and Predicted Potential



Comparison of Predicted Data with Measured Data
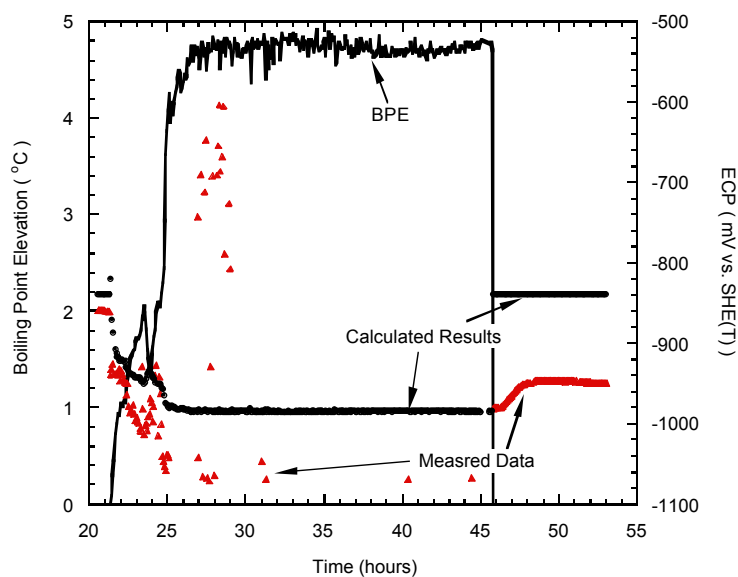
Boiling Point Elevation from Temperature Data vs. Boiling Point Elevation from Potential Data
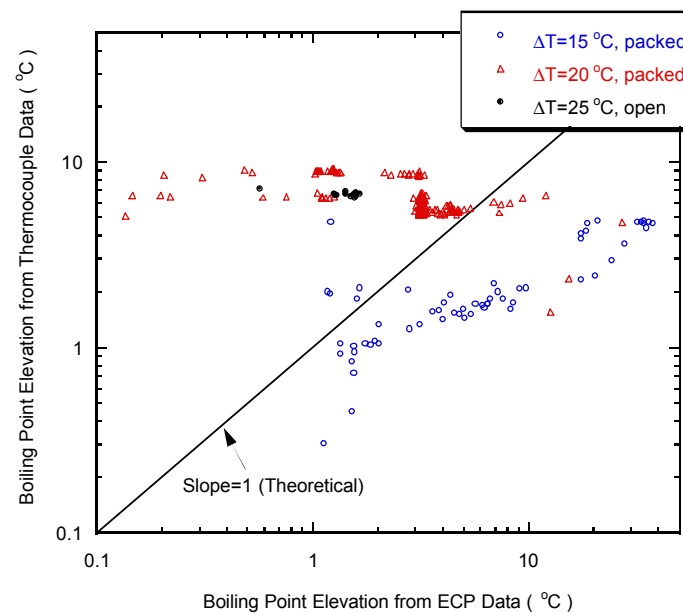
# Summary & Conclusions

- Heated crevice chemistry was studied by high temperature tests using a simulated PWR steam generator.

- Ag/AgCl reference electrode was developed for monitoring chemical concentration in the simulated SG tubesheet crevice, by using pure water as filling solution in order to solve potential drift problem.

- NaOH concentration process was confirmed in the tubesheet crevice with 0.15 mm radial gap based on temperature and electrochemical potential measurement data.

- As $\Delta T$ across the tube wall increased, the axial temperature gradient in crevice and time constant for concentration transient increased.

- A reasonable agreement was found between the measured and predicted data on the crevice potential.

- When the crevice was filled with magnetite particles, it showed the longer time constant for Na concentration and the severer concentration behavior compared with the case of open crevice.

# Experience of Heated Crevice Experiments at Studsvik

**H-P Hermansson[*], A. Molander[*]**
**P-O. Andersson[**] and H. Takiguchi [***]**

*) Studsvik Nuclear AB, SE-611 82 Nyköping, Sweden
**) Ringhals AB, SE-430 22 Väröbacka, Sweden
***) Japan Atomic Power Company, Mitoshiro Building, 1-1 Kanda-Mitoshiro-cho, Chiyoda-ku, Tokyo 101-0053, Japan

**Ringhals**
INGÅR I VATTENFALL

**Studsvik™ Nuclear**

**JAPC**

# Introduction

A facility was designed and constructed for characterization of crevice environments during realistic conditions. TSP intersections has been simulated. Crevices were open both at top and bottom.

The equipment has been used to study hideout of impurities relevant to the Ringhals 4 PWR and oxygenated conditions in PWR secondary systems, so called OWC.

A variety of testing conditions has been used. Different crevice gap and different crevice geometry have been used. The tests were carried out with or without crevice filling. The heat transfer conditions and the hydrodynamic conditions have also been varied within relatively wide conditions.

This presentation summarizes some of the results.

# Features of the equipment

Steam generator tube heated electrically or by pressurized high temperature water.

Measurements of corrosion potential, redox potential, pH and conductivity in bulk phase and in the crevice region.

Pressure drop over crevice simulated in some test by high flow recirc pump.

Temperature measurements in the SG tubing.

Crevice section easy to replace.

Different SG material has been used and TSP simulating part of both carbon and stainless steel have been used.

No crevice sampling.

# The Studsvik Loop for Heated Crevice Studies
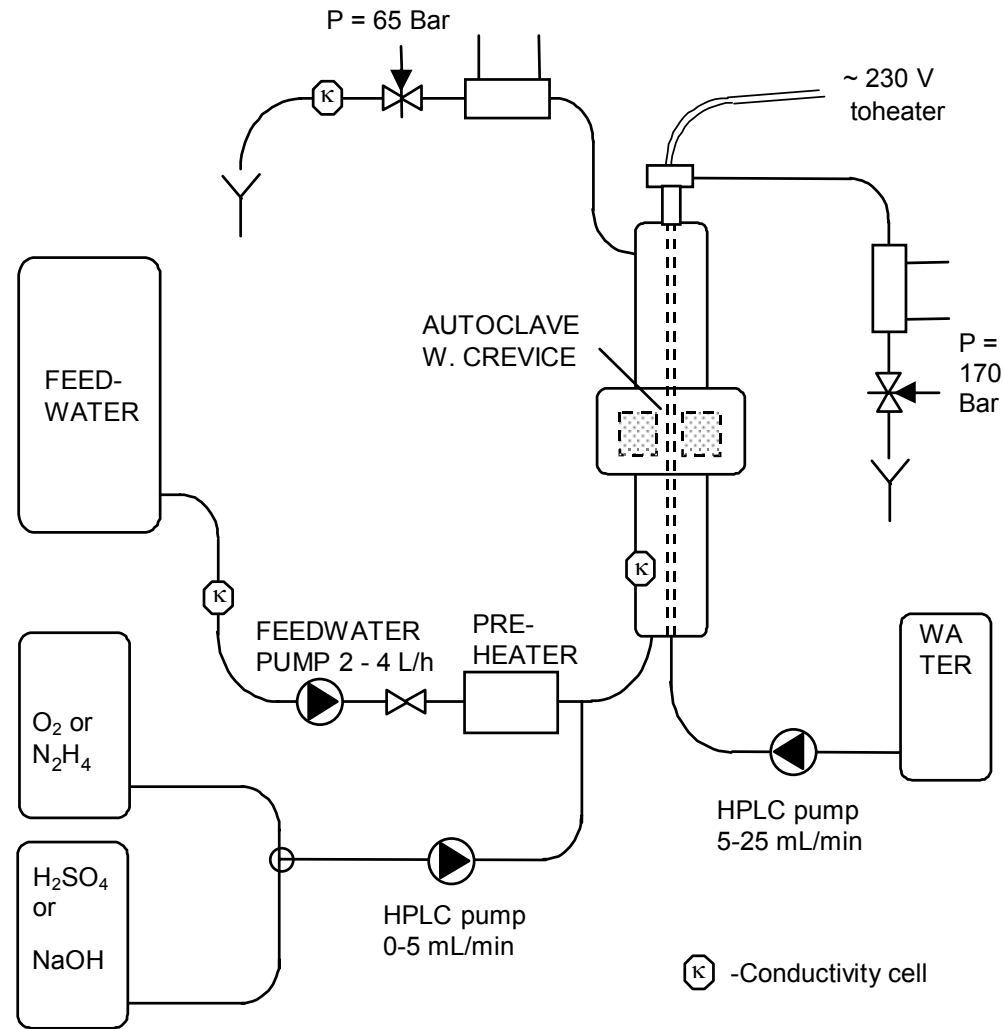


**Water heated version without high flow recirc.**

# Monitoring outside the crevice region
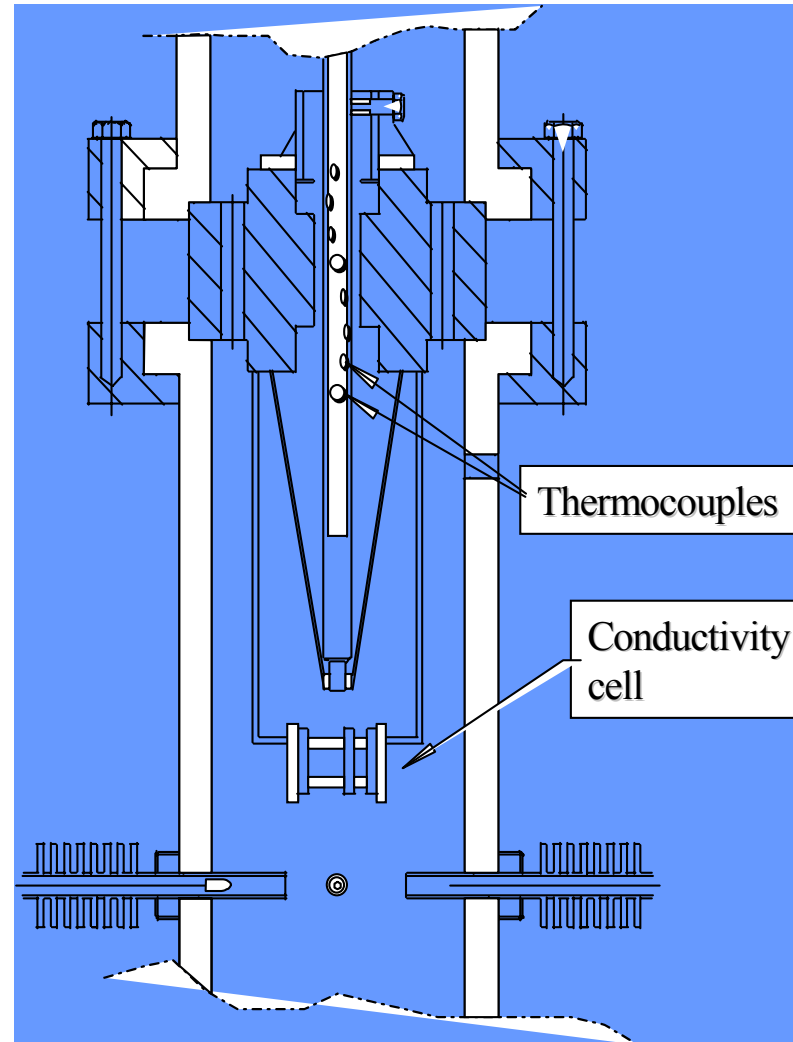
# Experimental

Steady autoclave conditions were established by boiling and decrease of the water level in the autoclave.

The water level was kept constant with a "feedwater pump" controlled by the signal from a differential pressure meter keeping the water level in the autoclave constant.

Controlled small amounts of impurities were added to the bulk phase.

Hideout was measured by a conductivity decrease and potential change in the bulk phase.

Simultaneous monitoring was made in the crevice to try to follow the hideout in-situ.

# Heated Crevice Arrangement
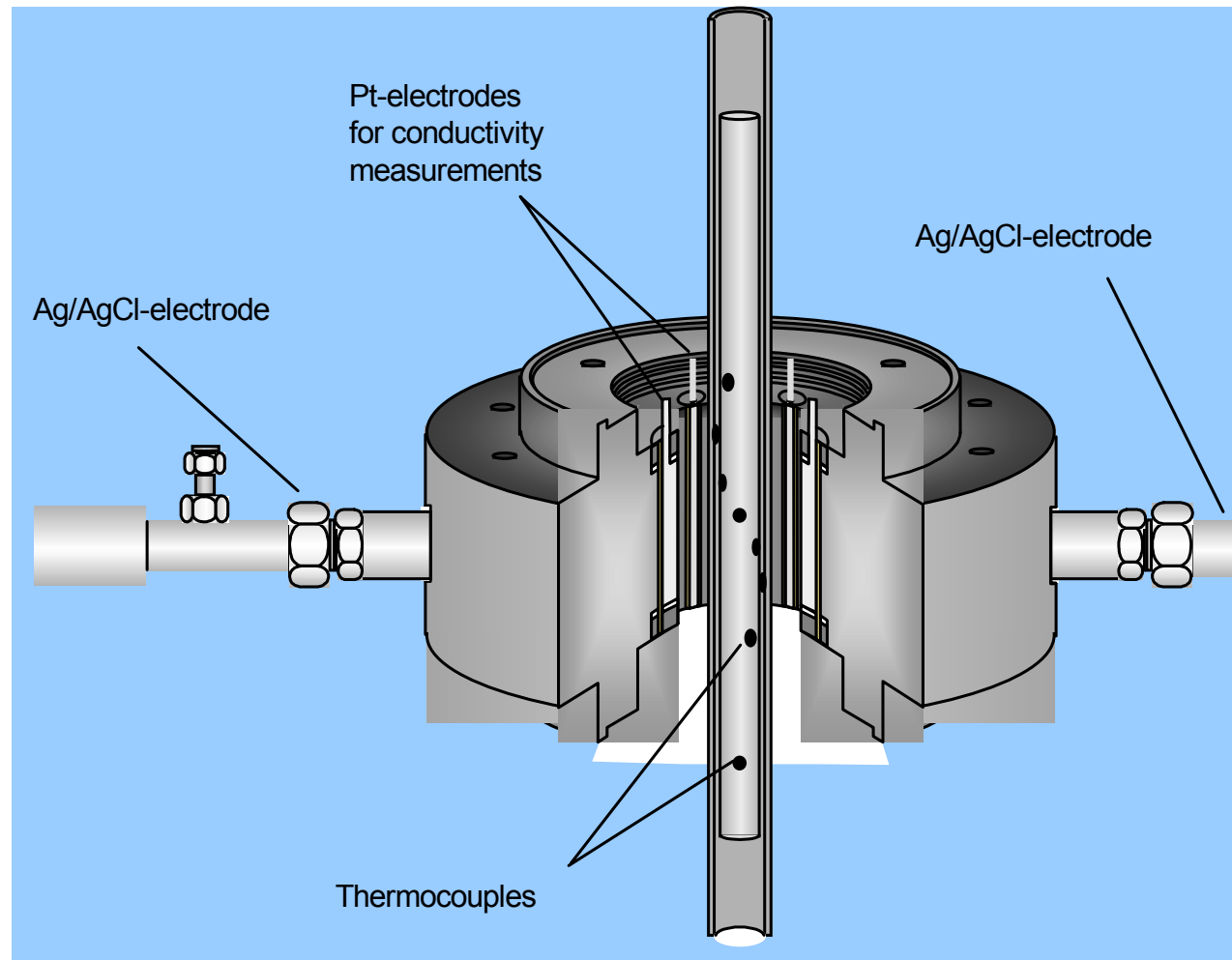
# Asymmetric filled crevice design
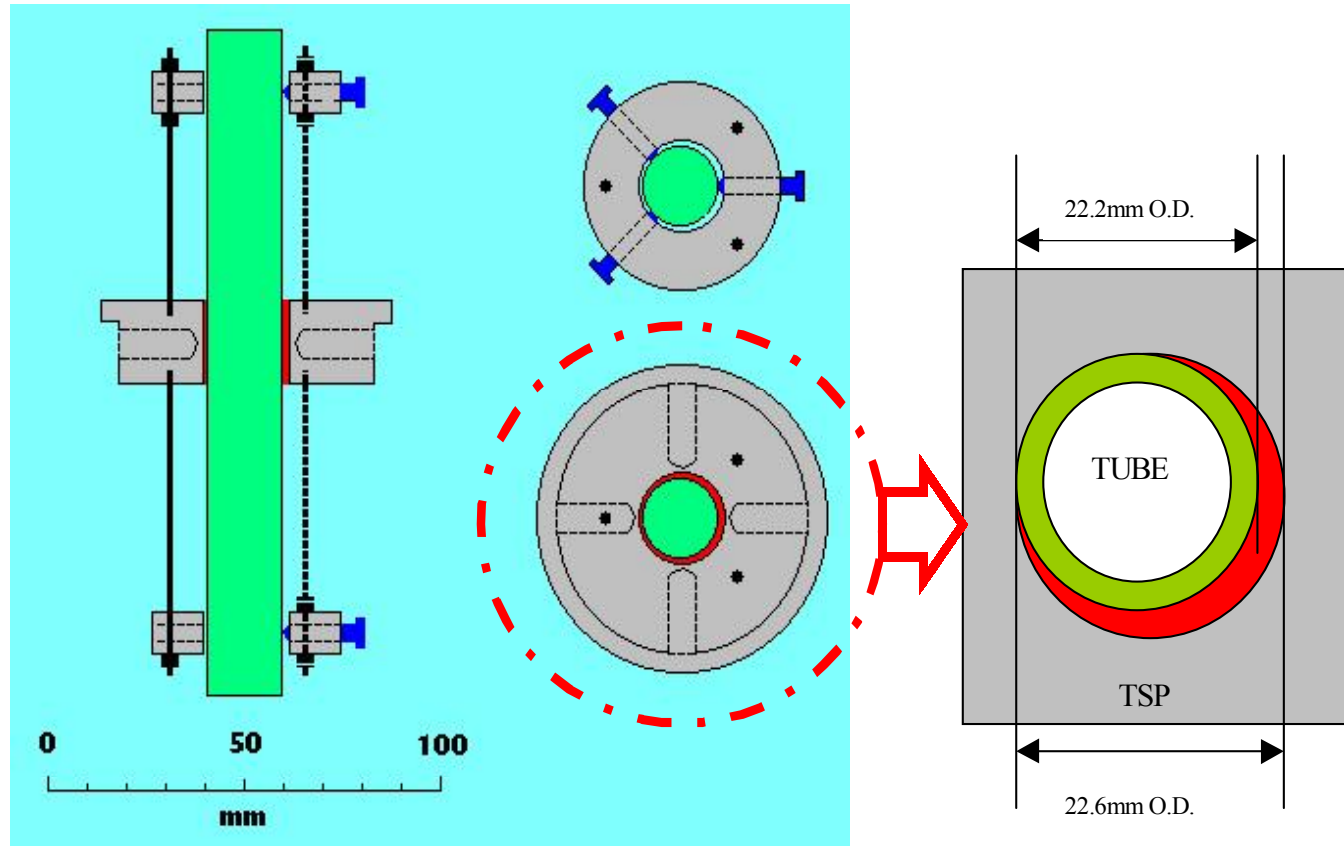


**Figure 1**
Schematic drawing of asymmetric crevice design.
<u>Legend</u>: Red is asymmetric crevice. Green is tube. Large gray part is TSP.

# Typical primary results

After the controlled amounts of impurities were added to the bulk phase hideout was easily measured by a conductivity decrease and potential change in the bulk phase.

Simultaneous monitoring was made in the crevice to try to follow the hideout in-situ. However, the crevice measurements were often hard to evaluate and understand. Results were often difficult (or impossible) to reproduce.

By interrupting the heating, return could be demonstrated.

The hideout/return was heavily dependent on the crevice gap and the crevice filling.

A pressure drop over the TSP significantly decreases the obtained hideout.

# Example: Crevice gap: 1 mm, unpacked

**Bulk**
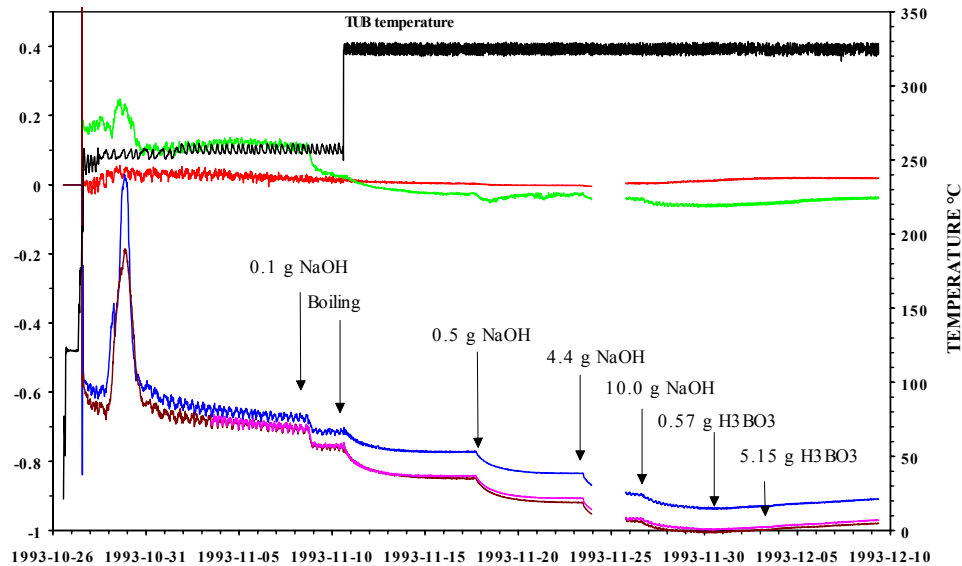
**Crevice**
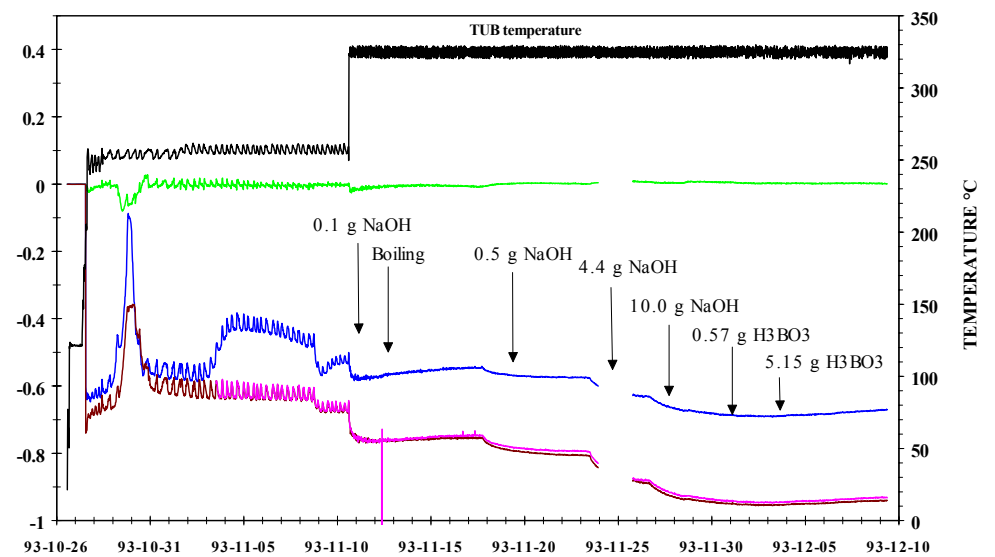


**Crevice and bulk reading are essentially the same at 1 mm crevice gap.**

# Example: Crevice gap: 0.2 mm, unpacked

**Bulk measurements**
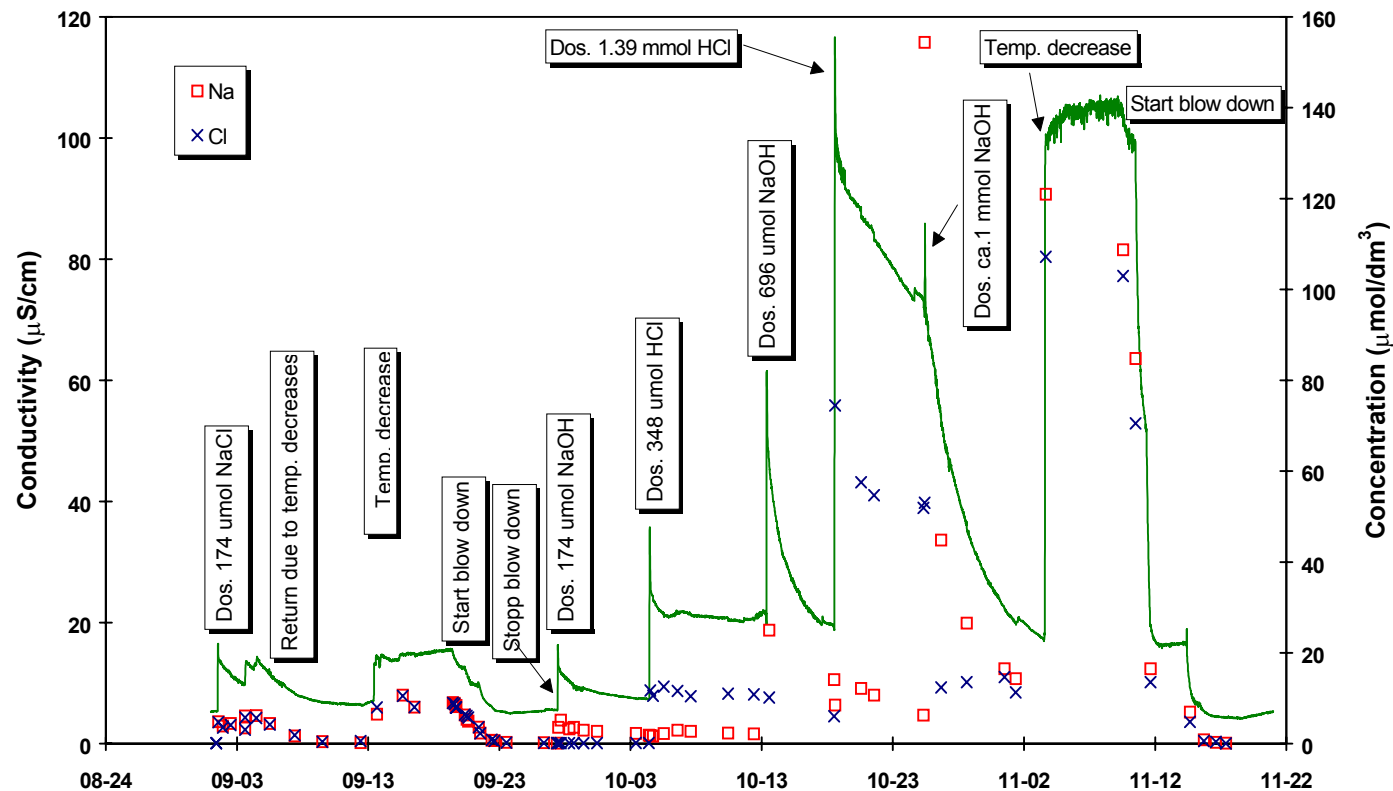
# Example: Crevice gap: 0.2 mm, unpacked

**Crevice conductivity**
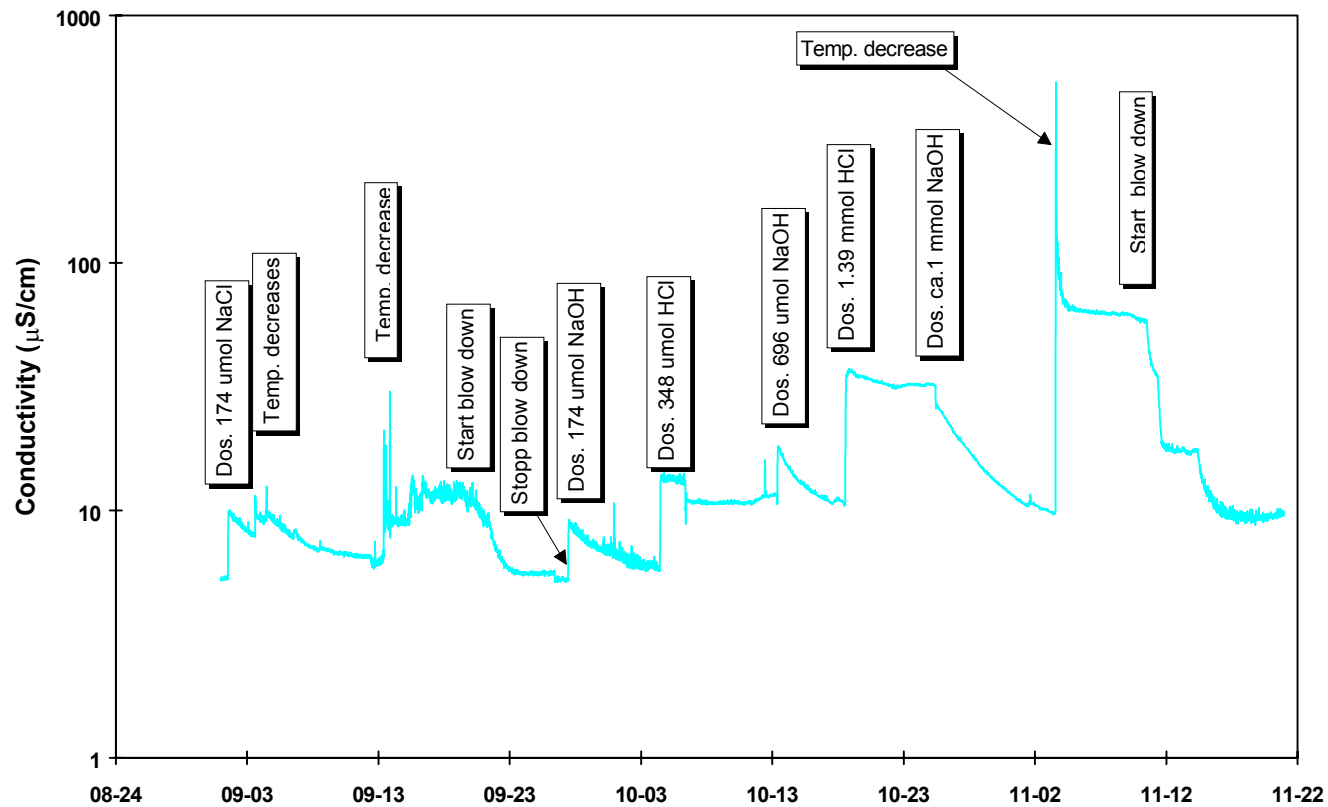
# Example: Crevice gap: 0.2 mm, unpacked

**Potential of PT inside crevice vs two reference electrodes**
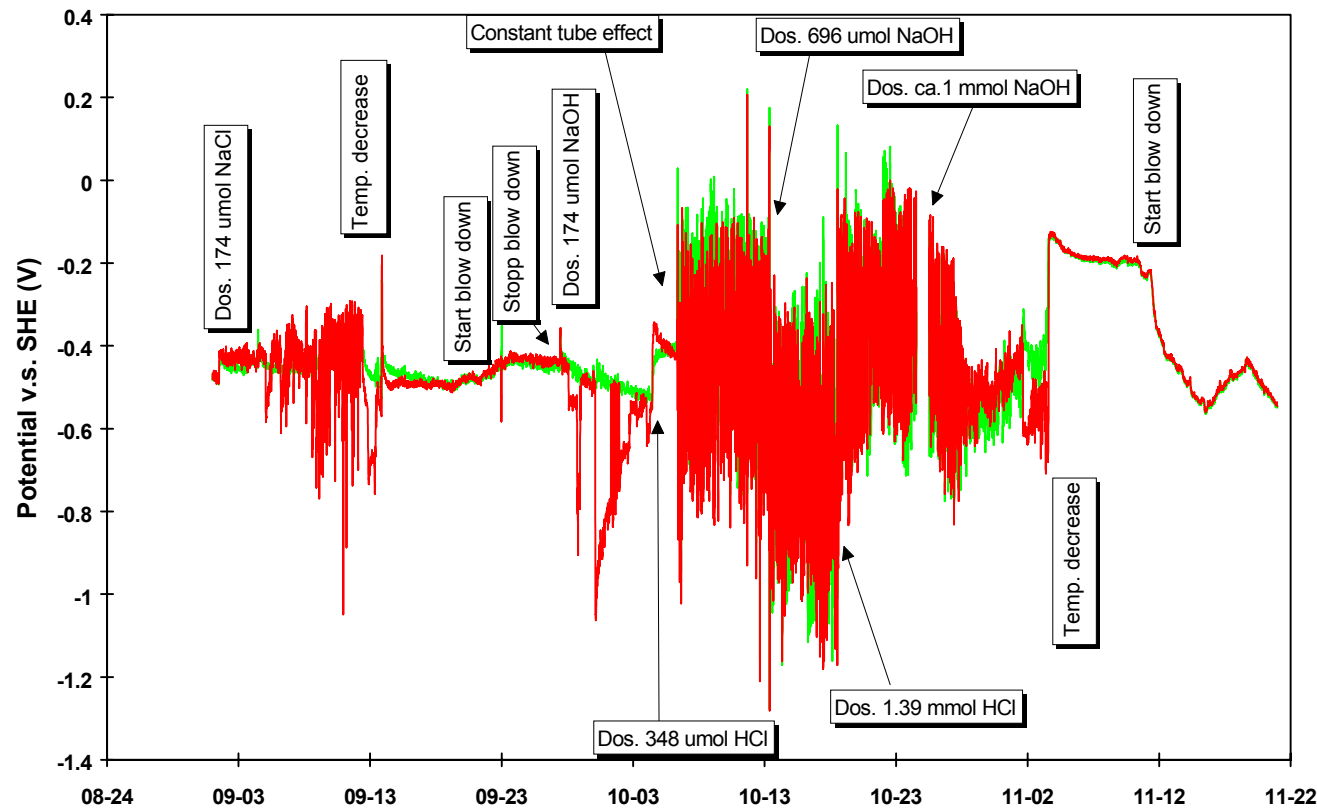
# Example: Crevice gap: 0.2 mm, unpacked

**Potential between two reference electrodes in the crevice**
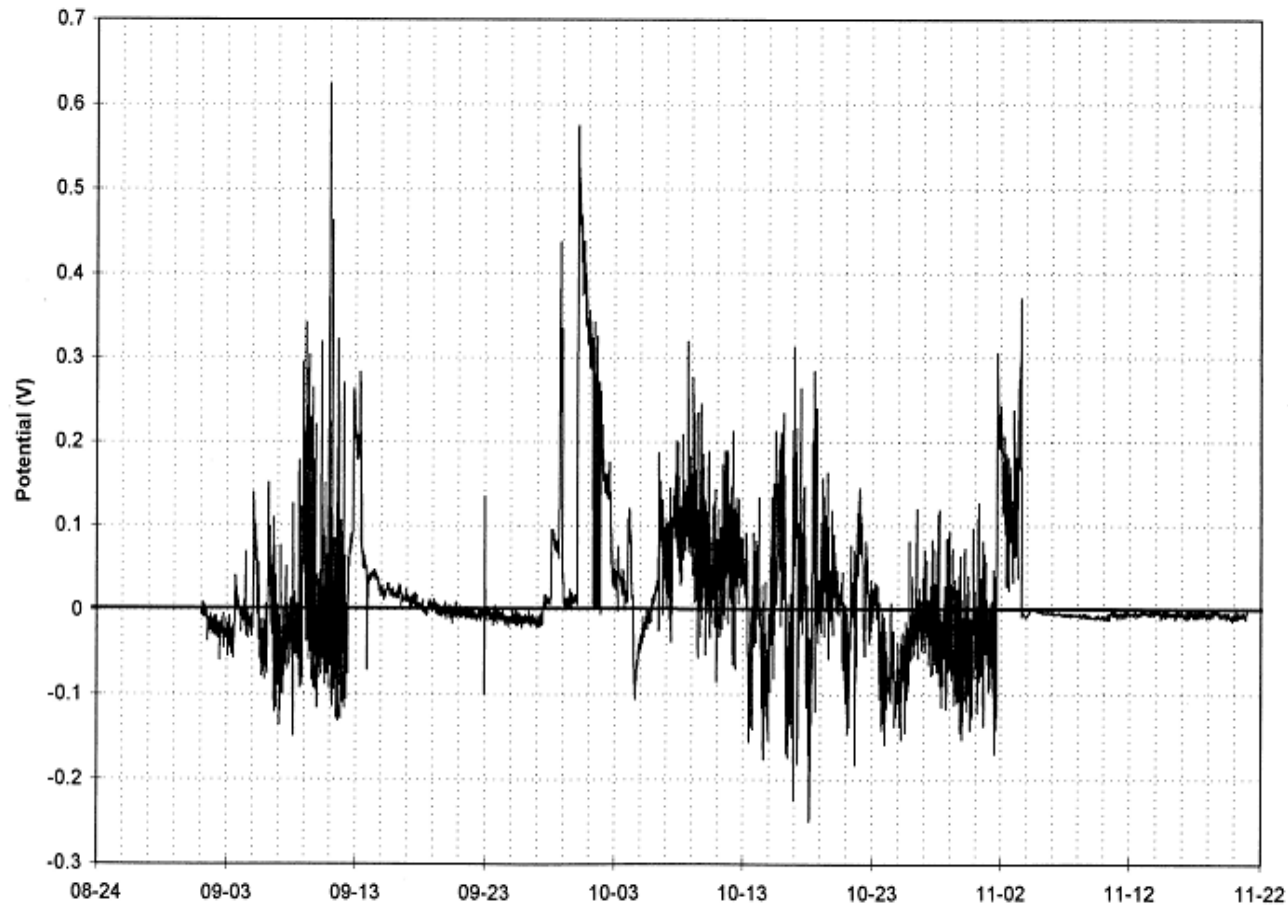
# Discussion

Hideout and return occur in the crevice of the loop if the crevice gap is small or filled with a porous filling.

Hideout is easily measured by bulk conductivity and corrosion/redox potentials.

Crevice measurements often confirm the hideout process but the measurements show large variations inside the crevice.

This means that just beside the measuring locations an even more aggressive solution can exist (which determines the corrosion attack).

So how shall we use data from heated crevice experiments?

# Discussion (cont.)

By modeling crevice concentrations can be calculated. The nominal crevice volume is used and the chemicals that "disappear" from the bulk are assumed to go into the crevice.

However:

Crevice volume is undefined (the void ratio inside the crevice is unknown).

The concentration of chemicals inside the crevice show a huge variation.

Calculated concentrations and concentration factors are not valid in these short term experiments and corrosion predictions are uncertain.

Can long term exposures help the situation?

# Filled crevices

Asymmetric crevices with a filling of about 25 % porosity.

**Hematite** in oxidizing ($O_2$) and **magnetite** in reducing ($N_2H_4$) environment.

Alkaline and acidic environment.

Temperature (°C), $pH_t$, and different $E_{SHE}$, were monitored in bulk and crevice.

The recordings were analyzed for hideout/return (amplitudes and time dependencies).

Ringhals
INGÅR I VATTENFALL

Studsvik™ Nuclear

JAPC

# Example of alkaline/ox. HTC
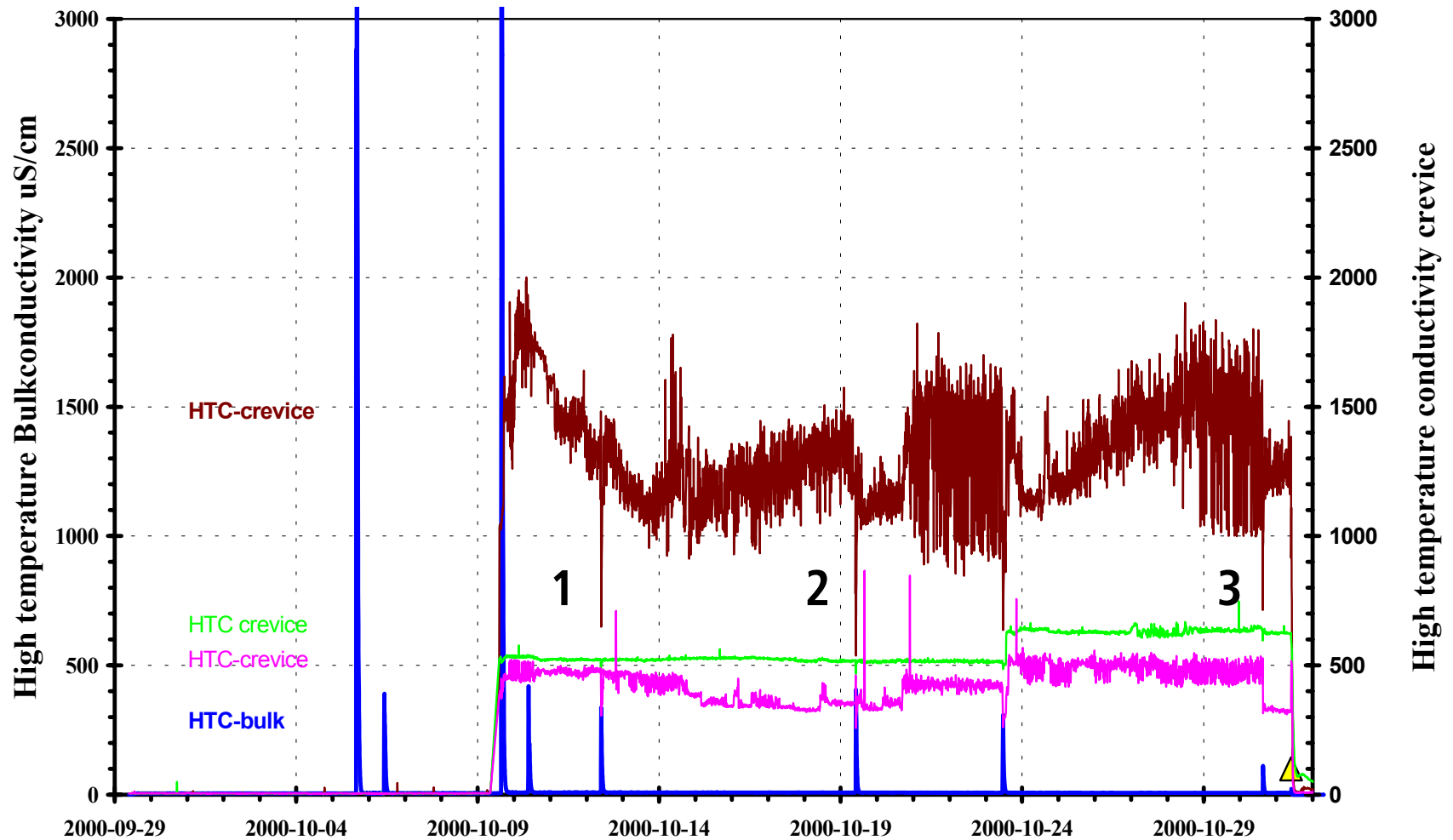
# Example of alkaline/ox. E$_{SHE}$
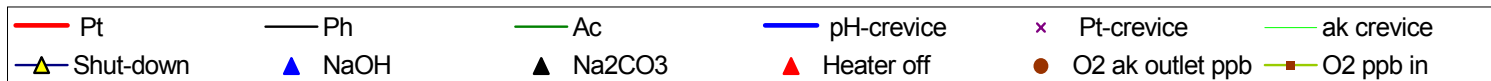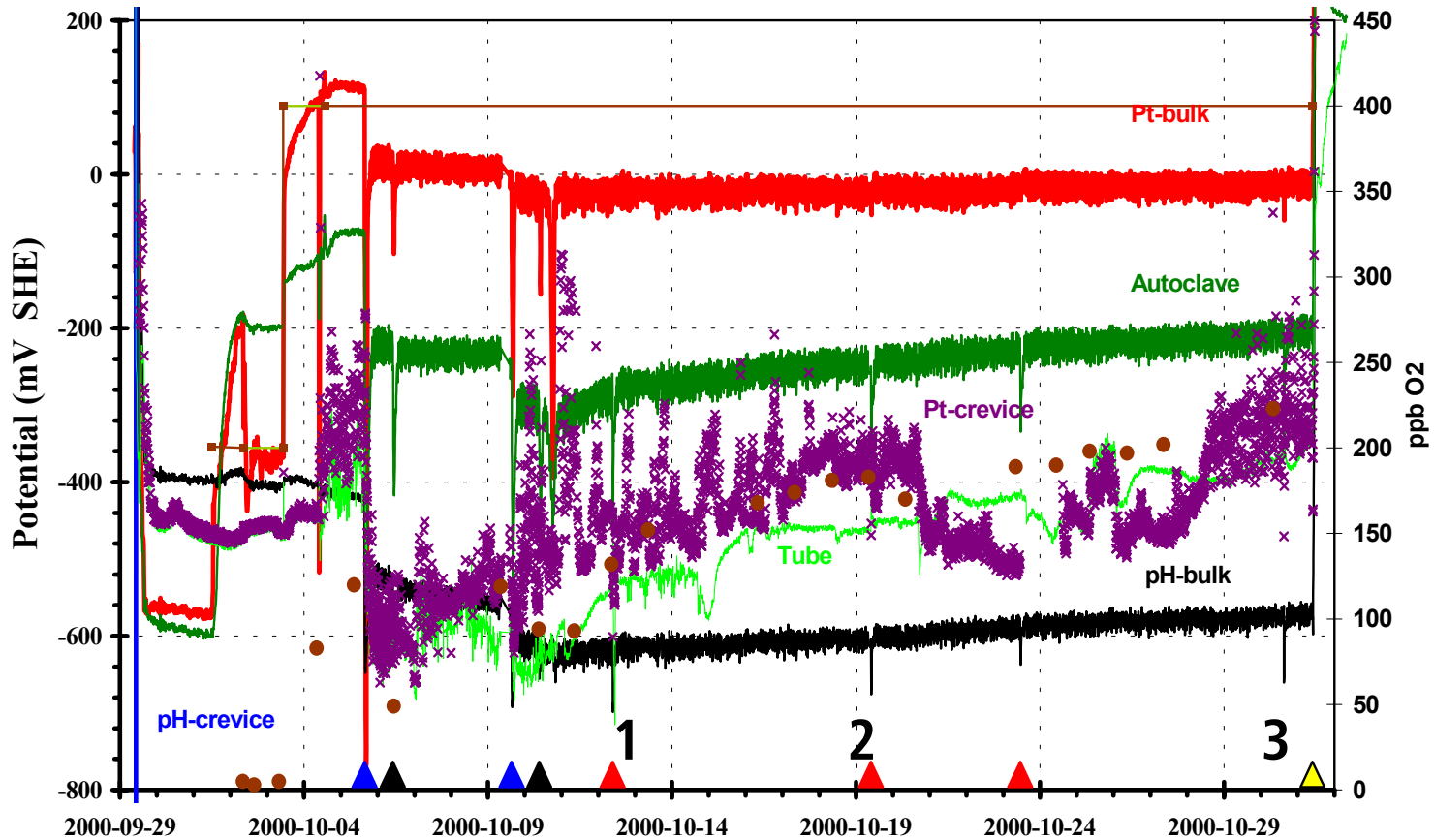
# Results for alkaline/ox/red. crevice

Simultaneous observations were made of decrease in the crevice HTC and increase of the bulk HTC indicating Hideout/return at temp. dips.

In between temperature dips, crevice HTC slowly increases again and bulk HTC falls back to very low values, indicating hideout.

Simultaneous temp and bulk   potential dips verify a return effect.

An ongoing increase of the Pt(crevice) potential in oxidizing and decrease in reducing environment indicates a slow reaction on the redox environment in the bulk.

# Example of acidic/ox. $E_{SHE}$
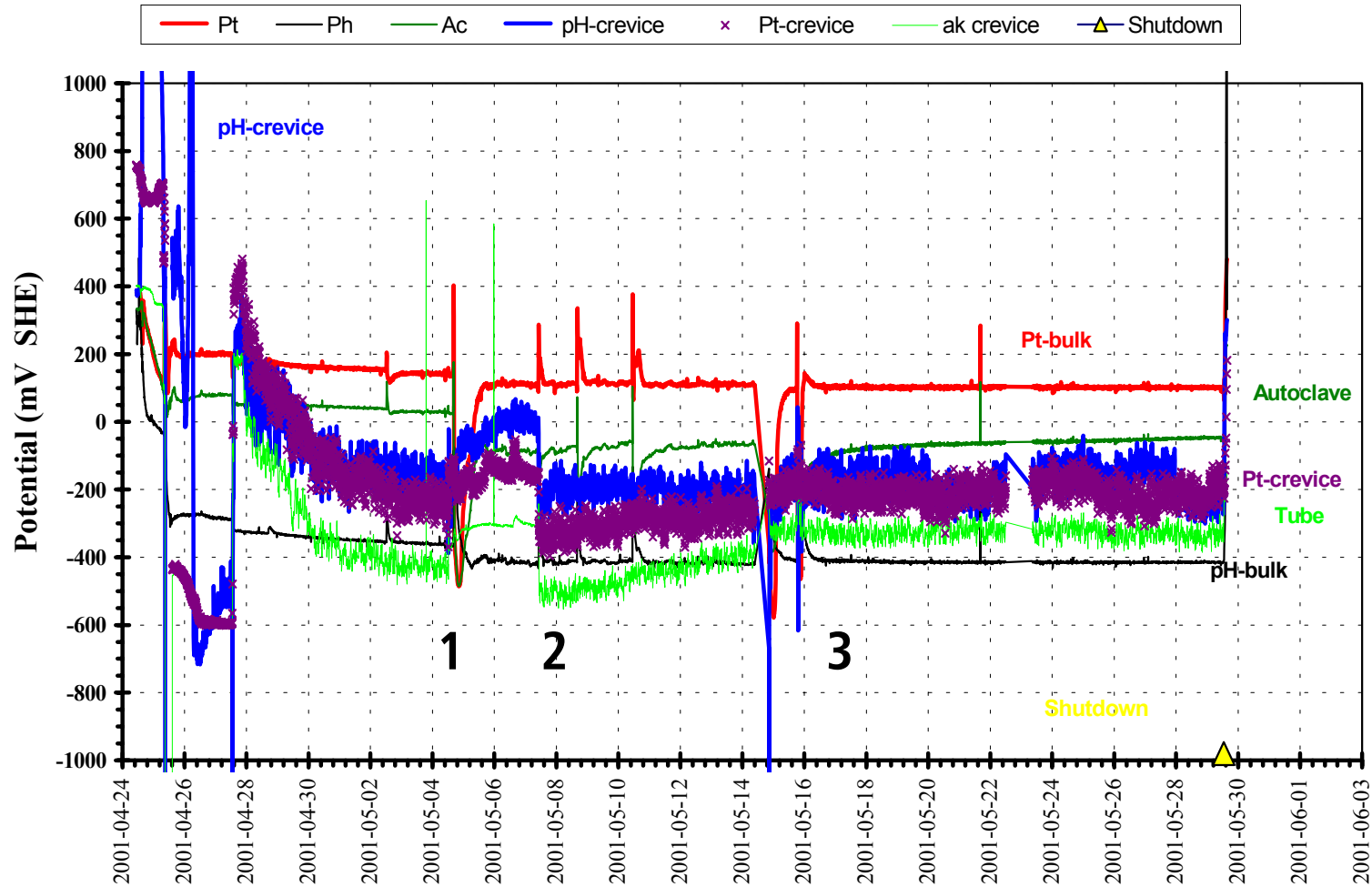
# Results for acidic/ox. crevice (8)

Simultaneous decrease in crevice HTC and increase of bulk HTC, but crevice HTC signals different from alkaline cases at temp. dips.

Crevice HTC did not change between temp. dips, but bulk HTC falls back to very low values. Main hideout level established very early?

The Pt(crevice) potential responds with dips on temperature dips, indicating an acidic return process.

The temperature dips also generate simultaneous increase in most bulk potentials, indicating an acidic return effect.

The crevice related potentials equilibrate more rapidly than in alkaline environment.

# Example of acidic/red. HTC (9)
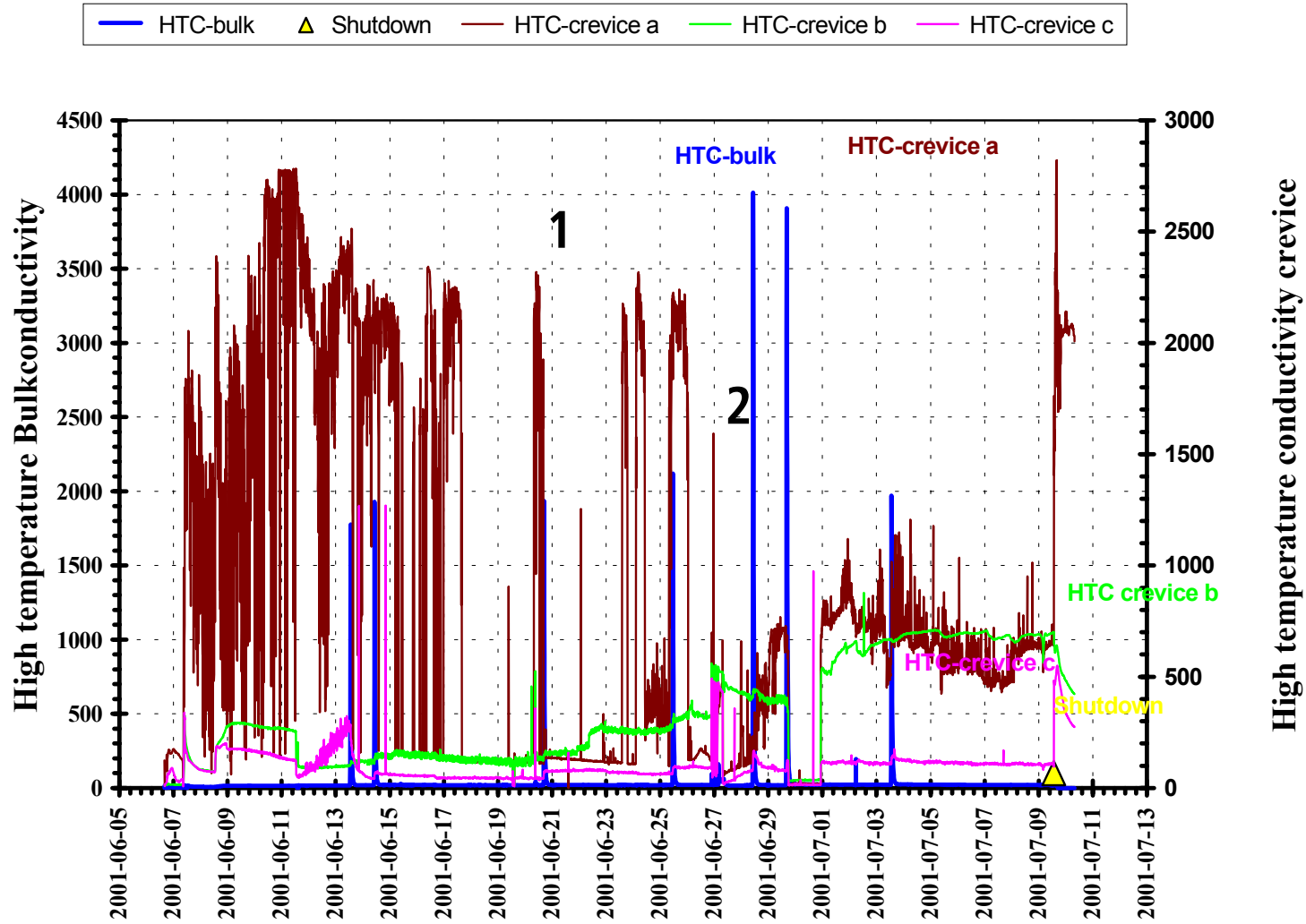
# Example of acidic/red. $E_{SHE}$ (9)
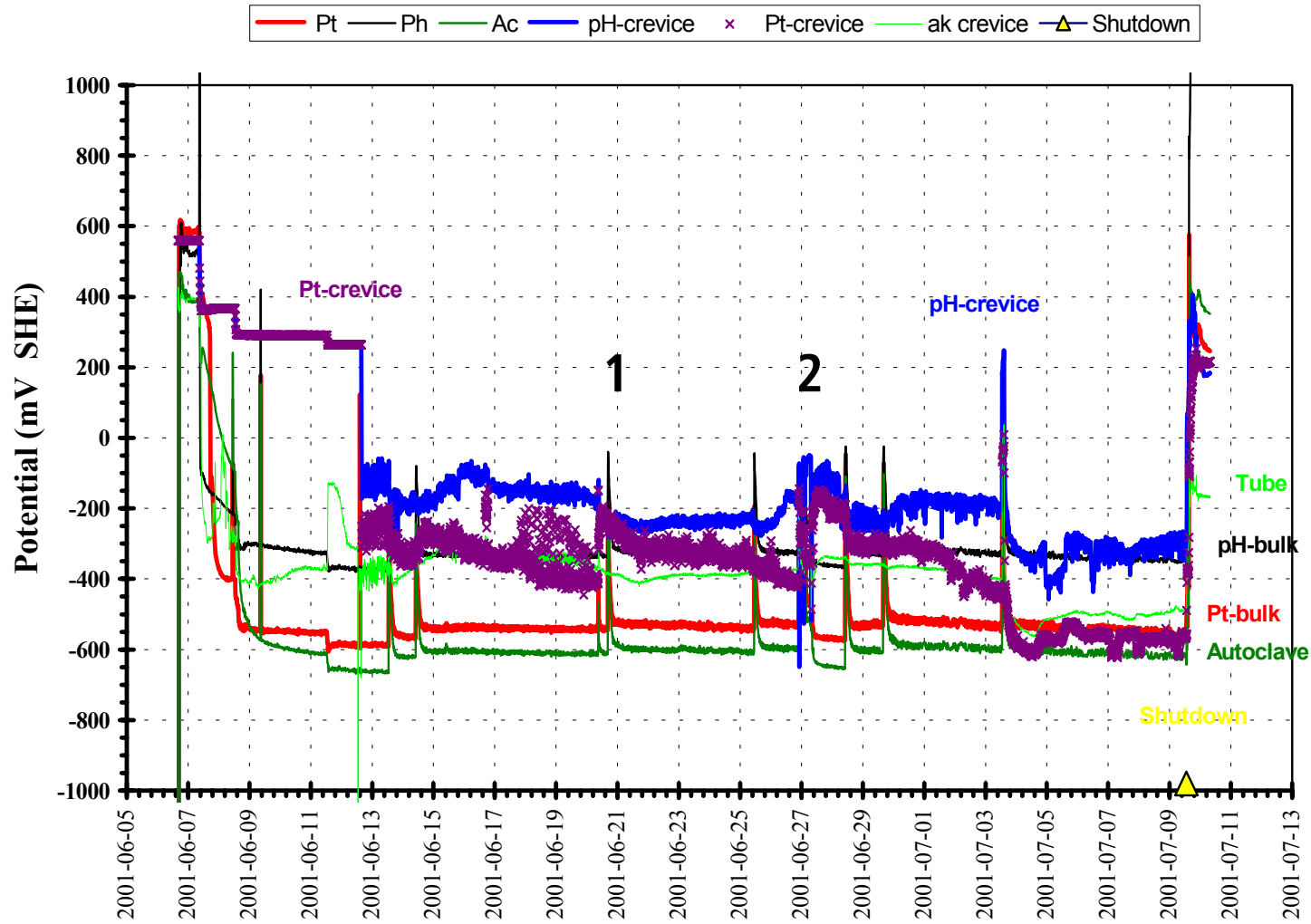
# Results for acidic/red. crevice (9)

One crevice HTC very scattered. Equals other after 2nd heater trip.

Bulk HTC always falls back to very low values, indicating hideout.

All E(bulk) increase at the heater trip, indicating return.

The pH(crevice) potential decreases, confirming the return.

The Pt(crevice) potential seems to be more dependent on hide-out and return of hydrazine than of acid as it goes in opposite direction.

After 0703 HTC(crevice)=HTC(bulk), E(crevice)=E(bulk) indicating total loss of the magnetite filling. The loss was confirmed at shut down.

# Discussion, Filled Crevices

HTC and pot. values indicate hideout and normally confirm each other.

Hideout/return observed in all alk./acidic - ox./red. conditions.

Acidic hideout/return more rapid than alkaline?

Protolythic hideout/return more rapid than redox hideout/return?

Final response stronger in a porous filling compared with no filling?

The wider and outer parts of the filled crevices seems to communicate with the bulk in the hideout/return process. The outer parts rapidly.

# Conclusions

It is difficult to draw firm conclusions about the crevice chemistry through heated crevice experiments.

The exposure times may not be enough to reach a steady state inside the crevice.

Results difficult to reproduce.

Improvements of the heated crevice technique may be possible but alternative methods would be attractive to improve corrosion/hideout predictions.

Combined radiotracer and chemical in-crevice monitoring may be such a possibility.

# High Temperature pH probes for crevice/ crack tip solution chemistry applications - A preliminary study

S. Rangarajan[*], Y. Takeda and T. Shoji

Fracture Research Institute, Tohoku University,
01 Aoba Aramaki Aobaku,
Sendai/980-8579, Japan

[*]Water and Steam Chemistry Laboratory,
BARC Facilities, Kalpakkam- 603102, India

## Abstract

The importance of water chemistry for economic, reliable and safe operation of water cooled power plants is well known. Among the various water chemistry parameters, pH plays an important role as it controls the local environmental chemistry through acid/ base equilibria of the dissolved electrolytes and various corrosion reactions of the structural materials with high temperature water. The pH of the crevice / crack tip solution rapidly changes due to occluded geometry and other associated phenomena like mass transport, thermal / potential gradients and boiling etc. This paper describes the fabrication of a few miniature pH probes based on YSZ membrane (with $Cu/Cu_2O$ and $Ni/NiO$ internals) and normal $W/W_xO_y$ systems by employing conventional, special electrochemical procedures and advanced methods like plasma spray techniques. The results on surface morphology and electrode interphases by Back scattered electron microscopy (BSM), EDAX and ESCA measurements were reported. Thermodynamic calculations are presented for arriving at the standard potential ($E^o$) values of these probes at different temperatures and the theoretical potential values (vs SHE) for various pH values of the solution were calculated. The pH measurements were carried out in bulk PWR water with hydrogenated conditions ( 1200 ppm Boric acid and 2 ppm LiOH; DO < 5 ppb; 0-2 ppm DH ) in the temperature range of 250-300 $^o$C by monitoring the potential of the pH probes with an external Ag/AgCl reference electrode. The results show that the electrode potentials are very stable at a constant temperature and change with temperature as the pH changes. The electrodes are also unaffected by the presence hydrogen in the solution. However, the electrodes performance were found to decrease beyond 200 hours and after repeated hydrogen cycling. The experimentally measured and theoretically calculated values are compared and discussed.

**Key words:** crevice chemistry, crack tip, pH, YSZ, high temperature

## Introduction

The operational safety of a power plant mainly depends on the structural materials and the environmental chemistry. The plant life can be extended by switching over to improved engineering materials and practicing a controlled environmental chemistry. However, for the operating power plants, changing of material is not only economical but also very difficult. On the other hand, controlling the environment is relatively easy and hence most of the plant utilities

adopt to this procedure for economical operation of their power plants. For water cooled power plants, the environment is nothing but water chemistry with deliberately added chemical components to minimize the corrosion damage of the structural materials. Of the various water chemistry parameters viz., dissolved oxygen, specific conductivity etc., pH plays an important role as it controls the local chemistry through acid/ base equilibria of the dissolved electrolytes and various corrosion reactions of the structural materials with high temperature water. The bulk water pH for a given composition of electrolytes does not change rapidly, but the crevice pH or the pH at the crack tip solution changes dynamically due to occluded geometry and other associated phenomena like mass transport, thermal / potential gradients and boiling etc. This leads to an aggressive chemistry in crevice or crack tip regions and influences the local corrosion reactions. Many studies have shown that the pH of crack tip solution is a function of the crack growth behavior of the material tested and in-situ pH measurements are always essential for validating the theoretical models of crack tip solution chemistry and hence the mechanism of environmentally assisted cracking (EAC) of the structural materials. This paper describes the fabrication of a few miniature pH probes based on YSZ membrane (with $Cu/Cu_2O$ and $Ni/NiO$ internals) and normal $W/W_xO_y$ systems by employing conventional, special electrochemical procedures and advanced methods like plasma spray techniques. Apart from surface morphology of the pH probes, the preliminary results of pH measurements in bulk PWR water with hydrogenated conditions (1200 ppm Boric acid and 2 ppm LiOH; DO < 5 ppb; 0-2 ppm DH) in the temperature range of 250-300 $^{o}$C) are reported. The experimentally measured and theoretically calculated values are compared and discussed.

**Experimental**

**Design and Fabrication of pH probes**

Earlier, standard hydrogen electrodes (SHE) based on Pt, Pd-H and Pd-Ag-H systems were used for high temperature pH measurements. However, these electrodes lost their popularity due to various problems viz., $H_2$ gas handling, difficulty in maintaining a particular partial pressure of hydrogen and their sensitivity to red-ox species. Later, pH electrodes based on yttria-stabilised zirconia (YSZ) with various internal metal / metal oxide systems gained importance as they don't have problems that are faced with standard hydrogen electrodes and since they are chemically inert to high temperature water [1-6]. The high temperature pH probes for bulk water applications can be prepared by filling a commercially available YSZ tubes (usually ¼ in. OD) with a suitable metal/ metal oxide powder and using a metallic wire as the contact and lead from the sensor. However, the crevice / crack tip solution chemistry applications require miniature probes.

In this study, three different miniature pH probes were prepared based on **$Cu/Cu_2O$, Ni/NiO and $W/W_xO_y$** systems by using a 0.5 mm metallic wire and sequentially forming the corresponding metal oxide and YSZ coating (only for Cu and Ni based systems) by various methods. The wire was then covered with heat shrinkage polytetrafluoroethylene (PTFE) tubing, leaving the sensor portion exposed to test solution. For copper, the oxide coating was obtained either by heating with a propane gas torch or at 1000 $^{o}$C in a muffle furnace under normal condition or at 800 $^{0}$C in Argon atmosphere. The upper layer of cupric oxide was naturally flacked off by slowly cooling the furnace and the remaining cupric oxide, if any, was brushed off to expose the inner

cuprous oxide film. In another procedure, a thin composite film of copper / cuprous oxide was formed by employing an electrodeposition method with a 0.6 M copper lactate solution (pH 9.0) using a current density of 1.5 mA/cm$^2$. For Ni/NiO and W/W$_x$O$_y$, the oxide coating was obtained by heating in air to a red heat for 3-5 minutes using a propane gas torch. Since the bonding characteristics of the YSZ depends on the substrate surface as well as the method of coating technique, different methods viz., Plasma Spray, Chemical Vapor Deposition (CVD) and Electrophoretic Deposition (ED) were proposed. However, for this study, only the electrodes coated with Plasma Spray technique were used for the pH measurements. The latter procedures are supposed to give more compact layer of YSZ and hence are now under way.

**Theoretical Calculation of Standard Potentials of the sensors**

Fig.1. gives the basic mechanism of potential development across the YSZ membrane. Based on the interphase potentials of the reactions at the various interfaces, one can show that the potential of these electrodes can be calculated from the free energy of the reaction,

$$xM + yH_2O \Leftrightarrow M_xO_y + 2yH^+ + 2ye^- \qquad \text{…. (1)}$$

and the potentials with respect to SHE can be obtained by coupling this half-reaction with that of hydrogen reduction,

$$yH_2 \Leftrightarrow 2yH^+ + 2ye^- \qquad \text{…. (2)}$$

Hence, the standard potential of these electrodes in a solution containing unit activity of hydrogen ion can be calculated from the free energy change for the overall reaction,

$$xM + yH_2O \Leftrightarrow M_xO_y + yH_2 \qquad \text{…. (3)}$$

For the above reaction, the metal oxides viz., Cu$_2$O, NiO and W$_4$O$_{12}$ [7] were used for the copper, Nickel and Tungston based systems respectively. Once the standard potential of these electrodes are known at a given temperature, the pH$_T$ of the solution can be calculated from the measured potential of the YSZ probe according to the expression:

$$E_{(YSZ\ VS\ SHE)} = E^o_{(M/MO)} - (2.303*RT/F)* pH_T \qquad \text{…. (4)}$$

where the symbols R, T, and F represent the usual meaning. However, if the YSZ probe potential is monitored with respect to an external Ag/AgCl reference electrode, the pH$_T$ of the solution can be given by the expression,

$$pH_T = [E^o_{(M/MO)} - \{E_{(YSZ\ VS\ Ag/AgCl)} + A\}] * [F/(2.303*RT)] \qquad \text{…. (5)}$$

where A is the correction term to convert the potentials from Ag/AgCl to SHE scale [8,9].

## Measurement system

A recirculating, high temperature and high pressure water loop with an autoclave facility having ports for introducing the pH probes and external Ag/AgCl reference electrode was used for this study. The measurements were carried out in simulated PWR water with hydrogenated conditions (1200 ppm Boric acid and 2 ppm LiOH; DO < 5 ppb; 0-2 ppm DH ) in the temperature range of 250-300 $^o$C. Electrodes of each kind were tested for a total duration more than 240 hours and the potentials were measured with a Keithley 6515 system electrometer and recorded in the computer for subsequent calculations.

## Results and Discussion

## Electrode surface morphology and characterisation studies

The photographs of copper based pH probe with cuprous oxide and YSZ films by various methods are given in Figure 2. A good adherent film of cuprous oxide was obtained by all the heating procedures. The electrolytic method gave a composite film of the cuprous oxide and metallic copper. Figure 2 (e) shows the YSZ coated Cu/Cu2O wire by Plasma Spray method while figure 2 (f) shows the outer and interior surfaces of the copper based pH probe. Figure 3. shows the XPS spectrum of the oxide coated copper wire. The cross-section of the coated film electrodes were studied by Back scattered electron microscopy (BSM) to identify the surface morphology and to evaluate the relative thickness of the films. Figure 4. gives the SEM pictures of the cross-section of the coated electrodes. It can be seen that for copper, the cuprous oxide film prepared in Argon atmosphere was not very uniform as compared to that prepared by propane gas torch. Of all the methods, the electrolytic method gave the thinner-most film. For nickel and Tungsten, the oxide films were quite uniform and very adherent. From the fabrication point of view, nickel and tungsten based electrodes are better than copper based electrodes. The tungsten based electrode has an additional advantage that it need not be coated with YSZ film for the pH measurements. Figure 5. gives the SEM images of YSZ coated Cu/Cu2O based pH probes. It can be observed that some delamination had occurred near the oxide/YSZ interface and this could have happened during the molding process used for sample preparation for SEM. This was clarified by EDAX measurements (not given here) which showed various interfaces. Figure 6. gives the photograph of Nickel & Tungsten probes after use. It shows the micro-crack that had developed on YSZ coating on nickel electrode towards the end of the test.

## Expressions for Standard Potential of the Electrodes:

A computer program was written in BASIC language to calculate the standard potential of the sensor from the free energy changes of the overall reaction (3) at various temperatures and to calculate the pH of the solution according to equation (5). The following expressions were derived from the results of the computer program to obtain the standard potentials, $E^o$ vs SHE in Volts for different pH probes.

$E^o_{(Cu/Cu2O)}$ $= 0.48381 - 0.462513.10^{-3}.T + 2.14013.10^{-7}.T^2 - 1.36749.10^{-10}.T^3$

$E^o_{(Ni/NiO)}$ $= 0.14099 - 0.363071.10^{-3}.T + 1.3041.10^{-7}.T^2 - 0.253191.10^{-10}.T^3$

$E^o_{(W/W4O12)}$ $= 0.08149 - 0.390169.10^{-3}.T + 1.62278.10^{-7}.T^2 + 0.395135.10^{-10}.T^3$

For converting the measured potentials of the pH probes to SHE scale from that of the Ag/AgCl/(0.1M KCl) reference electrode, the correction term, A is given by the expression

$A = 0.286637-1.003217.10^{-3}.(T-25) + 0.017447.10^{-5}.(T-25)^2 -0.303004.10^{-8}.(T-25)^3$

where T is the temperature in $^o$C.

**pH measurements**:

Electrodes of each kind were tested for a total duration more than 240 hours and the potentials were measured with a Keithley 6515 system electrometer and recorded in the computer for subsequent calculations.

Figure 7. (a-c), gives the potential measurements of the $Cu/Cu_2O/YSZ$ pH probe monitored over a period 12 days. All the potentials were measured with respect to autoclave frame and converted to SHE scale for pH calculations. The red-ox potential of the autoclave solution was also monitored by Pt electrode and were presented in some of the graphs for identifying the reason for the change in the potential values. For example, the change in potential in the first figure (labeled as 16$^{th}$) of 7 (a) can be reasoned out to change in temperature while the same in figure (labeled as 23$^{rd}$) of 7 (b) to introduction of hydrogen into the system. It can be seen that the potential of the pH probe and the Ag/AgCl reference electrode changed uniformly and the differences between the two potentials were almost constant. This behaviour is expected because at a given temperature the pH of the solution is constant and hence the potential of the pH probe should also remain constant. At this stage, both Ag/AgCl and pH probe function as a reference electrode. The potential of the pH probe did not change with the addition of hydrogen showing thereby its insensitivity to hydrogen or any redox changes to the system. However, after 24 hours of hydrogen addition the potential drifted to more negative value and remained constant and again after 36 hours the potential changed drastically and reached value of zero. The electrode was inspected after the test and was found to have micro-cracks. The rapid changes in potential could be due to development of the cracks which exposes the interior oxide phase to the test solution.

Figure 7. (d-f), gives the potential of the nickel and tungsten based pH probes with time. It can be seen that as the temperature is increased the potential of both the pH probes change to more negative values and become steady when the temperature remains steady. When the temperature was maintained for a number of days, the potentials were also remarkably constant. After a few days, when the temperature was decreased the potentials of both the probes moved in positive direction. It also was observed that the potential of the tungsten probe was more positive than that of nickel probe below 250 $^o$C and became more negative at higher temperature. The reverse trend was observed when the temperature was decreased from 300 $^o$C to 200 $^o$C and hence this change was found to be reversible. Similar to the copper based pH probe, the potential of the nickel and tungsten based pH probes also did not change when hydrogen was introduced into the system. This can be seen in the figure (labeled 06/12/02) of 7 (e) where the potential of a Pt

electrode is changing due to hydrogen addition while that of the pH probes remain at a constant value. However, while hydrogen was removed from the system, all the electrodes showed a change in potential. The nickel based YSZ probe showed a crack on the electrode surface ( see figure. 6) and this could be a reason for the changes in potential of this probe. But the reason for the potential shift of tungsten probe was not clear. The estimated pH values calculated from the potentials after the system had stabilized was found to be within two pH units from the theoretically calculated values for the copper and nickel based electrodes. But this deviation can be minimized by improving the YSZ coating and by calibrating the electrode over a wide range of pH.  However, for the tungsten electrode, the deviation was more which could be due to the uncertainty in the calculated standard potential because of a mixed oxide phase.

**Conclusion**

The copper and nickel based YSZ probes seem to work in the expected way. But needs to be calibrated for a wide range of pH. The standard potential, $E^o$ vs SHE for the various sensors were calculated from the free energy changes of the electrode reactions and expressions were derived to obtain the same at various temperatures. The estimated pH values (using the theoretically calculated standard potential) differed by two pH units from the theoretical pH values of the solution. However, the results can be improved by better fabrication procedures using Chemical Vapor Deposition (CVD) and Electrophoretic Deposition (ED) techniques to minimize the development of minor cracks and by calibration of the probes and using experimental $E^o$ values. Ni/NiO system seems to be better than $Cu/Cu_2O$, because NiO coating was more uniform, the deviation in pH values was relatively less and also doesn't pose any problem if nickel ions are released to the solution. Tungsten based electrode does not need YSZ coating and it is advantageous from the construction point of view. But the main draw back is the uncertainty in the theoretical $E^o$ value due to the mixed oxide phase. However, with proper calibration it can also be used as it is very simple in design and electrode dimension can be very small to suit Crevice / crack tip solution measurements.

**References**

1.  L.W. Niedrach, Science, Vol. 207, p. 1200 (1980).
2.  L.W. Niedrach, J. Electrochem. Soc., Vol. 127, p.2122 (1980).
3.  L.W. Niedrach and W.H. Stoddard, Corrosion, Vol. 41, No. 1, p 45 (1985).
4.  T. Tsuruta, D.D. Macdonald,  J. Electrochem. Soc., Vol. 129 p.1221 (1982).
5.  L.W. Niedrach, J. Electrochem. Soc., Vol 129, No.7, p 1445 (1982).
6.  D.D. Macdonald, S. Hettiarachchi, H. Song, K. Makela, R. Emerson and M. Haim, J. Solut. Chem., 21, 849 (1982)
7.  L.B. Kriksunov, D.D. Macdonald, and P.J. Millett, J. Electrochem. Soc., Vol. 141, No. 11, p. 3002 (1994).
8.  D.D. Macdonald, A.C. Scott and P.Wentrcek, J. Electrochem. Soc., Vol. 126, No. 6,  p. 908 (1979).
9.  D.D. Macdonald, A.C. Scott and P.Wentrcek, J. Electrochem. Soc., Vol. 126, No. 9,  p. 1618 (1979).

$$M \, / \, M^{n+} \quad O^{2-} \qquad \qquad O^{2-} \quad 2H^+$$

$$M \, / MO \qquad \qquad \text{YSZ}$$
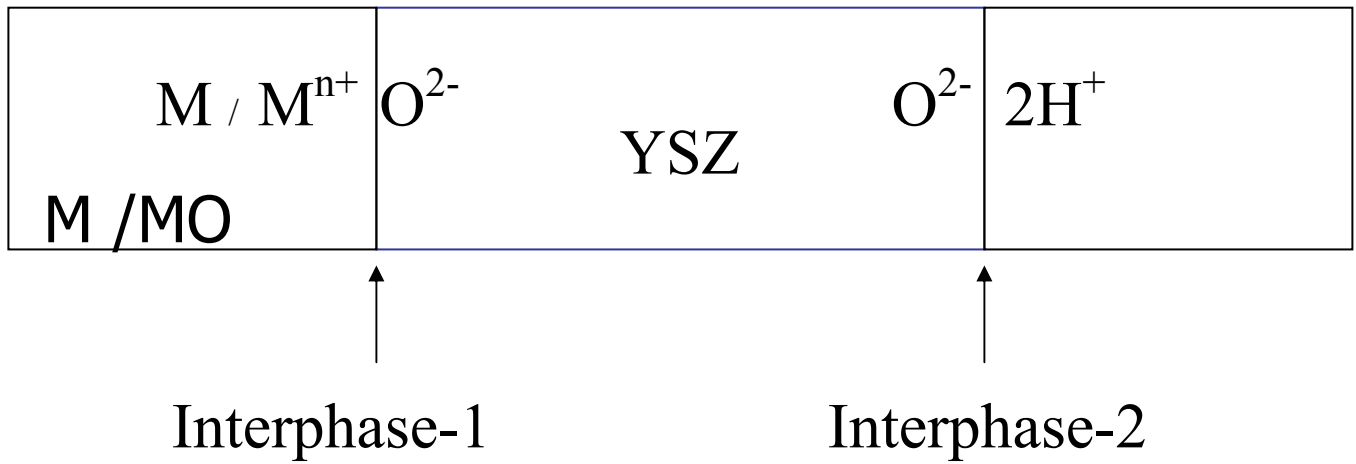
Interphase-1          Interphase-2

FIGURE 1. Basic mechanism of potential development across the YSZ membrane probe
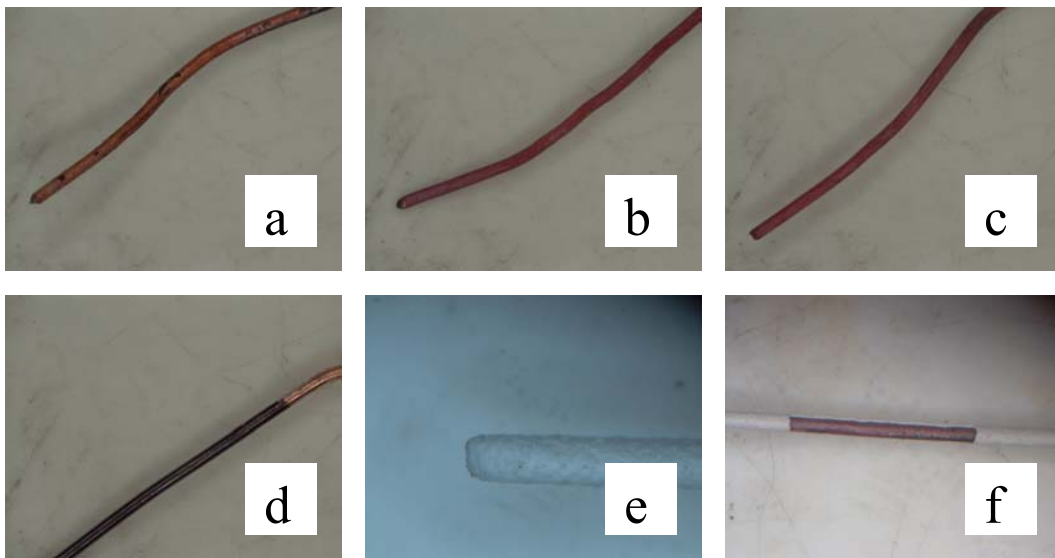


FIGURE 2. Photograph of Copper wire coated with $Cu_2O$ and YSZ: (a-c) $Cu_2O$ coating by heating in Argon atmosphere at 800 $^oC$ for 2, 8, 16 minutes respectively (d) $Cu_2O$ coating by electrolytic method (e) YSZ coated, (f) YSZ partially removed to show inner oxide layer
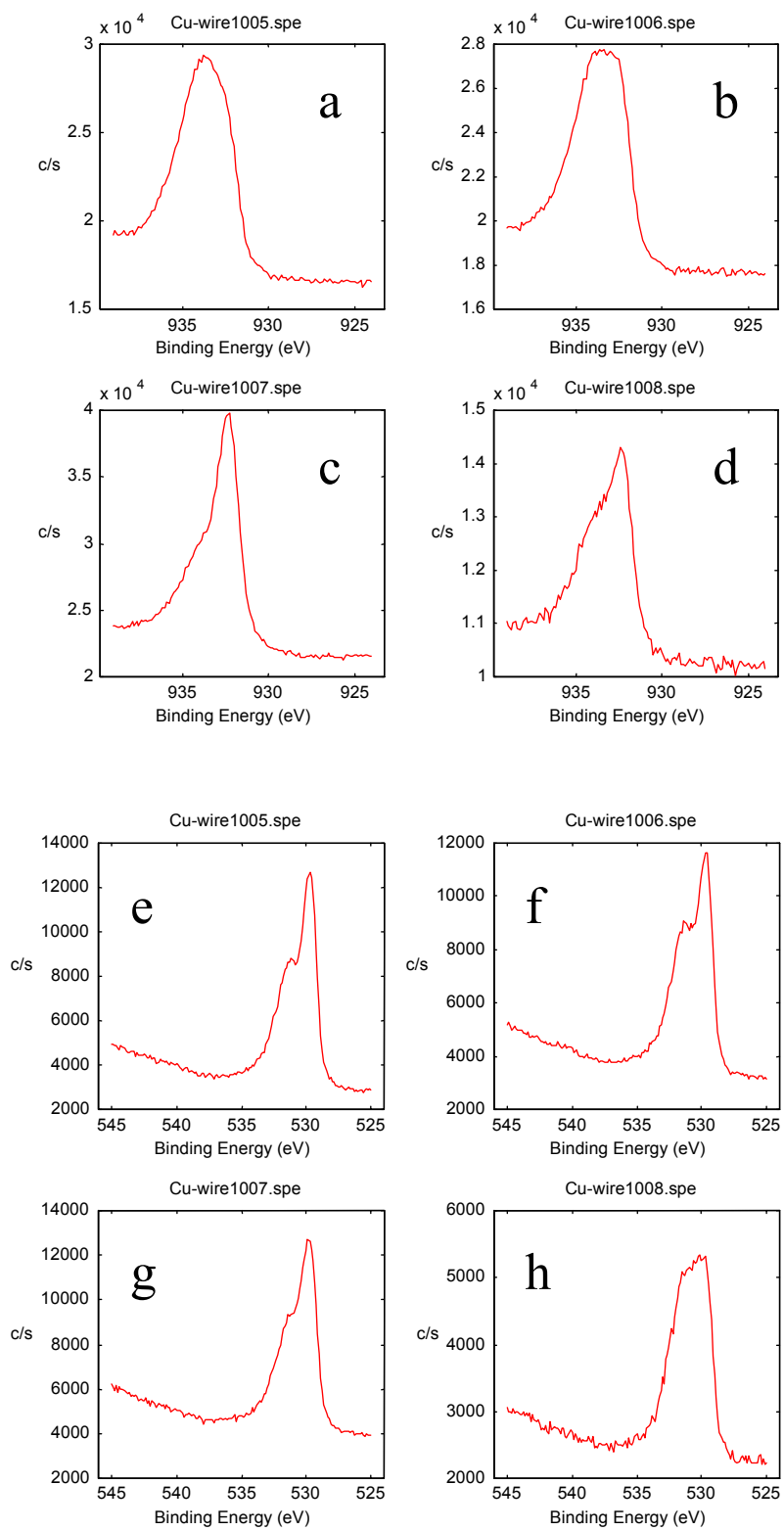
FIGURE 3. XPS spectrum of the oxide coated copper wire: (a-d) copper peaks (e-h) oxygen peaks ( a,,b, e & f - with top CuO layer; c,d,g & h – without top CuO layer)
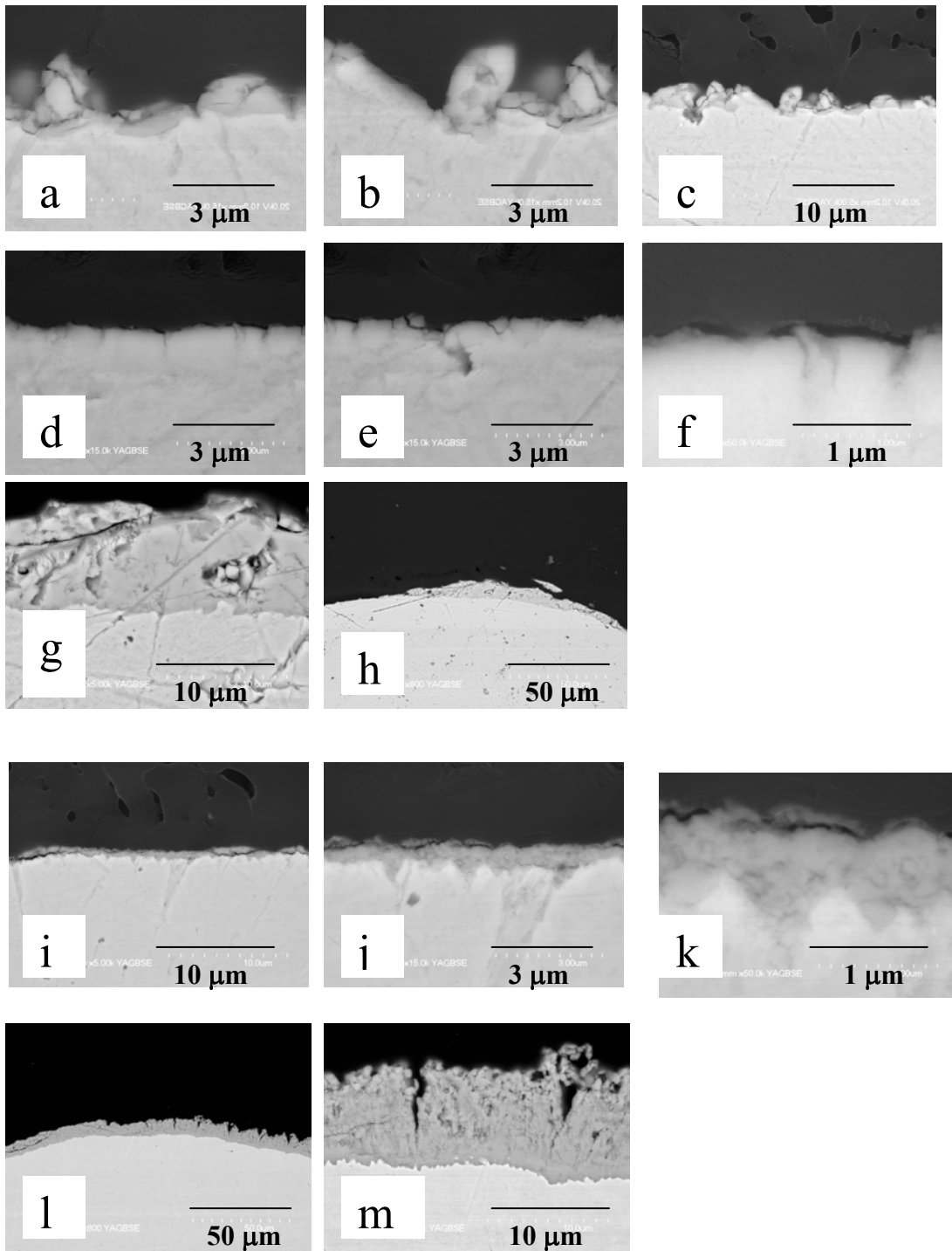
FIGURE 4. SEM Photographs of metal/metal oxide coating: (a-c) $Cu_2O$ prepared in Argon atmosphere at 800 $^0$C, (d-f) $Cu_2O$ prepared by Electrolytic method, (g-h) $Cu_2O$ prepared by Propane gas torch, (i-k) NiO prepared by Propane gas torch, (l-m) $W_xO_y$ prepared by Propane gas torch
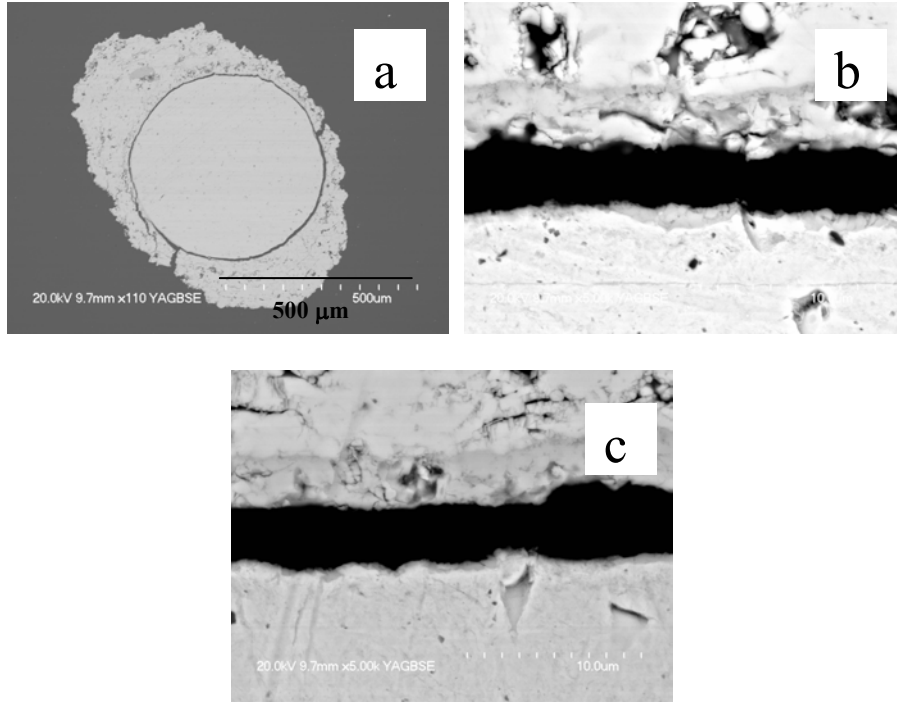
FIGURE 5. SEM images of YSZ coated Cu/Cu2O based pH probes: (a) Full cross-section (b) surface boundary on thickly coated side (c) surface boundary on thinly coated side
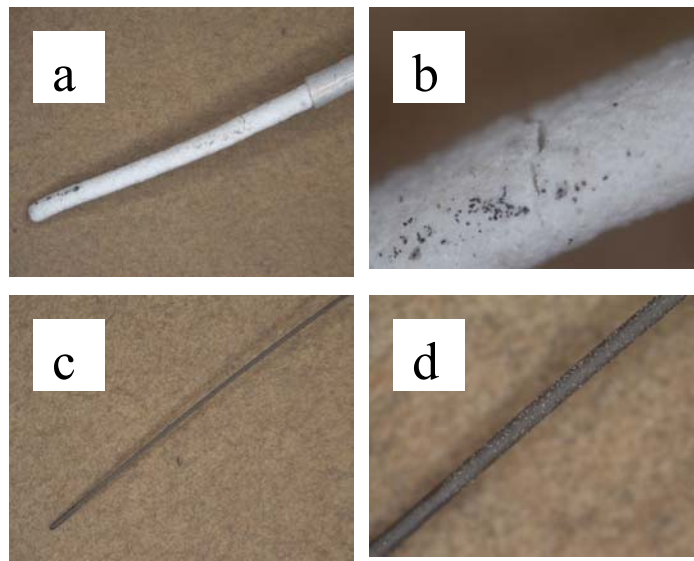


FIGURE 6. Photograph of Nickel & Tungsten probes after usage: (a) Ni/NiO/YSZ (b) same as (a), but enlarged for showing the micro- crack(c) W/$W_xO_y$ coating (d) same as (c), but enlarged

FIGURE 7. (a) Potential Measurements with Cu/Cu₂O/YSZ pH probe (Simulated PWR water, 1200 ppm Boric acid and 2 ppm LiOH; DO < 5 ppb; 0-2 ppm DH )

197
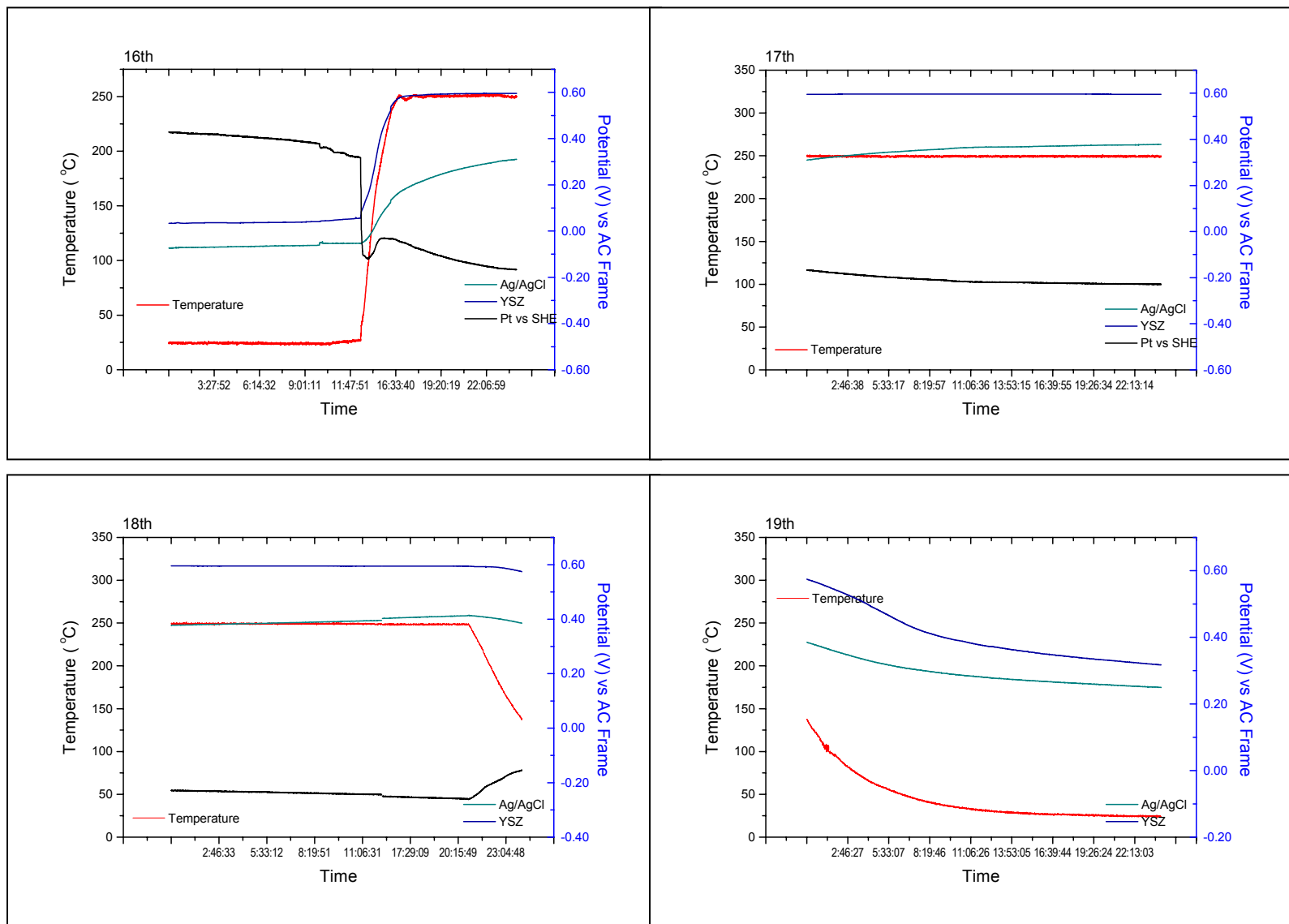
FIGURE 7. (b) Potential Measurements with Cu/Cu$_2$O/YSZ pH probe
(Con'td)
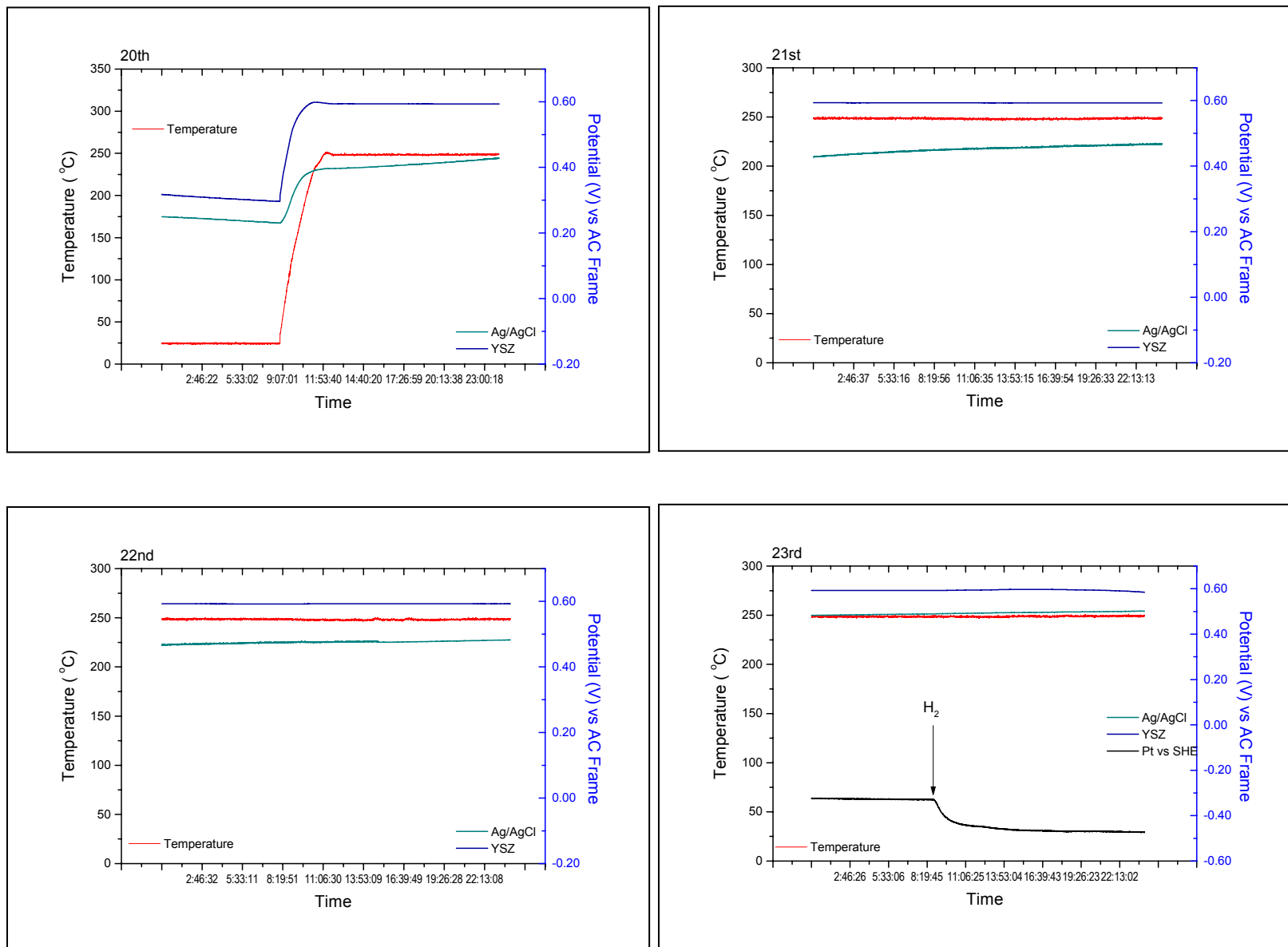
FIGURE 7. (c) Potential Measurements with Cu/Cu$_2$O/YSZ pH probe
(Con'td)
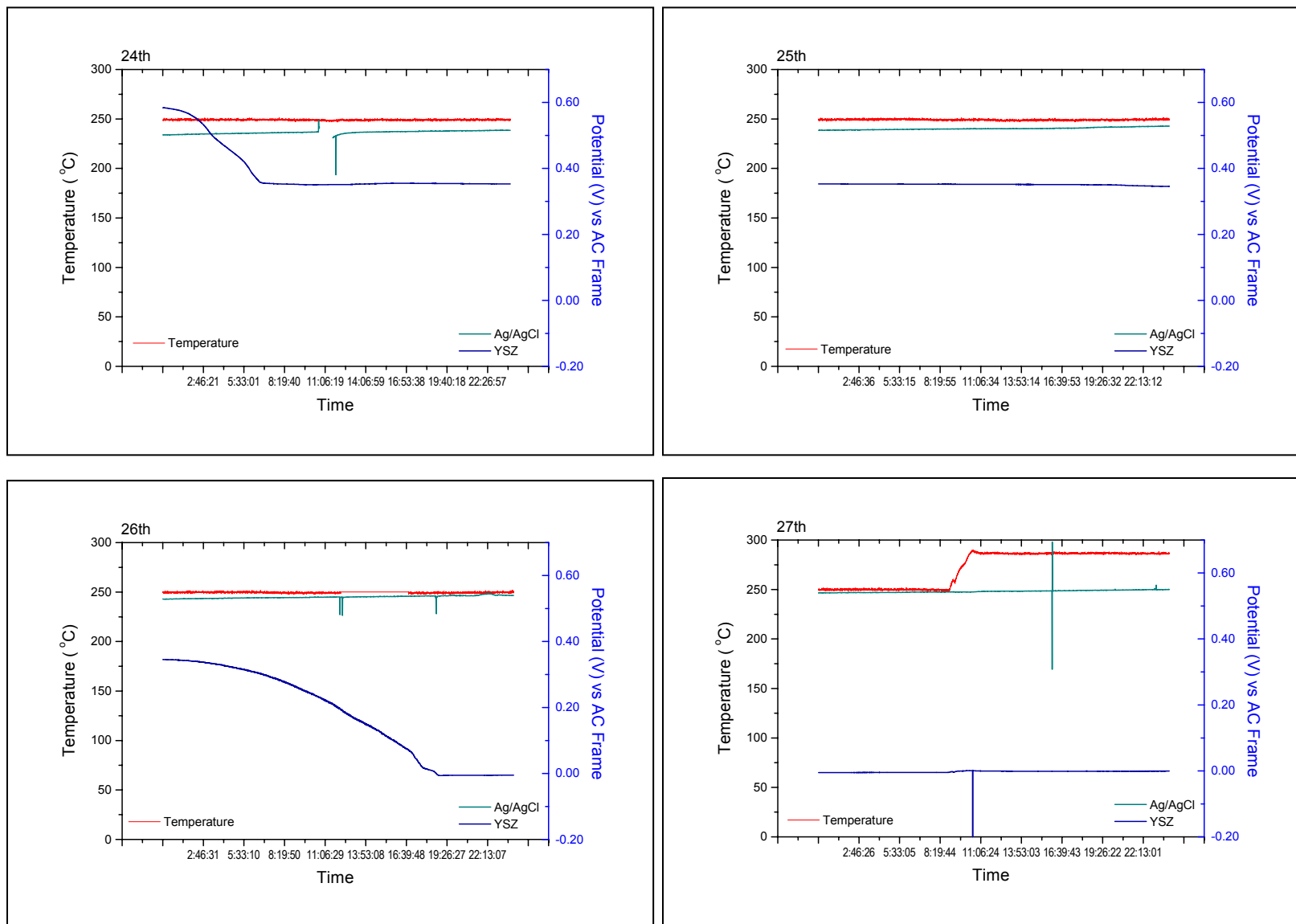
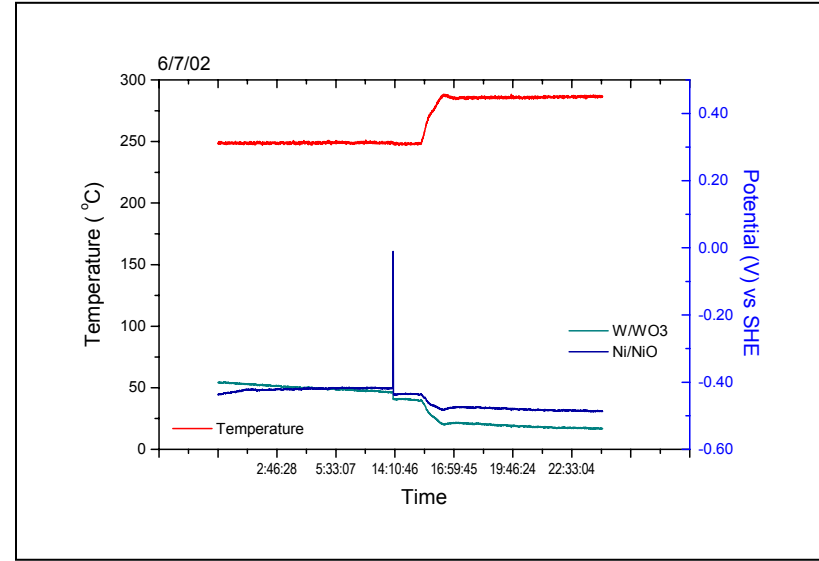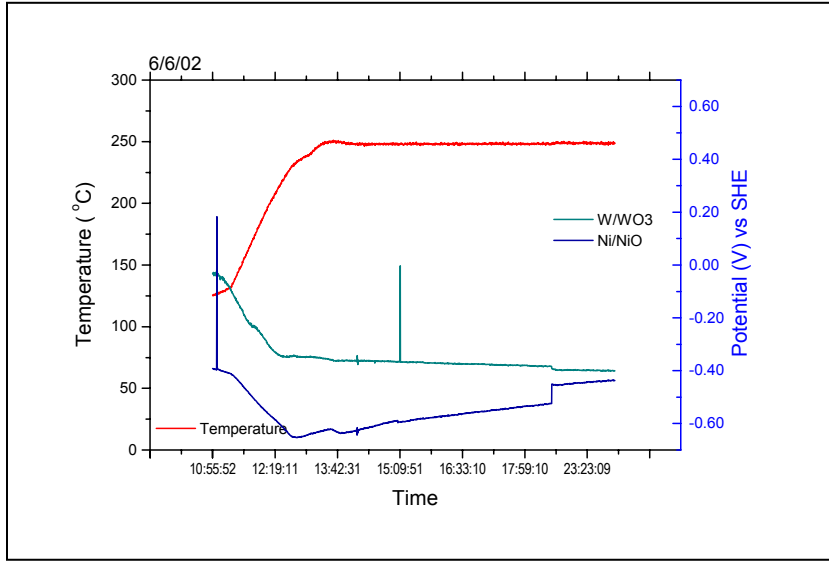FIGURE 7. (d) Potential Measurements with Ni/NiO/YSZ and W/W$_x$O$_y$ pH probes (Simulated PWR water (1200 ppm Boric acid and 2 ppm LiOH; DO < 5 ppb; 0-2 ppm DH )
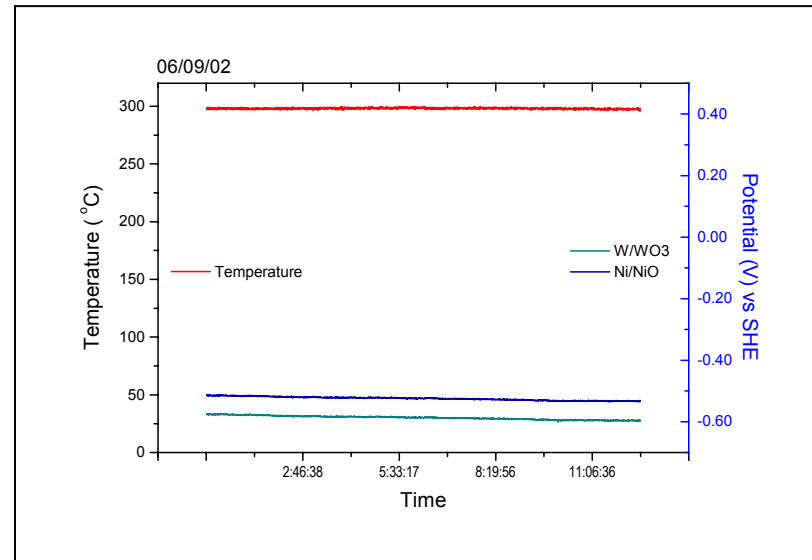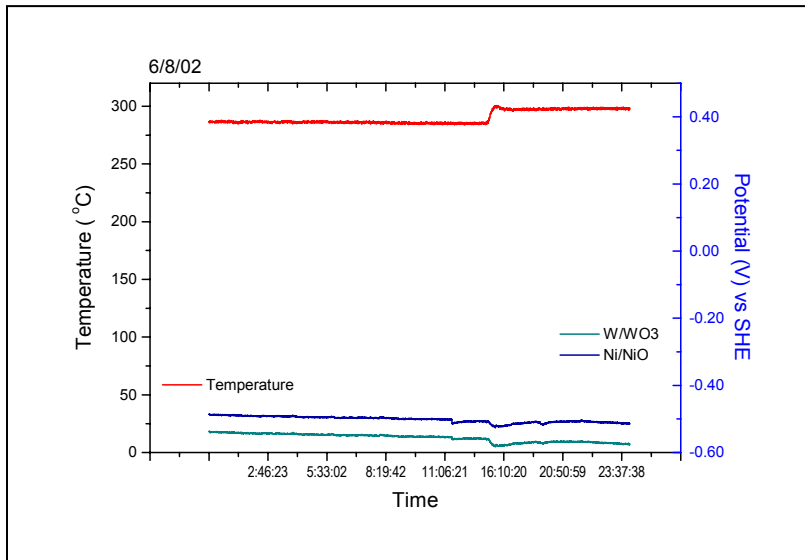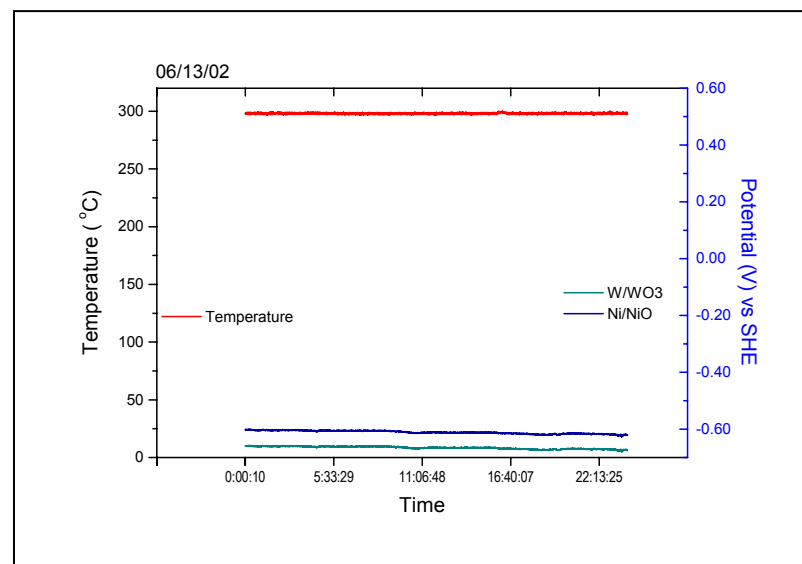
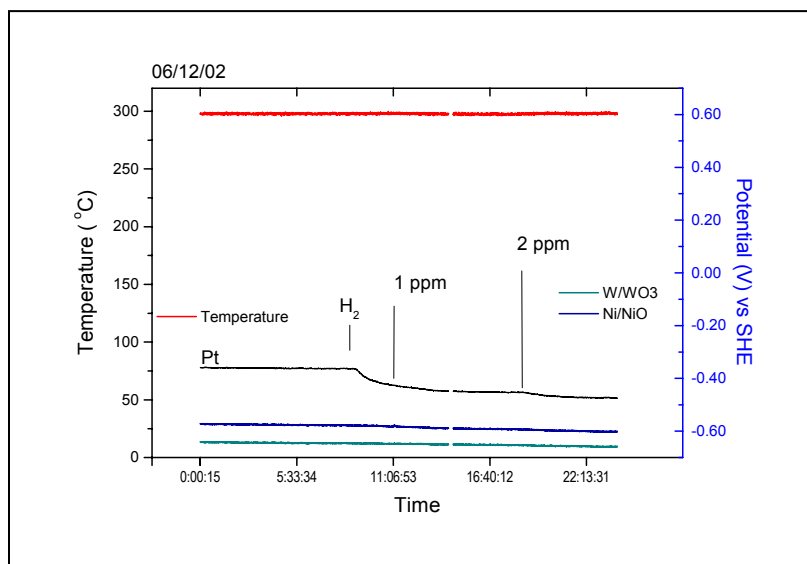FIGURE. 7 (e) Potential Measurements with Ni/NiO/YSZ and W/W$_x$O$_y$ pH probes
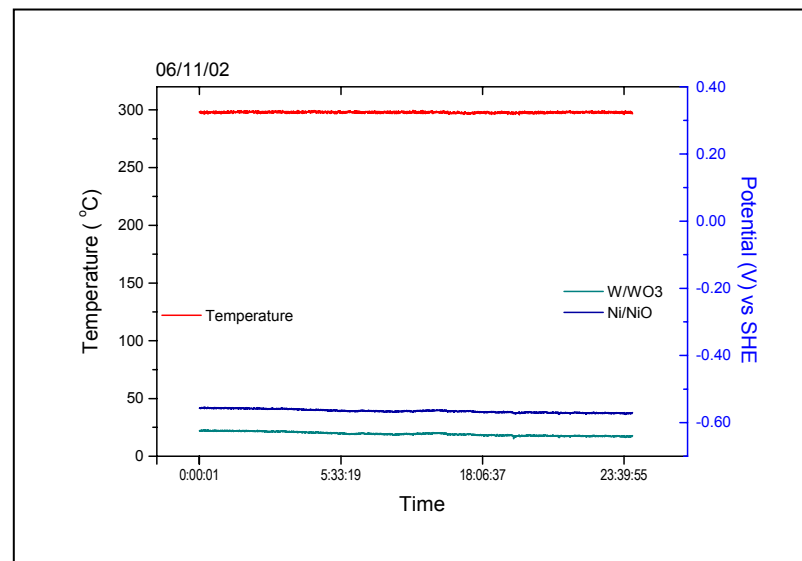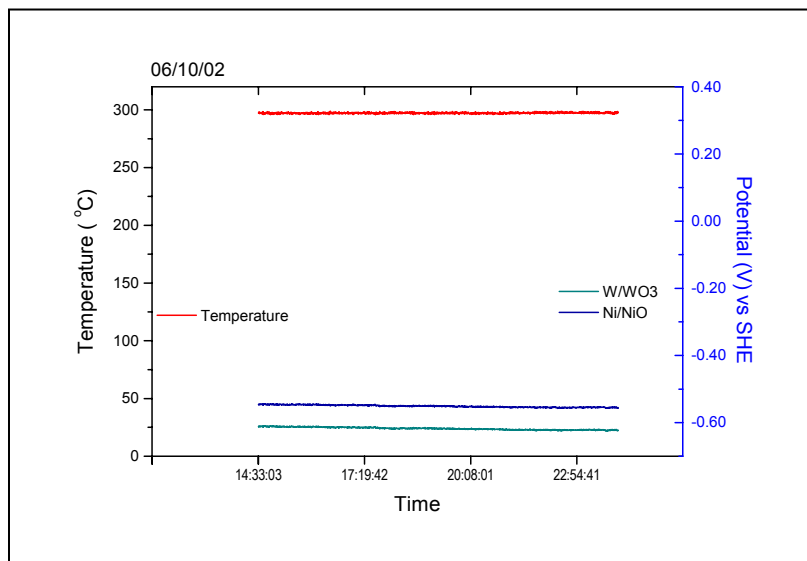(Con'td)

FIGURE. 7 (f) Potential Measurements with Ni/NiO/YSZ and W/W$_x$O$_y$ pH probes
(Con'td)